People's Democratic Republic of Algeria

Ministry of Higher Education and Scientific Research

University of El Oued

Faculty of Natural Sciences and Life

Laboratory of Biodiversity and Application of Biotechnology in the Agricultural Field

A Doctoral Thesis

Submitted in fulfillment of the requirements for the Doctorate degree in the third cycle (LMD)

Field: Biological Sciences

Specialization: Applied Biochemistry

Formulation of products based on copper and silver nano-particles and evaluation of their applications in biochemical processes.

Presented by: Chouia Maroua

Supervised by: Derouiche Samir

Defended in the presence of the Examination Committee:

Name	Rank	Affiliation	Role
TOUMI Ikram	Professor	University of El-Oued	**Chair**
DEROUICHE Samir	Professor	University of El-Oued	**Supervisor**
HADJADJ Soumia	Professor	Ouargla University	**Examiner**
BEKKOUCHE Amel	MCA	University of El-Oued	**Examiner**
FETNI Samira	MCA	University of Batna 2	**Examiner**

Academic Year: 1447-1448 AH / 2025-2026

إهداء

إلى النور الذي أنار دربي والسراج الذي لا ينطفئ نوره أبدا، إلى من بذل جهد السنين من أجل أن أعتلي سلالم النجاح، إلى من علمني النجاح والصبر، "*أبي الغالي*"

إلى الينبوع الذي لا يمل، إلى من حاكت سعادتي بخيوط منسوجة من قلبها، إلى من تتسابق الكلمات لتخرج معبرة عن مكنون ذاتها، جنة الله في أرضه "*أمي الغالية*".

إلى قرة عيني الذين ظفرت بهم هدية من الأقدار إخوة فعرفوا معنى الأخوة، إخوتي الأعزاء "*علاء الدين صفاء وإسراء*".

إلى رفيق الدرب الذي انضم إلى هذه الرحلة في وقتٍ لم يكن البدايات، لكنه اختار أن يحمل معي ما تبقّى من الطريق بثبات وصبر، في مرحلة كانت مثقلة بالتحديات، كان حضوره فارقًا وموقفه سندًا لا يُنسى، "*زوجي الكريم*".

إلى صاحب الشخصية العظيمة والأخلاق العالية الذي لا تسعني الكلمات لأشكر أفضاله علي، إلى الأستاذ القدوة الذي آمل السير على خطاه في يوم من الأيام، "*البروفيسور درويش سمير*".

إلى الوطن الصغير والكيان الذي يحتوينا، إلى الأعمدة الثابتة داخل القلب والدفء الأعمق الذي لا نملك إلا أن ننتمي إليه، إلى أغلى ما أملك، إلى كل أفراد عائلتي الذين لطالما شجعوني وكانوا لي خير السند وأخص بالذكر "*إكرام، رجاء، إيناس وأميمة*".

إلى رفيقات دربي والركن الجميل في حياتي الذين تذوقت معهم أسعد اللحظات، إلى صديقاتي ومهجة قلبي وأخص بالذكر" *وسام، ميساء، إيناس، ليلى و نسرين*".

إلى من كان لي عظيم الشرف أني تعلمت على أيديهم منذ المرحلة الابتدائية وحتى نهاية المطاف، إلى من أهداني من وقته، علمني حرفا ورفعني بكلماته، " *إلى كل أساتذتي الأفاضل*".

Acknowledgements

First and foremost, I am profoundly grateful to **Allah**, whose infinite wisdom and blessings have sustained me through the challenges of this research and the journey of my academic life.

I am deeply thankful to my supervisor, **Pr. DEROUICHE Samir,** for their valuable guidance, continuous support, and constructive feedback throughout the course of this research. Throughout this thesis, his advices he generously gave me with listening, kindness and patience allowed my work to come to fruition and see the light of day.

I appreciate the honor given to me by **Pr. TOUMI Ikram** of chairing the jury for this work, also I would like to sincerely thank the honorable jury members **Pr. HADJADJ Soumia**, **Dr. BEKKOUCHE Amel** and **Dr FETNI Samira**, for accepting to be part of my thesis committee and for the honor of their academic contribution.

I am deeply grateful to my beloved family for their unwavering support, encouragement, and patience throughout the course of my academic journey. Their constant presence and belief in me have been a source of strength and motivation at every stage.

I would like to express my deepest appreciation to my dear husband for his support and understanding. His encouragement and quiet sacrifices have been invaluable throughout this journey.

I would like to extend my sincere thanks to **Pr. Bouras Biya** and **Dr. Laarbi Haddad** for generously sharing their knowledge and expertise, which greatly enriched the quality of my research.

I would like to extend my heartfelt thanks to my dear friend, **Dr. Benmoussa Wissam**, whose constant support, encouragement, and presence throughout this journey meant more than words can express. Your help and companionship made even the hardest moments easier to bear.

A heartfelt thank to **Dr. Frahtia Ahlam** for being so generous with her time, knowledge, and support. Your help made a real difference in my research, and I am truly grateful.

I would like to express my gratitude to **Dr. Hammadi Maroua**, **Dr. Boulaares Islam** and **Dr. Chetehouna Sara**, for their valuable assistance and support during my practical training period.

I would also like to extend my sincere thanks to the pedagogic laboratory technicians for their technical assistance and continuous support throughout the experimental phases of my research. Their professionalism and dedication greatly contributed to the success of my work.

Abstract

This study aimed to synthesize eco-friendly bio-based nanomaterials and evaluate their efficiency in enzyme immobilization and biomedical applications. Starch-copper (St-CuNPs), alginate-copper (Alg-CuNPs), starch-silver (St-AgNPs), and alginate-silver nanoparticles (Alg-AgNPs) were synthesized via a green approach and characterized using SEM, FTIR, and XRD analyses. Enzyme immobilization experiments were carried out using invertase from *Saccharomyces cerevisiae* and rennet extract. Optimization was performed by varying pH, temperature, immobilization time, and nanoparticle concentration. Response Surface Methodology (RSM) with Central Composite Design (CCD) was used for rennet immobilization. Antioxidant and anti-inflammatory activities of AgNPs were evaluated using FRAP, DPPH, protein denaturation, and hemolysis inhibition assays. Characterization confirmed the formation of crystalline nanoparticles stabilized by starch and alginate functional groups. CuNPs exhibited mixed metallic and oxide phases while AgNPs displayed pure face-centered cubic metallic phases. Optimal invertase immobilization occurred at 4 h, pH 9, 30 °C, and 3% St-CuNPs, while the optimization of enzyme activity revealed that the optimal conditions were 40 °C and pH 4.5 for the immobilized enzyme, and 35 °C and pH 5 for the free enzyme. Reusability tests showed that the immobilized enzyme retained about 49% of its initial activity after ten successive cycles. Rennet immobilization was optimal at pH 2.3, 24 °C, and 8% Alg-CuNPs, achieving a maximum coagulant activity of 6.5 RU/mLThe immobilized enzyme showed more stable thermal and pH performance than the free enzyme, retaining activity across 30–50 °C and pH 4–8, and exhibited slower activity loss during six weeks of storage. Antioxidant and anti-inflammatory assays showed that St-AgNPs had the highest FRAP and DPPH activity (IC_{50} = 401 and 844.8 µg/mL), Alg-AgNPs exhibited stronger protein stabilization (IC_{50} = 131.7 µg/mL), and St-AgNPs had better membrane-stabilizing effects (IC_{50} = 889.6 µg/mL). The results confirm that starch- and alginate-based nanomaterials effectively reduce and stabilize nanoparticles, making them suitable for enzyme immobilization.These green nanomaterials demonstrated excellent reusability, enhanced enzyme stability, and notable antioxidant and anti-inflammatory potential, highlighting their promising applications in biotechnology and biomedicine.

Keywords : Invertase, rennet, Nanotechnology, AgNPs, CuNPs, Starch, alginate, antioxidant, anti-inflammatory.

Résumé

Cette étude visait à synthétiser des nanomatériaux bio-sourcés respectueux de l'environnement et à évaluer leur efficacité pour l'immobilisation d'enzymes et les applications biomédicales. Des nanoparticules de cuivre–amidon (St-CuNPs), cuivre–alginate (Alg-CuNPs), argent–amidon (St-AgNPs) et argent–alginate (Alg-AgNPs) ont été synthétisées par une approche verte et caractérisées par SEM, FTIR et XRD. Des expériences d'immobilisation d'enzymes ont été réalisées en utilisant l'invertase de *Saccharomyces cerevisiae* et un extrait de présure. L'optimisation a été effectuée en faisant varier le pH, la température, le temps d'immobilisation et la concentration en nanoparticules. La méthodologie de surfaces de réponse (RSM) avec un plan composite central (CCD) a été utilisée pour l'immobilisation de la présure. Les activités antioxydantes et anti-inflammatoires des AgNPs ont été évaluées par les tests FRAP, DPPH, dénaturation protéique et inhibition de l'hémolyse. La caractérisation a confirmé la formation de nanoparticules cristallines stabilisées par les groupes fonctionnels de l'amidon et de l'alginate. Les CuNPs présentaient des phases métalliques et oxydées mixtes, tandis que les AgNPs présentaient des phases métalliques cubiques centrées sur les faces pures.

L'immobilisation optimale de l'invertase a été obtenue après 4 h, à pH 9, 30 °C et 3 % de St-CuNPs. L'optimisation de l'activité enzymatique a montré que les conditions optimales étaient de 40 °C et pH 4,5 pour l'enzyme immobilisée, et 35 °C et pH 5 pour l'enzyme libre. Les tests de réutilisabilité ont montré que l'enzyme immobilisée conservait environ 49 % de son activité initiale après dix cycles successifs. L'immobilisation de la présure était optimale à pH 2,3, 24 °C et 8 % d'Alg-CuNPs, atteignant une activité coagulante maximale de 6,5 RU/mL. L'enzyme immobilisée présentait une stabilité thermique et un comportement au pH plus constants que l'enzyme libre, conservant son activité entre 30–50 °C et pH 4–8, et subissant une perte d'activité plus lente pendant six semaines de stockage. Les tests antioxydants et anti-inflammatoires ont montré que les St-AgNPs présentaient les plus fortes activités FRAP et DPPH (IC_{50} = 401 et 844,8 µg/mL), que les Alg-AgNPs avaient une meilleure stabilisation des protéines (IC_{50} = 131,7 µg/mL), et que les St-AgNPs avaient de meilleurs effets de stabilisation membranaire (IC_{50} = 889,6 µg/mL). Ces résultats confirment que les nanomatériaux à base d'amidon et d'alginate réduisent et stabilisent efficacement les nanoparticules, les rendant adaptés à l'immobilisation enzymatique. Ces nanomatériaux verts ont démontré une excellente réutilisabilité, une stabilité enzymatique améliorée et un potentiel antioxydant et anti-inflammatoire notable, soulignant leurs applications prometteuses en biotechnologie et en biomédecine.

Mots-clés : Invertase, présure, nanotechnologie, AgNPs, CuNPs, amidon, alginate, antioxydant, anti-inflammatoire.

الملخص

هدفت هذه الدراسة إلى تصنيع مواد نانوية صديقة للبيئة ومستخلصة من مصادر حيوية، وتقييم فعاليتها في تثبيت الإنزيمات والتطبيقات الطبية الحيوية. تم تحضير جزيئات نانوية من النحاس–النشاء(St-CuNPs) ، والنحاس–ألجينات-Alg) (CuNPs، والفضة–النشاء(St-AgNPs) ، والفضة–ألغينات (Alg-AgNPs) باستخدام طريقة صديقة للبيئة، وتمت دراسة خصائصها باستخدام المجهر الإلكتروني الماسح (SEM) والتحليل الطيفي بالأشعة تحت الحمراء (FTIR) وتحليل حيود الأشعة السينية .(XRD) أُجريت تجارب تثبيت الإنزيمات باستخدام الإنفيرتاز من *Saccharomyces cerevisiae* ومستخلص المنفحة. تم تحسين ظروف التثبيت من خلال تعديل درجة الحموضة، ودرجة الحرارة، ووقت التثبيت، وتركيز الجزيئات النانوية. كما تم استخدام منهجية السطح الاستجابي (RSM) مع التصميم المركب المركزي (CCD) لتحسين تثبيت المنفحة. أظهرت التحليلات تكوين جزيئات نانوية متبلورة مستقرّة بواسطة مجموعات النشاء والألجينات. كانت جزيئات النحاس مزيجًا من الطور المعدني والأكسيدي، بينما عرضت جزيئات الفضة أطوارًا معدنية نقية مكعبة الوجه. تم الحصول على تثبيت أمثل للإنفيرتاز عند 4 ساعات، $pH = 9$، $30°C$ ، وتركيز 3% منSt-CuNPs ، بينما كانت ظروف النشاط الأمثل للإنزيم المثبت عند $40\ °C$ و$pH = 4.5$، وللإنزيم الحر عند $35\ °C$ و .$pH = 5$أظهرت اختبارات إعادة الاستخدام أن الإنزيم المثبت احتفظ بحوالي 49% من نشاطه الأصلي بعد عشرة دورات متتالية. كان تثبيت المنفحة الأمثل عند $pH = 2.3$، ودرجة حرارة $24°C$ ، وتركيز 8% منAlg-CuNPs ، محققًا أعلى نشاط تخثر قدره 6.5 .RU/mL كما أظهر الإنزيم المثبت أداءً أكثر استقرارًا حراريًا وpH، محافظًا على نشاطه بين $30–50\ °C$ و$pH\ 4–8$، وفقدان نشاط أبطأ خلال ستة أسابيع من التخزين .أظهرت الاختبارات المضادة للأكسدة ومضادة للالتهاب أن St-AgNPs أظهرت أعلى نشاط FRAPو DPPH (IC_{50} = 401 و844.8 µg/mL) ، بينما أظهرت Alg-AgNPs قدرة أكبر على تثبيت البروتينات (IC_{50} = 131.7 µg/mL)، وأظهرت St-AgNPs أفضل تأثير في تثبيت أغشية الخلايا .(IC_{50} = 889.6 µg/mL) تؤكد النتائج أن المواد النانوية المستندة إلى النشاء والألجينات تقلل وتثبت الجزيئات النانوية بفعالية، مما يجعلها مناسبة لتثبيت الإنزيمات. أظهرت هذه المواد النانوية الخضراء إعادة استخدام ممتازة، واستقرارًا محسّنًا للإنزيمات، وإمكانات مضادة للأكسدة ومضادة للالتهاب ملحوظة، مما يبرز تطبيقاتها الواعدة في مجال التكنولوجيا الحيوية والطب الحيوي.

الكلمات المفتاحية :إينفرتاز، منفحة، تكنولوجيا النانو، جسيمات الفضة النانوية، جسيمات النحاس النانوية، نشاء، ألجينات، مضاد أكسدة، مضاد التهاب.

Figures list

Tables list

Abbreviation list

Ag	**Silver**
ALG	**Alginate**
Alg-AgNPs	**Alginate-silver nanoparticles**
Alg-CuNPs	**Alginate-copper nanoparticles**
BSA	**Bovin serum albumin**
CAU	**Coagulant activity unit**
$CaCl_2$	**Calcium chloride**
Cu	**Copper**
$Cu\ [NO_3]_2$	**Copper nitrate**
DNS	**3,5-dinitrosalicylic acid**
DPPH	**1,1-diphenyl-2-picryhydrazyl**
EDTA	**Ethylenediaminetetraacetic acid**
EDX	**Energy Dispersive X-ray**
FeCl3	**Ferric chloride**
FRAP	**Ferric reducing ability of plasma**
FTIR	**Fourier Transform Infrared spectroscopy**
HCl	**Hydrochloric acid**
IY	**Immobilization yield**
$K_3Fe(CN)_6$	**potassium ferricyanide**
NaAlg	**Sodium alginate**
NaCl	**Sodium chloride**
$NaHCO_3$	**Sodium bicarbonate**
NaOH	**Sodium hydroxide**
NPs	**Nanoparticles**
RE	**Raw extract**
RS	**Reducing sugars**
RBC	**Red blood cells**

Abbreviation list

Rpm	**Round per minute**
RU	**Rennet unit**
SEM	**Scanning electron microscopy**
St-AgNPs	**Starch-silver nanoparticles**
St-CuNPs	**Starch-copper nanoparticles**
TCA	**Trichloroacetic acid**
UV-VIS	**Ultraviolet-visible spectroscopy**
XRD	**X-ray powder diffraction**

Content

Introduction

Introduction

All living organisms are made of cells, which rely on highly efficient enzymes to catalyze specific biochemical reactions with great precision and minimal side effects.(Bhatia, 2018) The term "enzyme" derives etymologically from the Greek enzymos ('in leaven'), reflecting its initial discovery in fermentation processes. (Robinson P. K, 2015). Enzymes are biological catalysts that lower activation energy to speed up biochemical reactions, remain unchanged after catalysis, and enhance reaction rates without altering the equilibrium between reactants and products. (A. Kumar, Asthana, Jain, & Singh, 2017; Mohamad, Marzuki, Buang, Huyop, & Wahab, 2015).

Despite their catalytic advantages, enzymes present significant practical limitations that constrain industrial implementation. These biomolecules exhibit pronounced sensitivity to environmental parameters, demonstrate restricted functional durability, and are particularly susceptible to inhibition by elevated substrate concentrations (Hernandez & Fernandez-Lafuente, 2011). Operational challenges are further compounded by intrinsic molecular instability, which frequently restricts continuous industrial utilization due to insufficient functional longevity and complex recovery protocols for enzyme recycling (R. A. Sheldon, 2007). Fundamental biochemical constraints also exist, as native protein architectures evolve to meet only baseline functional requirements rather than optimal performance metrics, with residue-residue interactions and sequence configurations representing evolutionary compromises rather than engineered perfection (Mohamad et al., 2015).

Recent years have witnessed growing scientific and industrial interest in immobilized enzyme technology as a promising strategy to overcome the limitations of free enzymes (AS & BR, 2004). Enzyme immobilization involves the confinement or attachment of enzymes to solid matrices, thereby converting them into heterogeneous biocatalytic systems. This approach confers significant advantages over soluble enzymes, particularly enhanced structural stability and improved tolerance to fluctuating process conditions (Massolini & Calleri, 2005) .

These advances have encouraged the exploration of innovative material platforms, such as nanotechnology, which can provide superior support, control, and functionality for immobilized enzymes. Nanotechnology represents a cutting-edge scientific discipline focused on the manipulation and application of materials at the nanometer scale (1-100 nm), with broad interdisciplinary applications across various scientific domains (Mansoori & Soelaiman, 2005) The rapid progress in nanoscience has facilitated the engineering of diverse organic and inorganic nanomaterials, particularly nanoparticles, which have demonstrated remarkable potential across multiple industries. These applications span from advanced electronics and targeted drug delivery systems to innovative solutions in food packaging and textile manufacturing (Saallah et al., 2016)

The physicochemical and biological characteristics of nanoparticles are profoundly influenced by their synthesis methodologies. Furthermore, the choice of precursor materials, including specific salts employed in the fabrication process, plays a critical role in determining the resultant nanoparticles (Scott, Vadalasetty, Chwalibog, & Sawosz, 2018).

The main goal of this study is

- The green synthesis and physicochemical characterization of starch-copper, alginate-copper, starch-silver and alginate-silver nanoparticles.
- Extraction of the invertase enzyme from Saccharomyces cerevisiae and optimization of its immobilization on starch–copper nanoparticles, followed by optimization of the activity parameters of both free and immobilized enzymes with reusability assessment.
- Extraction of rennet and optimization of its immobilization on alginate–copper nanoparticles using Response Surface Methodology (RSM) with a Central Composite Design (CCD), followed by evaluation of the stability and storage properties of both free and immobilized rennet.
- Evaluation of antioxidant and anti-inflammatory activities of AgNPs using FRAP, DPPH, protein denaturation, and hemolysis inhibition assays.

This work aims to explore sustainable nanomaterials that enhance enzyme functionality and provide potential added value through their bioactivity.

Literature Review

Chapter I
Enzyme Immobilization

I. Enzymes

Enzymes represent a class of proteinaceous biocatalysts that significantly accelerate both biochemical and chemical transformations. These biomolecules are universally distributed across biological systems, from multicellular organisms to microorganisms, where they mediate essential metabolic and catabolic pathways critical for sustaining life (Homaei, Sariri, Vianello, & Stevanato, 2013). Historically employed to streamline complex industrial processes, enzymes have recently gained renewed prominence as green alternatives in manufacturing. The global shift toward sustainable bioprocessing has dramatically expanded their utilization across diverse industries, ranging from pharmaceuticals to biofuel production(Maghraby, El-Shabasy, Ibrahim, & Azzazy, 2023). Recent advancements in protein biotechnology have revolutionized enzyme production, enabling the isolation of research-grade biocatalysts with exceptional purity for both scientific and industrial applications. These biological catalysts have been integral to traditional food processing methodologies for centuries, playing indispensable roles in dairy fermentation (e.g., cheese production), alcoholic beverage preparation (including beer and wine manufacturing), and other heritage food technologies (Homaei et al., 2013). The industrial enzyme sector has experienced particularly remarkable expansion since the early 21st century, with biotechnology innovations driving unprecedented adoption across manufacturing sectors (Maghraby et al., 2023)

II. Useful Enzymes for Industrial Applications

II.1. Invertase

Invertase (EC 3.2.1.26), classified as β-D-fructofuranoside fructohydrolase or β-fructofuranosidase, represents a catalytically important glycoprotein characterized by significant mannose-rich glycosylation. This enzyme is taxonomically categorized within the glycoside hydrolase (GH) family based on its structural and mechanistic properties (Lombard, Golaconda Ramulu, Drula, Coutinho, & Henrissat, 2014). Its primary biochemical function involves the stereospecific hydrolysis of sucrose, yielding an equimolar ratio of fructose to glucose - a product mixture commercially designated as inverted sugar (Kotwal & Shankar, 2009) as showed in Figure 01.

Commercial invertase production primarily utilizes Saccharomyces species due to their efficient β-fructosidase activity. This yeast-derived enzyme differs fundamentally from fungal α-glucosidase invertases in their catalytic mechanisms - while β-fructosidases cleave sucrose molecules at the fructose moiety, α-glucosidases attack the glucose terminus. The resulting invert syrup exhibits greater sweetness than sucrose, primarily due to fructose's enhanced sweetening properties. Beyond taste improvement, fructose offers nutritional advantages including better suitability for diabetic diets and enhanced iron absorption in pediatric populations (Linde et al., 2012). Invertase plays a crucial role in food manufacturing by enabling significantly higher sugar concentrations while preventing crystallization. This property makes it particularly valuable for producing non-crystallizing syrups from sucrose. The enzyme finds widespread application in confectionery production, where it effectively prevents sugar crystal formation in products such as marzipan, gingerbread dough, and praline fillings, ensuring smooth texture and consistent quality. (Alam, Hubbard, Oliver, & Rattray, 2007).

Beyond its extensive applications in food processing, invertase plays a significant role in pharmaceutical manufacturing. This versatile enzyme is commonly incorporated into various medicinal formulations, including digestive aids, pediatric nutrition products, cough syrups, and nutraceutical preparations. (Bhalla, Thakur, & Thakur, 2017). A particularly valuable application lies in its ability to synthesize fructooligosaccharides (FOS) - short-chain fructose polymers that serve as non-digestible carbohydrates. These functional oligosaccharides have gained prominence as prebiotic additives in health-oriented foods, beverages, and baked goods. Their reduced caloric content coupled with satisfactory sweetness makes FOS particularly suitable for diabetic-friendly products. (Khandekar, Palai, Agarwal, & Bhattacharya, 2014).

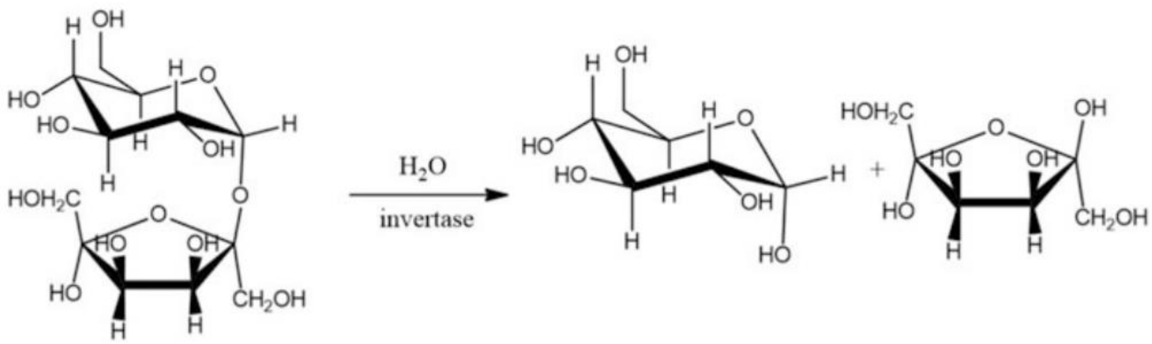

Figure 01: Hydrolysis of sucrose to glucose and fructose.

II.2. Rennet

Rennet represents a crucial enzymatic preparation traditionally sourced from the gastric mucosa of young ruminants, including calves, lambs, and goat. This natural enzyme complex, predominantly produced in milk-fed juveniles, exhibits specific proteolytic activity that induces milk coagulation through casein cleavage. The dairy industry extensively utilizes rennet as a primary coagulant in cheese manufacturing, where it serves as the key agent in developing the characteristic texture and structure of numerous cheese varieties. (Kaushal, Singh, & Arya, 2022)

The enzymatic extract primarily consists of chymosin (EC 3.4.23.4), accounting for approximately 95% of the total milk-clotting activity. The remaining proteolytic activity derives from pepsin A (EC 3.4.23.1), pepsin B (EC 3.4.23.2), and gastricsin (EC 3.4.23.3). Notably, the enzyme composition varies significantly with age: calf rennet typically contains 90% chymosin and 10% pepsin, while adult bovine rennet exhibits the inverse ratio of these enzymes.

Chymosin (32-39 kDa), an aspartic protease of gastric origin, demonstrates exceptional substrate specificity by cleaving the Phe105-Met106 peptide bond in κ-casein. This targeted proteolysis disrupts casein micelle stability, initiating the milk coagulation cascade. The enzyme exhibits greater stability at refrigeration temperatures (2°C) compared to ambient conditions, with complete thermal inactivation occurring above 55°C. Its optimal catalytic activity occurs at pH 4.0, reflecting its natural gastric environment.

In contrast to chymosin, pepsin exhibits broader substrate specificity and significantly greater nonspecific proteolytic activity. This enzymatic characteristic leads to extensive casein hydrolysis, which can adversely affect cheese production through three primary mechanisms: (1) reduced product yield due to excessive protein breakdown, (2) development of off-flavors from generated peptides, and (3) compromised shelf stability resulting from accelerated proteolytic degradation. (de Castro Leite Júnior et al., 2022).

Cheese represents one of the most widely consumed fermented dairy products globally, with production encompassing over one hundred distinct varieties. This nutritionally valuable food provides an excellent source of dietary protein, essential vitamins, and critical minerals including calcium. Rennet-mediated coagulation stands as one of the most significant enzymatic applications in food biotechnology. However, the growing global cheese demand coupled with declining calf rennet availability has necessitated the development of alternative coagulant sources. (Rachana Singh, Singh, & Sachan, 2019).

III. Introduction to Enzyme Immobilization

Although enzymes offer significant advantages over conventional chemical catalysts, several practical limitations hinder their industrial implementation. The production costs remain a primary constraint, as enzyme isolation and purification processes are substantially more expensive than synthetic catalyst preparation. Furthermore, their proteinaceous nature renders them particularly vulnerable to denaturation when removed from native biological environments, limiting operational stability under industrial conditions. (Hernandez & Fernandez-Lafuente, 2011).

Enzyme immobilization has emerged as a highly effective strategy to address these limitations. This biotechnology approach involves the stabilization of enzymes through attachment to or encapsulation within solid matrices, thereby generating robust heterogeneous biocatalytic systems. The immobilized enzyme configuration offers numerous operational advantages while maintaining catalytic efficiency. (Datta, Christena, & Rajaram, 2013). Immobilized enzyme systems replicate the natural organization of enzymes in biological systems, where they are typically associated with cellular membranes, organelles, or cytoskeletal elements. The solid-phase matrix confers structural stabilization to the enzyme, thereby preserving its catalytic activity. Compared to soluble enzymes, immobilized preparations demonstrate superior robustness and enhanced tolerance to environmental fluctuations. Furthermore, heterogeneous biocatalyst systems offer multiple practical advantages including: (1) facile biocatalyst and product separation, (2) capacity for repeated enzyme utilization, (3) continuous process operation capability, (4) immediate reaction control, and (5) expanded bioreactor configuration options. (Kress et al., 2002).

The scientific foundation for enzyme immobilization was established in 1916 with a seminal discovery demonstrating that invertase maintained full catalytic activity when adsorbed onto solid substrates such as activated charcoal or aluminum hydroxide. Remarkably, the immobilized enzyme exhibited equivalent performance to its free-floating counterparts in solution. This pivotal observation marked the genesis of immobilized enzyme technology and directly informed contemporary immobilization methodologies. (Gomes-Ruffi, da Cunha, Almeida, Chang, & Steel, 2012).

Initial enzyme immobilization approaches suffered from suboptimal loading capacities relative to the theoretical binding potential of support matrices. The field underwent transformative advancement during the mid-20th century (1950s-1960s) with the development of covalent attachment methodologies. Subsequent decades witnessed exponential growth in immobilization research, as evidenced by the current corpus of over 5,000 peer-reviewed publications and patents addressing this technology. Contemporary biotechnology has successfully immobilized hundreds of enzymes through various methodologies, with numerous industrial applications employing over a dozen biocatalysts—notably penicillin G acylase, invertase, lipases, and proteases—in large-scale processes. Despite decades of intensive research, the persistent publication of novel studies and comprehensive reviews in this domain reflects both the sustained scientific interest and continued technological evolution of enzyme immobilization techniques. (Hartmann, 2005).

Enzyme immobilization offers significant advantages across multiple domains, including enhanced economic viability, improved environmental sustainability, and superior technical performance—primarily through increased operational stability and reusability. This biotechnology approach has been successfully implemented across diverse industrial sectors, spanning food processing, pharmaceutical manufacturing, animal feed production, textile engineering, healthcare products, and detergent formulations, as well as environmental applications such as bioremediation and effluent treatment. Modern immobilization strategies employ various techniques (e.g., entrapment, covalent bonding) with advanced support matrices, enabling large-scale industrial implementation of biocatalytic processes. (Maghraby et al., 2023).

IV. Methods of Enzyme Immobilization

The strategic selection of an immobilization method constitutes a fundamental aspect of biocatalyst development, critically influencing enzymatic performance and operational characteristics (Chiou & Wu, 2004). Five principal immobilization techniques are currently employed (Figure 2): adsorption, covalent binding, entrapment, encapsulation, and cross-linking (Wahba & Hassan, 2015). These approaches utilize either physical interactions (characterized by weaker intermolecular forces) or chemical conjugation (involving stronger covalent bonds). However, physically adsorbed enzymes often demonstrate insufficient binding affinity to withstand the rigorous conditions encountered in industrial applications (Cao, van Langen, & Sheldon, 2003).

IV.1. Adsorption

The physical adsorption technique represents one of the most straightforward enzyme immobilization approaches, involving the non-covalent attachment of enzymes to either organic or inorganic support matrices (Sugahara & Varéa, 2014) This method relies on relatively weak intermolecular interactions, including van der Waals forces, electrostatic attractions, hydrophobic effects, hydrogen bonding, and ionic associations between the enzyme and carrier surface (Jegannathan, Abang, Poncelet, Chan, & Ravindra, 2008)

The resulting enzyme orientation and binding strength are highly dependent on both protein conformation and matrix surface characteristics, which can yield either tightly bound, structurally preserved enzymes or weakly associated, conformationally altered forms. This approach offers exceptional versatility in carrier material selection, though enzyme-carrier compatibility remains crucial for successful immobilization. Effective adsorption requires specific biochemical affinities between the enzyme and support matrix (Wong, Thirlway, & Micklefield, 2008).

The adsorption method presents several distinct advantages: minimal carrier pretreatment requirements, reduced reagent consumption, cost-effectiveness, and straightforward implementation (Guisan, 2013).

The non-covalent immobilization approach is inherently limited by the weak, reversible nature of its interactions. This frequently leads to enzyme leaching from the support matrix, causing both progressive activity depletion and product contamination. Such limitations significantly compromise system durability and reusability, especially in analytical and biosensing applications. Furthermore, surface-induced protein adsorption often triggers conformational rearrangements and partial denaturation, frequently resulting in substantial activity loss. (Homaei et al., 2013)

IV.2. Covalent Binding

Covalent immobilization has become the predominant approach for enzyme stabilization since its introduction (Porath & Axén, 1976). This technique relies on forming stable covalent linkages between reactive amino acid residues (e.g., $-NH_2$, -COOH, -OH, -SH) on the enzyme surface and complementary functional groups on the support matrix. Many carrier materials require chemical activation to generate these reactive sites prior to enzyme conjugation (Hashem, Gamal, Hassan, Hassanein, & Esawy, 2016). Among various matrices, hydrophilic polysaccharides have demonstrated particular effectiveness as supports for covalent immobilization. (D.-M. Liu & Dong, 2020)

Covalent immobilization offers several significant advantages, including enhanced enzyme durability and high recovery rates for repeated use. This method improves enzymatic stereospecificity while substantially increasing operational stability(Fernández-Lorente et al., 2001). A key benefit is the minimal risk of enzyme leaching, even when exposed to high substrate concentrations or harsh buffer conditions that would typically promote protein denaturation. The robust covalent linkages effectively maintain enzyme integrity under challenging reaction conditions.(Liang, Li, & Yang, 2000).

Despite its advantages, covalent immobilization presents several practical limitations. The technique requires complex procedural steps and extended incubation periods to achieve effective enzyme conjugation (Marrazza, 2014). In many cases, structural modifications of the enzyme are necessary to expose reactive groups for covalent attachment, potentially compromising protein integrity. The method also yields relatively low enzyme loading capacities (~0.02 g enzyme/g support), limiting its industrial scalability (Marrazza, 2014). Moreover, the restricted mobility of covalently immobilized enzymes may impede essential conformational changes during catalysis, thereby reducing enzymatic activity (Shen et al., 2011).

IV.3. Entrapment

Enzyme entrapment represents one of the most straightforward immobilization techniques, involving physical confinement of enzymes within a porous support matrix. This approach enhances enzyme stability while preserving catalytic activity, as it avoids direct chemical modification of the protein. The method's effectiveness primarily depends on two key factors: the selection of an appropriate support material and optimization of pore size to ensure adequate substrate-enzyme interaction. Unlike covalent binding or adsorption methods, entrapped enzymes maintain their conformational freedom within the solution-filled matrix pores while being spatially constrained within the support structure. (Mohy Eldin, Hassan, & El-Aassar, 2005).

The entrapment approach preserves enzyme integrity by avoiding direct chemical interactions with the polymer matrix, thereby minimizing denaturation risks. This technique offers several significant advantages: high enzyme loading capacity, cost-effective fabrication, improved mechanical stability of the immobilized enzymes, and controlled mass transfer characteristics (Costa, Azevedo, & Reis, 2005). Furthermore, the encapsulation material can be precisely engineered to create an optimal microenvironment through modulation of pH, polarity, or amphiphilic properties (Liang et al., 2000).

The entrapment method presents several notable limitations. A primary constraint involves mass transfer resistance, where increasing matrix thickness during polymerization impedes substrate diffusion to active sites. Additional challenges include: potential enzyme leakage through oversized matrix pores, relatively low enzyme loading capacity, and structural degradation of the support material during polymerization processes. These factors collectively restrict the technique's efficiency and applicability. (Nguyen & Kim, 2017).

IV.4. Encapsulation

The encapsulation technique immobilizes biomolecules within polymeric matrices by confining them in discrete, semi-permeable vesicles (Beatriz, Paula, & Batista-Viera, 2013). Similar to entrapment, this approach maintains enzymes in solution while restricting their spatial distribution. Encapsulation is particularly advantageous for fragile enzymes, as it protects them within microenvironments bounded by porous membranes. The semi-permeable nature of these membranes permits free diffusion of small substrate and product molecules while retaining larger enzyme complexes within the capsules. (Kurzbaum et al., 2020). Encapsulation immobilizes biological systems within a protective polymeric film, shielding biocatalysts from potentially damaging environmental factors while preserving their catalytic efficiency. This protective barrier significantly extends biocatalyst operational longevity (Patil, Kamalapur, Marapur, & Kadam, 2010).

Similar to entrapment, encapsulation maintains enzyme mobility while restricting spatial distribution. However, a key limitation arises from molecular size exclusion - many enzymes and cellular components exceed the capsule's pore dimensions, preventing their migration across the semipermeable membrane. The technique's effectiveness is predominantly governed by the capsule's pore size characteristics(Kierstan & Coughlan, 1991).

IV.5. cross-linking

Cross-linking represents an irreversible immobilization technique that operates without carrier materials. This method utilizes polyfunctional reagents to create covalent linkages between enzyme molecules (or cells), forming stable three-dimensional networks. The resulting macromolecular complexes maintain enzymatic activity while exhibiting enhanced structural stability. Cross-linking immobilization employs various bi- or polyfunctional reagents including glutaraldehyde, hexamethylene diisocyanate, diazobenzidine, and toluene diisothiocyanate to form intermolecular bridges between enzyme amino groups. This process can be achieved through either chemical or physical approaches. The technique offers significant advantages: preservation of native enzymatic activity, and direct substrate accessibility to the catalytic sites. However, potential limitations include: possible enzyme denaturation due to harsh cross-linking conditions, and toxicity of certain cross-linking agents to biological systems. (Govardhan, 1999).

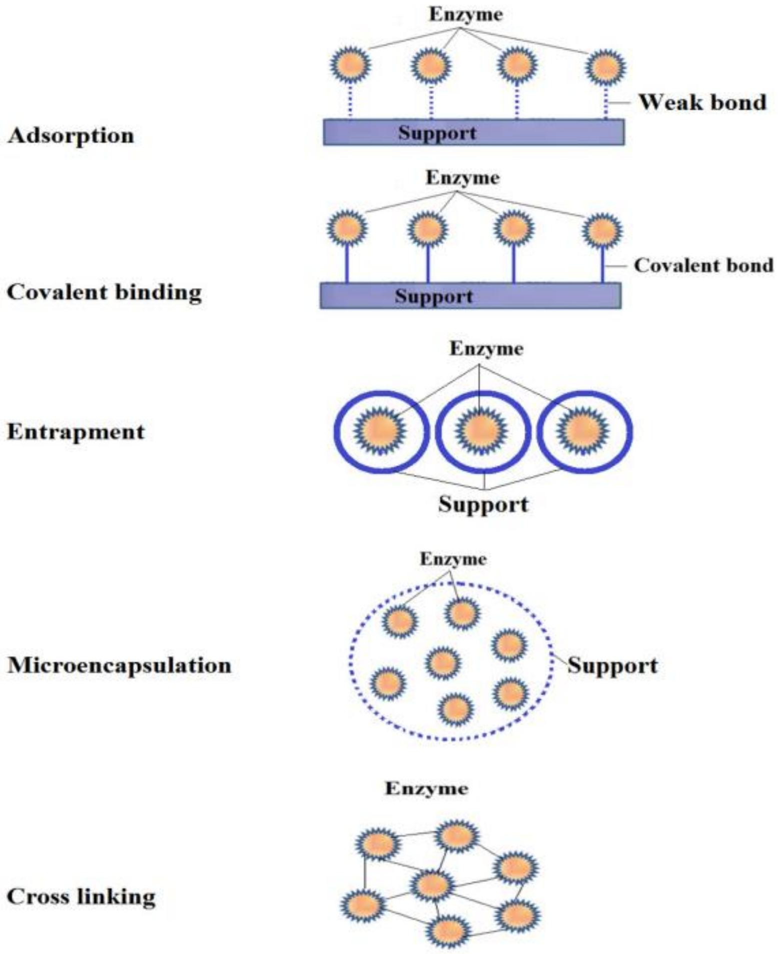

Figure 02: Immobilization methods.

Table 01: Advantages and disadvantages of immobilization methods

Characteristic	Immobilization method				
	Physical adsorption	Covalent binding	Entrapping method	Encapsulation	Cross-linking method
Preparation	Easy	Difficult	Difficult	Easy	Difficult
Enzyme activity	Low	High	High	High	Moderate
Substrate specificity	Unchangeable	Changeable	Unchangeable	Unchangeable	Changeable
Binding force	Weak	Strong	Strong	Moderate	Strong
Regeneration	Possible	Impossible	Impossible	Possible	Impossible
General applicability	Low	Moderate	High	Moderate	Low

Cost of immobilization	Low	High	Low	Low	Moderate

V. Support Materials

The functional characteristics of immobilized enzyme systems are determined by the synergistic interplay between the enzyme's intrinsic properties and the carrier material's physicochemical attributes. This enzyme-support interaction dictates the resulting biocatalyst's chemical stability, biochemical functionality, mechanical robustness, and kinetic behavior. Carrier materials span three principal categories: synthetic organic polymers, natural biopolymers, and inorganic matrices (R. Sheldon, 2007). Extensive research has documented the successful application of diverse support materials for enzyme immobilization (Girelli & Mattei, 2005).

V.1. Synthetic Polymers

Among synthetic polymer supports for enzyme immobilization, acrylic resins—particularly Eupergit® C (Evonik Industries)—have emerged as predominant matrices. These macroporous copolymers consist of N,N′-methylene-bis(methacrylamide), glycidyl methacrylate, allyl glycidyl ether, and methacrylamide, exhibiting an average particle size of ∼170 μm and pore diameters of 20-30 nm (Figure 3). The resins demonstrate exceptional hydrophilicity and maintain remarkable structural integrity across the entire pH spectrum (0-14), showing negligible swelling or contraction even under extreme pH fluctuations. Their chemical and mechanical stability under harsh conditions makes them particularly suitable for industrial biocatalysis applications. (Boller, Meier, & Menzler, 2002) . Polyketone polymers (–[–CO–CH2–CH2–]n–) represent particularly promising immobilization matrices due to their exceptional mechanical robustness, high protein-binding capacity and straightforward immobilization protocol requiring only reactant mixing. Notably, their application eliminates the need for bifunctional crosslinkers or spacer arms, significantly simplifying the immobilization process while maintaining protein integrity. (Agostinelli et al., 2007). .

While hydrophilic resins offer significant advantages for enzyme immobilization, they present notable diffusion limitations that particularly impact kinetically controlled bioconversion processes. Despite this constraint, covalent immobilization onto acrylic resins has proven commercially viable for numerous industrial enzymes, demonstrating the method's practical utility in large-scale applications. (Katchalski-Katzir & Kraemer, 2000).

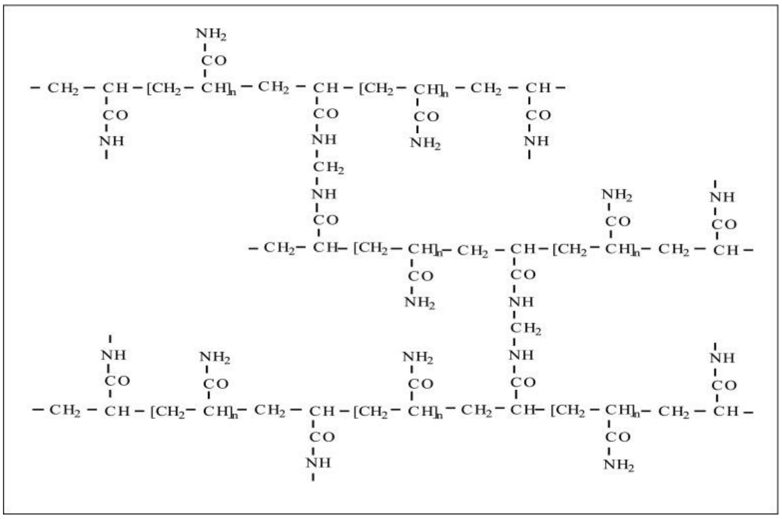

Figure 03: Structure of polyacrylamide gel matrix.

V.2. Biopolymers

Water-insoluble polysaccharides—including cellulose, starch, agarose, carrageenans, and chitosan—represent a prominent class of biopolymeric supports for enzyme immobilization. These matrices spontaneously form robust aqueous gels exhibiting two key characteristics: exceptional chemical inertness, and remarkable mechanical strength even at low polymer concentrations (<2% w/v). Their high hydroxyl group density and hydrophilic nature create optimal microenvironments for maintaining enzyme stability and activity. (Van de Velde, Lourenço, Pinheiro, & Bakker, 2002). The versatile chemical functionality of these biopolymers enables facile activation for both reversible and irreversible protein conjugation. Through strategic application of bifunctional crosslinking agents, the polymeric matrices can be structurally reinforced to enhance their mechanical stability and thermal resistance. These unique properties establish polysaccharide-based resins as nearly ideal matrices for biomolecular purification (via reversible interactions) and enzyme immobilization (through irreversible covalent attachment).

V.2.1 Chitosan and chitin

Chitin and chitosan have emerged as effective natural polymer supports for enzyme immobilization. These polysaccharides facilitate enzyme conjugation through interactions with protein surface residues or carbohydrate moieties (Hsieh, Liu, & Liao, 2000). Composite systems demonstrate superior performance, as evidenced by: chitosan-alginate blends showing reduced enzyme leaching compared to pure alginate matrices due to enhanced physical and ionic interactions, and chitosan-clay composites providing exceptional enzyme retention through synergistic effects of abundant hydroxyl/amino groups for covalent linkage, optimal hydrophilicity, and highly porous architectures. (Chang & Juang, 2007).

V.2.2 Cellulose

As the most abundant natural polymer, cellulose has been extensively utilized for enzyme immobilization. Modified cellulose derivatives demonstrate enhanced performance characteristics: Diethylaminoethyl (DEAE)-functionalized cellulose exhibits superior enzyme storage stability (Al-Adhami, Bryjak, Greb-Markiewicz, & Peczyńska-Czoch, 2002) and cellulose-coated magnetite nanoparticles enable efficient starch degradation systems when conjugated with α-amylase (Namdeo & Bajpai, 2009). Advanced cellulose composites, such as glutaraldehyde-activated ionic liquid-cellulose films, offer additional advantages including improved mechanical formability and operational flexibility. (Klein et al., 2011).

V.3. Inorganic supports

In contrast to polymeric supports, rigid inorganic matrices offer distinct advantages for enzyme immobilization. Various mineral-based materials—including alumina, silica, zeolites, and mesoporous silicates—have demonstrated exceptional utility as immobilization carriers. Among these, silica-derived supports have emerged as particularly advantageous for both industrial biocatalysis and research applications, owing to their exceptional mechanical stability, tunable porosity and compatibility with large-scale manufacturing processes (Vianello et al., 2000). Silica-based matrices offer three principal advantages over soft gel supports: Superior mechanical robustness enabling operation across extended pressure ranges and harsh processing conditions - a characteristic that has established their dominance in high-performance liquid chromatography media fabrication (Cabrera, 2004), Facile surface functionalization through diverse chemical modifications, permitting tailored ligand conjugation, and Unparalleled surface area density, as demonstrated by exceptional enzyme loading capacities (e.g., invertase immobilization via amino-functionalized surfaces). These combined properties make silica gels particularly versatile for demanding biocatalytic applications. Silica gels offer exceptional tunability in morphological design, enabling precise control over pore architecture and microchannel configuration to optimize substrate-ligand interactions. These matrices combine three critical industrial advantages: outstanding mechanical stability under operational stress, chemical inertness across diverse solvent systems, and environmental compatibility, making them ideal for sustainable manufacturing processes. (David, Wang, Yang, & Yang, 2006).

V.4. Smart polymers

Smart polymer-based enzyme immobilization represents an innovative approach utilizing stimuli-responsive matrices that undergo reversible conformational transitions in response to subtle environmental changes (temperature, pH, or ionic strength) (Klouda & Mikos, 2008). The thermo-responsive polymer poly(N-isopropylacrylamide) (PNIPAAm) has emerged as a particularly promising candidate, exhibiting a lower critical solution temperature (LCST) of ~32°C. Below this threshold, PNIPAAm maintains a hydrated, soluble state, while above the LCST, it undergoes rapid phase separation through hydrophobic collapse and water expulsion from the polymer matrix. This smart immobilization approach enables biotransformations under homogeneous conditions (below LCST), where dissolved enzymes exhibit minimized mass transfer limitations and preserved native conformation, avoiding activity loss from surface-induced denaturation. Subsequent temperature increase above the LCST triggers three simultaneous benefits: rapid biocatalyst precipitation for facile recovery, enabled enzyme reuse, and inherent process safety through thermal self-regulation. The latter occurs when exceeding the LCST causes immediate catalyst precipitation and reaction termination, effectively preventing thermal runaway scenarios. (Klis, Karbarz, Stojek, Rogalski, & Bilewicz, 2009).

V.5. Nanomaterial-based supports

Engineered nanomaterials represent an advanced immobilization platform, offering three key structural advantages: exceptional surface-to-volume ratios, tunable surface functionalities, and nanoscale diffusion pathways (El-Khawaga, Zidan, & Abd El-Mageed, 2023). These characteristics enable: significantly higher enzyme loading capacities, enhanced immobilization efficiency, and simultaneous multi-enzyme co-localization, making them particularly suitable for cascade biocatalysis (Giannakopoulou, Gkantzou, Polydera, & Stamatis, 2020; Zdarta et al., 2023). The shortened mass transfer distances inherent to nanocarriers reduce diffusion limitations, thereby accelerating substrate turnover rates and improving overall catalytic efficiency. Nanocarriers demonstrate four principal advantages over conventional immobilization supports:

- **Enhanced Stability**: Nanomaterials exhibit high chemical and thermal stability, resisting degradation and preventing enzyme inactivation. They protect enzymes, extend their functional lifetime, and improve stabilization and recyclability in co-immobilization systems.

- **Tunable Surface Properties**: Nanocarrier surfaces can be precisely modified through functionalization to meet specific co-immobilization requirements. Introducing targeted functional groups enhances enzyme-carrier interactions and immobilization efficiency.

- **High Catalytic Efficiency**: The large specific surface area of nanomaterials provides more active sites for enzyme binding compared to conventional supports. This increases enzyme loading density and, combined with superior mass transfer properties, enables more effective enzyme-substrate contact and significantly improved catalytic efficiency.

- **Biocompatibility**: Many nanocarriers demonstrate excellent biocompatibility, creating favorable environments that help maintain enzymes' natural conformation and activity, thereby enhancing immobilization and stabilization outcomes.

Despite their advantages, certain nanocarriers remain technically and economically disadvantaged compared to conventional supports in three aspects: greater fabrication complexity, reduced operational stability, and higher processing costs. Nevertheless, nanomaterial-based carriers significantly broaden enzymatic applications through their structural diversity, including nanoparticles, nanofilms, and nanofibers. These versatile platforms enable effective immobilization of diverse enzyme classes, facilitating expanded utilization across multiple domains of industrial biocatalysis, biosensing systems, diagnostic medicine, and therapeutic development. (J. Zhang, Lovell, Shi, & Zhang, 2025).

VI. Applications of immobilized enzymes

Immobilized enzymes find diverse applications across industrial processes, medical technologies, and research methodologies. For commercial implementation, selecting an appropriate immobilized enzyme system requires careful evaluation of the trade-offs between immobilized and free enzyme characteristics. Additional industrial utilizations encompass: small-scale organic synthesis, analytical procedures, and clinical diagnostic applications. (Taylor et al., 2004)

VI.1. Industrial Applications

Researchers have extensively pursued cost reduction in industrial processes through enzyme reuse strategies. Immobilization technology has been identified as an effective solution that enables repeated enzyme utilization, maintained catalytic stability, and preserved enzymatic effectiveness, collectively contributing to significant production cost savings.

VI.1.1 Food Industry Application

Enzymes play a vital role in food processing (Table 02), though their purified forms are often vulnerable to denaturation during extraction and handling. To overcome this limitation, immobilization techniques are employed to enhance enzyme stability and facilitate their separation from reaction mixtures. Immobilized enzymes, in particular, have proven valuable in industrial applications such as syrup manufacturing. A key example is the use of immobilized β-galactosidase, which efficiently hydrolyzes lactose found in whey, enabling the conversion of dairy waste into glucose and supporting the production of lactose-free milk (Wahba & Hassan, 2015). Beyond enzymatic applications, food preservation also benefits from bioactive compounds. Essential oils derived from plants like fennel and cumin can be encapsulated within polymeric carriers, allowing their gradual release as natural preservatives. These oils not only extend shelf life but also contribute health-enhancing properties to a range of food items, including baked goods, beverages, dairy products, pickles, and confectioneries. (Abdel Wahab et al., 2018).

Table 02: Immobilized enzymes for food applications

Enzyme	Immobilization method	Support	Application	Results	Ref
Protease	Entrapment	Mesoporous silica and zeolite	Milk coagulant for dairy products	Immobilized protease converted milk into cheeses in <90 min	(Kumari, Kaur, Srivastava, & Sangwan, 2015)
Protease	Cross-linking	Chitosan beads	Production of gluten-eliminated beer	Gluten content was decreased from 65 to 15 mg/kg	(Benucci et al., 2020)
Amylase	Covalent binding	Chitosan	Barley malt hydrolysis	Increasing the product yield	(Raspopova & Krasnoshtanova, 2016)

Pectinase	Encapsulati-on	Polyvinyl alcohol gel	Apple juice clarification	80% turbidity reduction	(Cerreti, Markošová, Esti, Rosenberg, & Rebroš, 2017)
Pectinase	Adsorption/ cross-linking	Polymeric matrix	Apple juice clarification	Immobilized pectinase was recycled 10 times	(Rajdeo, Harini, Lavanya, & Fadnavis, 2016)
Lipase	Encapsulati-on	α-lactalbumin nanotubes	Flavor enhancement for low-fat cheeses	Immobilization enhanced the flavor of cheese	(Guan et al., 2021)
Lipase	Adsorption	Hydroxyapatite	Production of methyl acetate aroma	Immobilized lipase activity was preserved after 3 h at 60 °C	(Trbojević Ivić et al., 2016)
β-galactosidase	Covalent binding	Chitosan/silica	Lactose hydrolysis in dairy products	High efficiency of lactose hydrolysis reaching up to 62%	(Ricardi et al., 2018)
β-galactosidase	Covalent binding	Polyvinyl alcohol	Lactose hydrolysis in dairy products	High efficiency of lactose hydrolysis reaching up to 75%	(Batsalova, Kunchev, Popova, Kozhukharova, & Kirova, 1987)

The integration of immobilized lipases into food technology has significantly advanced both dairy and beverage manufacturing. In cheese production, these enzymes play a crucial role by accelerating ripening and intensifying flavor through targeted fat hydrolysis. Their function extends to butter processing, where they contribute to butterfat breakdown, enhancing texture and taste. Beyond dairy, immobilized lipases are also instrumental in flavor development within the beverage industry. By enabling the synthesis of short-chain esters—such as methyl acetate—these enzymes help generate aromatic compounds that serve as key flavoring agents.

Collectively, these diverse applications highlight the pivotal contribution of immobilized enzymes to innovation and quality enhancement across modern food and beverage systems. (Memarpoor-Yazdi, Karbalaei-Heidari, & Khajeh, 2017).

VI.1.2 Textile Industry

The textile industry, a traditional yet economically vital sector in many countries, increasingly relies on microbial enzymes to enhance efficiency and sustainability. Enzymes such as, cellulase, amylase, laccase, pectinase , and cutinase have found broad application in processes like scouring, bio-polishing and wool treatment (M. A. Hassan, Haroun, Amara, & Serour, 2013). Among them, cellulase has remained the most extensively utilized enzyme from early developments in the industry to present-day practices. However, textile processing often involves harsh conditions, including elevated temperatures and extreme pH levels, which can compromise the activity of free enzymes. To address this limitation, immobilization techniques have been adopted, enabling enzymes to function effectively under such stress while retaining their catalytic activity over multiple use cycles. A notable advancement includes the covalent attachment of cellulase to synthesized nanoparticles of polymethyl methacrylate, enhancing its stability and operational lifespan in industrial applications. (Chen, Wang, Hua, & Du, 2007).

VI.1.3 Wastewater Treatment

Heavy metal pollution represents one of the most pressing global environmental challenges. Industrial wastewater frequently contains toxic metals including chromium (Cr), lead (Pb), cadmium (Cd), zinc (Zn), nickel (Ni), arsenic (As), silver (Ag), copper (Cu), and mercury (Hg) (Abdel-Hameed, Hameed, & Ebrahim, 2007). Conventional remediation approaches primarily employ: chemical precipitation, ion-exchange separation, solvent extraction, and solid-phase extraction to mitigate matrix interference. Recent advancements have introduced biosorption technologies utilizing immobilized algal biomass, where cyanobacteria and other microbial cells selectively isolate and immobilize soluble metal species through natural bioaccumulation processes. Conversely, biopolymeric substances like carrageenan and alginate have shown promising potential in water treatment, particularly in softening applications through immobilization techniques (Figure 04). In this approach, metal ions present in water are adsorbed and immobilized onto the surface of activated biopolymer matrices, facilitating their effective removal. This environmentally friendly method leverages the natural binding properties of these polymers, offering a sustainable alternative for reducing water hardness. (Elnashar & Hassan, 2017).

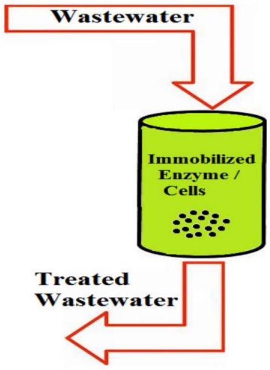

Figure 04: Wastewater treatment diagram using immobilization technology.

VI.2. Pharmaceutical Applications

Enzyme production for pharmaceutical applications constitutes a vital component of modern drug manufacturing. Research institutions worldwide have actively explored the therapeutic potential of enzymatic drugs, with nearly all major pharmaceutical research centers investigating their medicinal applications.

VI.2.1 Diabetics

Suye, Kumon, and Ishigaki (2010) demonstrated a method for immobilizing glucose oxidase onto a polycarbonate membrane modified via urethane coupling with poly(L-lysine), followed by activation using glutaraldehyde (Suye, Kumon, & Ishigaki, 2010). his immobilization approach significantly enhanced both the pH and thermal stability of the enzyme compared to its free form. Experimental comparisons revealed that traditional polycarbonate membranes adsorbed only minimal amounts of the enzyme. In contrast, the modified membranes—featuring aldehyde-functionalized surfaces—enabled strong covalent attachment of glucose oxidase, effectively preventing enzyme leakage. This stable immobilization makes the modified membrane a promising platform for use in glucose sensing technologies. (Mohammadi, Rezaei Mokarram, Ghorbani, & Hamishehkar, 2019)

VI.2.2 Biomedical Analysis

Enzyme immobilization has enabled the development of highly selective and accurate analytical methods for detecting a wide range of biochemical compounds. These assays operate on a fundamental principle: the interaction between a specific substrate and its corresponding immobilized enzyme. The effectiveness of the assay is determined by measuring either the increase in product concentration or the depletion of the substrate during the reaction(Maslova, Senko, & Efremenko, 2018). Table 03 show a list of some examples.

Table 03: Immobilized enzymes used in biomedical analysis.

Immobilized Enzyme	Substance Assayed	References
Glucose oxidase	Glucose	(Ren et al., 2006)
Urease	Urea	(Helman, Pacheco-Colón, & Gropman, 2014)
Cholesterol oxidase	Cholesterol	(R. Singh, Kumar, Mittal, & Mehta, 2016)
Lactate dehydrogenase	Lactate	(Makler, Piper, & Milhous, 1998)
Alcohol oxidase	Alcohol	(Edalli et al., 2016)
Hexokinase	ATP	(O'Driscoll, 1976)
Galactose oxidase	Galactose	(Fujiwara, Yokoi, & Nakajima, 2016)
Penicillinase	Penicillin	(M. Hassan et al., 2012)
Ascorbic acid oxidase	Ascorbic acid	(Garman, 2007)
L-Amino acid oxidase	L-Amino acids	(Tamer, Omer, & Hassan, 2016)
Cephalosporinase	Cephalosporin	(M. Hassan et al., 2012)

Chapter II
Nanotechnology

I. Nanotechnology

Nanotechnology represents both the scientific discipline and engineering practice of precisely controlling matter at the nanoscale (approximately 1/100,000th the width of human hair) to develop novel materials and technologies with transformative societal impacts (Roszek, Jong, & Re, 2005). More specifically, nanotechnology encompasses: the deliberate design, precise characterization, controlled fabrication and targeted application of functional structures, devices, and systems through nanometer-scale manipulation of size and morphology. Complementary to this, nanoscience involves the fundamental study of material properties at atomic (0.1-1 nm), molecular (1-100 nm), and macromolecular (100-1000 nm) scales, where observed phenomena markedly diverge from bulk material behavior.

The conceptual foundations of nanotechnology emerged in 1959 when physicist Richard Feynman delivered his seminal lecture "There's Plenty of Room at the Bottom" at the American Physical Society annual meeting. In this groundbreaking presentation, Feynman proposed revolutionary concepts for manipulating and imaging matter at atomic scales using nanoscale machinery. The field gained its formal nomenclature in 1974 when Professor Norio Taniguchi of Tokyo Science University first introduced the term "nanotechnology" to describe precision engineering at the nanometer scale.(Haleem, Javaid, Singh, Rab, & Suman, 2023).

II. Nanotechnology Applications

II.1. Nanotechnology and Food Industry

Nanotechnology has introduced transformative capabilities across various sectors of the food industry, ranging from production and packaging to quality control and targeted delivery systems (Yu et al., 2018). One significant application involves the use of polymer or clay nanocomposites in food packaging, offering superior resistance to environmental factors due to their excellent barrier properties (Huang, Wang, Zhu, Seeger, & Chu, 2022). In addition, nanoparticle formulations function as antimicrobial agents, helping to extend shelf life by preventing microbial spoilage—particularly in canned and preserved food products. Advanced nanosensors and nanoassembly-based diagnostic tools have also been developed to detect microbial contamination during storage and processing stages (Biswas et al., 2022). Moreover, nanoassemblies are capable of identifying trace gases, organic and inorganic pollutants, and even microscopic pathogens, making them valuable assets in ensuring food safety and quality (Rashidi, 2021).

The global dairy sector is undergoing significant transformation through the integration of nanotechnology (T. Singh et al., 2017). Emerging innovations in this field are enhancing various aspects of dairy production, including more efficient processing systems, improved interaction between ingredients, higher product yields, extended preservation periods, and increased safety standards (Hamad, Han, Kim, & Rather, 2017). Packaging techniques have also seen marked improvements, with materials offering superior performance and protection. Furthermore, the use of nanocarrier systems is gaining traction for delivering functional ingredients—such as bioactive compounds, therapeutic agents, intensified flavors, coloring agents, and aroma enhancers—directly into dairy formulations, enriching both their nutritional value and sensory appeal. (Chellaram et al., 2014)

II.2. Nanotechnology in the Medical Field

The use of nanoscale technologies in diagnostic medicine is rapidly advancing, enabling earlier and more accurate detection of diseases, which is critical for guiding subsequent clinical interventions. Nanotechnological approaches are also being applied to study disease susceptibility at the molecular and cellular levels, offering valuable perspectives for personalized treatment strategies (Dessale, Mengistu, & Mengist, 2022). As research progresses, nanotech-based innovations promise to transform medical diagnostics by significantly enhancing test precision, sensitivity, and turnaround time (Fox, Tran, Nguyen, Nguyen, & Tran, 2019). One notable development in this area is the emergence of advanced biosensors, made possible by nanomaterials, which can identify minute concentrations of biological markers in body fluids such as urine and blood. These ultra-sensitive tools are instrumental in supporting early diagnosis and proactive disease management(Xu, Tan, Liao, & Wang, 2021).

Advancements in nanotechnology have significantly transformed drug delivery systems, allowing for precise targeting of therapeutic agents while reducing adverse effects and enhancing overall treatment outcomes. In this approach, engineered nanoparticles serve as carriers, guiding pharmaceutical compounds directly to specific biological sites where intervention is needed. This strategic delivery not only improves drug bioavailability but also maximizes its therapeutic potential by concentrating the effect at the intended location. (Sahu et al., 2021). Nanotechnology offers a range of benefits in the realm of pharmaceutical delivery systems. One major advantage lies in its capacity to direct therapeutic agents precisely to affected regions—such as tumor sites, areas of inflammation, or infections—thereby reducing off-target exposure and limiting adverse effects (Sahu et al., 2021). Additionally, the incorporation of drugs into nanoparticle carriers can significantly enhance their chemical stability and aqueous solubility, improving their clinical effectiveness (Oroojalian et al., 2020). Moreover, nano delivery platforms contribute to improved drug absorption and distribution within the body, which in turn increases bioavailability. This efficiency often allows for lower dosages, decreasing the risk of systemic toxicity. (Enrico, 2019)

III. Green Synthesis of Metal Oxide Nanoparticles

Green synthesis has emerged as a promising approach within bio-nanotechnology, offering both environmentally sustainable and cost-effective alternatives to traditional chemical and physical fabrication methods. This technique relies on the use of non-toxic, biologically compatible agents that are safe for both human health and the environment. A diverse range of naturally derived sources—including plant-based extracts, microbes such as yeast and fungi, bacterial strains, algae, and other biological materials—have been explored for their potential in facilitating the synthesis of metal oxide nanoparticles. (Mtibe, Mokhothu, John, Mokhena, & Mochane, 2018).

IV. Factors involved in the green synthesis of nanoparticles

As with other synthesis approaches, factors like reaction temperature, acidity or alkalinity levels (pH), and duration of the reaction significantly influence the morphology, dimensions, and overall production efficiency of the resulting nanoparticles. (Makarov et al., 2014).

Temperature: plays a critical role in nanoparticle synthesis, significantly affecting both particle morphology and production efficiency. Variations in thermal conditions influence how reactants interact, which in turn dictates the final shape, ranging from spherical and prismatic to flake-like, triangular, or octahedral structures. Elevated temperatures generally accelerate reaction kinetics and increase the formation of nucleation sites, thereby enhancing overall yield. Furthermore, the extent of thermal input not only governs particle shape but also contributes to size enlargement, with higher temperatures typically leading to the generation of larger nanoparticles. (Thanh, Maclean, & Mahiddine, 2014).

pH: is a crucial parameter that directly impacts the formation of nucleation sites during nanoparticle synthesis. Higher pH levels often result in an increased number of these sites, influencing both the quantity and quality of the particles formed. Additionally, the pH environment determines the feasibility of synthesizing specific types of nanoparticles, as certain materials require strictly acidic or basic conditions. For instance, magnetic nanoparticles are typically produced in alkaline settings, whereas metal oxides are more commonly synthesized in neutral to acidic media. (Handayani, Ningrum, & Imawan, 2020).

Time: Reaction duration is a key variable influencing the final characteristics of nanoparticles, particularly their size. Extended synthesis times generally lead to larger particle dimensions and greater product yield, as the prolonged exposure allows more sustained interaction among the reacting species. This extended contact enhances the growth phase of nanoparticles, contributing to both size expansion and increased synthesis efficiency. (De Oliveira et al., 2020).

V. Copper (Cu) Nanoparticle

Copper-based nanoparticles have shown significant promise in the biomedical field due to their potent antimicrobial properties, including antifungal, antibacterial, and antiviral effects (Ali et al., 2021). As an essential trace element, copper plays diverse physiological roles in the human body—contributing to the integrity of skin and blood vessels, supporting connective tissue function, and facilitating the synthesis of hemoglobin, melanin, myelin, and proper thyroid activity (Palecek, 2020). Beyond their biological significance, copper nanoparticles also exhibit a wide range of functional characteristics such as electrical conductivity, magnetic responsiveness, mechanical durability, and thermal stability. These properties make them highly suitable for applications like antimicrobial coatings on surgical instruments, water purification systems, and thermal management technologies (Mohamed, 2020)

Extensive research supports the effectiveness of copper nanoparticles as potent antiviral agents (Jahan, Erci, & Isildak, 2021). In particular, eco-friendly synthesis methods have yielded particles approximately 160 nm in size that exhibit strong inhibitory effects against the influenza virus, primarily through the suppression of viral protein expression. This antiviral property has led to their incorporation in protective items such as face masks and antimicrobial kitchen fabrics. Additionally, smaller spherical copper nanoparticles—averaging 39.3 nm in diameter and applied in concentrations between 40 and 120 µg/mL—have demonstrated significant cytotoxicity within 24 hours against human skin carcinoma (B16F10) and normal mouse fibroblast (NiH3T3) cell lines. (Edis, Haj Bloukh, Ashames, & Ibrahim, 2019).

VI. Silver (Ag) Nanoparticle

Silver nanoparticles (AgNPs), broadly studied within the 1–100 nm size range, have emerged as a promising alternative for enhancing biomedical applications, including drug delivery, wound healing, tissue scaffolding, and protective coatings. Their notably high accessible surface area facilitates efficient ligand binding, while their inherent antimicrobial properties—historically recognized in silver nitrate formulations—make them a unique and rapidly advancing solution against pathogenic microbes. AgNPs exhibit significant physical, chemical, and biological advantages, such as broad-spectrum antimicrobial activity, anticancer potential, and therapeutic versatility. Additionally, their capacity to form diverse nanostructures, coupled with cost-effective production, further underscores their utility in medical and industrial contexts. (Cadinoiu et al., 2022; Safaya & Rotliwala, 2022)

Numerous studies have demonstrated that silver nanoparticles possess potent antibacterial activity against a broad spectrum of pathogenic bacteria, including *Escherichia coli*, *Staphylococcus aureus*, *Salmonella typhimurium*, *Pseudomonas aeruginosa*, *Vibrio cholerae*, and *Bacillus subtilis*. (Azeem, Ahmed, Shaban, & Elsayed, 2022; Kanniah et al., 2022).

VII. Gold (Au) Nanoparticle

Gold nanoparticles produced through green synthesis are derived from natural sources and exhibit both chemical stability and thermal resilience. These eco-friendly nanoparticles can be effectively conjugated with photosensitizing agents, enabling their use in photodynamic antimicrobial therapy (V. Kumar, Shriram, Shukla, & Gosavi, 2022; Shivaramakrishnan, Gurumurthy, & Balasubramanian, 2017). Notably, such biosynthesized AuNPs have demonstrated efficient catalytic activity without requiring additional capping agents or toxic carriers. This characteristic enhances their suitability for biomedical applications, particularly in facilitating drug and gene delivery systems. (Y. Liu et al., 2022). AuNPs exhibit unique properties that make them valuable for biomedical applications. Their gold core stabilizes molecular assemblies through monolayer surface modifications, enabling precise control over surface characteristics such as charge distribution and hydrophobicity. A key functional feature of AuNPs is their ability to form stable thiol linkages, which facilitates efficient intracellular release mechanisms (Karuvantevida et al., 2022). These nanoparticles offer tunable physical properties, as their performance characteristics can be systematically modified by adjusting size, shape, and aspect ratio. Importantly, AuNPs demonstrate excellent biocompatibility and minimal toxicity, making them ideal candidates for drug delivery and gene therapy applications. Their diagnostic potential is particularly noteworthy, with demonstrated efficacy in detecting and diagnosing various conditions including cardiovascular diseases, malignancies, and infectious pathogens. (Aminabad, Farshbaf, & Akbarzadeh, 2019).

VIII. Polysaccharide-Based Nanoparticles

Nanoparticles engineered from natural biopolymers, particularly proteins and polysaccharides, have emerged as effective carriers for bioactive compounds. These systems are fundamentally characterized as solid colloidal particles with a size distribution typically spanning 1 to 1000 nanometers in diameter. Their biopolymeric composition offers distinct advantages for bioactive encapsulation and delivery, combining the biocompatibility of natural materials with the tunable physical properties of nanoscale systems. (Nagpal, Singh, & Mishra, 2010).

The growing scientific interest in renewable polysaccharide-based nanoparticles as advanced biomaterials has attracted significant attention across multiple disciplines, including biomedicine, bioengineering, pharmaceutical sciences, chemistry, and materials science. Polysaccharides have become increasingly important for designing protective nanoparticle delivery systems for bioactive compounds and nutrients, owing to their remarkable capacity to form stable supramolecular assemblies. These natural polymers offer numerous advantages as biopolymeric precursors, including inherent biocompatibility, tunable biodegradability, potential bioactive properties in certain cases, and cost-effectiveness due to their abundant natural sources such as plant-derived materials and crustacean exoskeletons. These characteristics make polysaccharide nanoparticles highly suitable for diverse industrial applications (Salatin & Yari Khosroushahi, 2017). Polysaccharide-derived nanomaterials have found wide-ranging applications across fields such as food preservation, functional food delivery, packaging, wound care, pharmaceuticals, biomedical engineering, and cosmetic formulations. Their molecular backbone, rich in reactive functional groups, supports straightforward chemical modification, enabling the fabrication of nanoparticles with diverse architectures. Among these, polysaccharide-based nanocarriers and nano-hydrogels are especially prominent in the targeted delivery of nutraceuticals and therapeutics, as well as in bioimaging and tissue engineering. Additionally, their ability to undergo reversible self-assembly—mediated by hydrophobic interactions and hydrogen bonding—makes them ideal for constructing stimuli-responsive systems.(Jaiswal, Limayem, & Shankar, 2022)

VIII.1. Alginate

Alginate (ALG) is a naturally occurring polyanionic linear polysaccharide extracted from the cell walls of marine brown algae. Its chemical structure consists of (1→4)-linked α-L-guluronic acid and β-D-mannuronic acid residues. A distinctive property of ALG is its capacity for ionotropic gelation in the presence of divalent cations (e.g., Ca^{2+}, Ba^{2+}, Al^{3+}), which occurs through coordination between the metal ions and carboxylate groups of guluronic acid residues, forming stable electrostatic crosslinks. This biopolymer exhibits three key characteristics that make it particularly valuable for therapeutic applications: mucoadhesive properties, inherent biocompatibility, and controlled biodegradability. These attributes have established ALG as a promising material for pharmaceutical and biomedical uses, especially in controlled drug delivery systems. (Anis et al., 2021).

Alginate has been widely employed in enzyme immobilization systems, demonstrating particular effectiveness in three principal formulations: xanthan-alginate composite beads, alginate-polyacrylamide hybrid gels, and calcium alginate beads. These systems consistently exhibit enhanced enzymatic activity and improved reusability compared to free enzymes. The stability of immobilized enzymes can be further optimized through dual cross-linking approaches involving both divalent cations (particularly Ca^{2+}) and glutaraldehyde, which synergistically reinforce the alginate matrix structure. (Flores-Maltos et al., 2011).

VIII.2. Starch

Starch is composed of α-D-glucopyranose units organized into two distinct structural forms: (1) linear amylose chains connected by α(1→4) glycosidic bonds, and (2) branched amylopectin with additional α (1→6) linkages extending from the linear backbone. As a natural polysaccharide, starch offers multiple advantages as a nanomaterial precursor, being safe, cost-effective, renewable, and biodegradable, with wide availability across plant species (Le Corre, Bras, & Dufresne, 2010). For enzyme immobilization, starch has demonstrated particular utility in calcium alginate-starch composite systems. When used for bitter gourd peroxidase immobilization, these hybrid supports exhibit complementary advantages depending on the immobilization approach: entrapped enzymes show enhanced stability against denaturants (e.g., urea) due to protective interactions with carbohydrate moieties, while surface-immobilized enzymes maintain higher catalytic activity. (Matto & Husain, 2009). One of the commonly adopted industrial strategies for enhancing product yield involves the radiation-induced grafting of monomers such as acrylamide and dimethylaminoethyl methacrylate onto starch-based substrates. (Raafat, Araby, & Lotfy, 2012).

Experimental Part

Chapter I
Materials & Methods

I. Green Synthesis of Nanoparticles

I.1 Synthesis of Starch-Copper Nanoparticles (St-CuNPs)

Using corn starch as a capping agent and copper (II) sulfate pentahydrate as a precursor salt, the Cu nanoparticles were created via a chemical reduction method. The first step in the preparation process is to add 0.1 M copper (II) sulfate pentahydrate solution to 120 mL of 1.2% starch solution, stirring vigorously for 30 minutes. The synthesis solution is mixed continuously and quickly while 50 mL of a 0.2 M ascorbic acid solution is added in the second stage. The resulting solution was then heated to 80°C for two hours while 30 mL of a 1 M sodium hydroxide solution was gradually added and constantly stirred. The solution changed from yellow to ocher in color. Following the reaction's completion, the mixture was removed from the heat source and let to settle for the entire night before the supernatant solution was carefully disposed of. To remove the excess starch bonded to the nanoparticles, the precipitates were filtered out of the solution and then three times rinsed with deionized water and ethanol (Khan, Rashid, Younas, & Chong, 2016)

I.2. Synthesis of Alginate-Copper Nanoparticles (Alg-CuNPs)

Copper nitrate (0.1 M, Cu $[NO^3]^2$) was completely dissolved in 100 mL of nanopure water under magnetic stirring. Then this solution was heated to the synthesis temperature (80°C). Once the synthesis temperature was reached, 50 mL of ascorbic acid solution (containing the proper quantities of reducing agent) was added to the hot solution and stirred continuously. After ascorbic acid addition, the blue solution turned dark green, thus indicating the immediate nucleation of CuNPs. Finally, the colloidal dispersions were deposited onto NaAlg and heated for 1 hour (88°C) (Díaz-Visurraga et al., 2012)

I.3. Synthesis of Starch-Silver and Alginate-Silver Nanoparticles (St-AgNPs, Alg-AgNPs)

In a typical experiment, 85 mg of soluble starch or sodium alginate was dissolved in 25 mL of distilled water at 85˚C for 30 min. 10 mL of a 6.10^{-2} M silver nitrate was added into 25 mL of hot aqueous solution under vigorous stirring away from light. Then 15 mL of a glucose solution (0.12 M) was added into the reactive system, which was held at 85 ± 0.5˚C with 700 rpm stirring. A magnetic stirrer was used to maintain a constant stirring throughout the reaction process. The obtained colloidal suspension was cooled down at room temperature after 04 hours reaction time and characterized. To avoid any photochemical reactions, all colloidal dispersions were kept in a dark place (Jain, Pawar, Sarkar, Junnuthula, & Dyawanapelly, 2021).

II. Characterization of Nanoparticles

To confirm the functional groups involved in the formation and stabilization of the nanoparticles, Fourier Transform Infrared Spectroscopy (FTIR) was performed in the range of 4000–400 cm^{-1}. Surface morphology and particle size were analyzed using Scanning Electron Microscopy (SEM), which provided visual evidence of particle shape, size distribution, and degree of agglomeration. The crystalline structure and phase composition of the nanoparticles were investigated using X-ray Diffraction (XRD). Diffraction patterns were recorded using Cu Kα radiation (λ = 1.5406 Å) over a 2θ range of 10° to 80°. The observed peaks were compared with standard data from the Joint Committee on Powder Diffraction Standards (JCPDS) to confirm the formation of crystalline silver and copper nanoparticles.

III. Invertase Immobilization on Starch-Copper Nanoparticles

III.1. Extraction of Invertase Enzyme

The study of (Ferreira, Rossler, Toralles, Ruiz, & Rombaldi, 2018) presented the autolysis approach used to extract invertase. 40 mL of 100 mM $NaHCO_3$ was added to 10 g samples of lyophilized yeast, and the mixture was stirred for 24 hours at 200 rpm and 35–40°C in an orbital shaker, next, the sample was centrifuged for five minutes at 5000 rpm, the liquid supernatant was named raw extract (RE) because it included invertase that had been liberated by autolysis. The protein content was then measured using Bradford's technique (Pedrol & Tamayo, 2001). RE was kept in storage at -20°C.

III.2. Invertase Activity

The reaction medium contained 1.0 mL of enzyme source, 1.0 mL of buffers (pH 5.0), and 1.0 mL of 120 mM sucrose solution as substrate, in the blank test, the substrate was replaced with 1.0 mL of water, the reaction was conducted at 25°C and pH 5.0. Using glucose as a standard, 3,5-DNS (3,5-dinitrosalicylic acid, Inlab) was used to determine the amount of RS, equal volumes of sample and DNS reagent were mixed (300 µL each, 1:1 ratio), heated, and after 10 minutes the absorbance was subsequently measured using a microplate reader at a transmittance of 490 nm (Miller, 1959).

III.3. Preparation of Immobilized Invertase Enzyme System

Enzyme source solution (2 mL) was kept in a 30 mL tube with 2 mL of concentrated starch CuNPs to create immobilized enzyme. Using buffer solution, the volume was increased to 10 mL, fully mixed, and rotated at a steady 500 rpm. The samples were centrifuged after four hours, and the resulting immobilized enzyme was then rinsed twice with distilled water and stored in a refrigerator at 4°C for additional research (H R, Hosamani, D N, & Sneharani, 2020). In order to compute the immobilization yield (IY), which was determined by Eq. (1), the free and immobilized invertase were subjected to protein estimation by the Bradford method (Pedrol & Tamayo, 2001);

$$IY\ (\%) = \frac{C1 - C2}{C1} \times 100 \qquad \textbf{Eq. (1)}$$

where C1 represents the protein concentration added during immobilization and C2 represents the protein concentration found in the supernatant following immobilization.

III.4. Optimization of Invertase Immobilization and activity

III.4.1 Effect of Experimental Parameters on Immobilization Efficiency

At a pH of 7 and 20°C, the impact of time on immobilization efficiency was assessed throughout a range of time intervals (2–18 hours). In a buffer solution with a pH range of 6 to 10 (phosphate buffer for 6,7 pH, Tris-HCl for 8,9 pH and carbonate bicarbonate for10 pH), the impact of pH on immobilization efficiency was assessed at 20°C. The 20–50 °C temperature range was used to assess the impact of temperature. By adjusting the concentration between 0.5 and 7%, the impact of St-CuNPs concentration on immobilization was evaluated. To choose the ideal parameter for the experiment, we rely on the activity of the immobilized enzyme. Following each experiment, we fix the optimal parameter.

III.4.2 Effect of pH and Temperature on free and immobilized enzyme activity

The impact of pH on invertase activity was assessed at 25°C using sodium acetate buffer (20 mM) in the 3.5–5.5 pH range. All further testing were conducted using the pH that was determined to be ideal. With the use of a temperature-controlled water bath, the impact of temperature on the activity of free and immobilized invertase was assessed between 30°C and 50°C.

III.5. Reusability of immobilized enzyme

Since immobilized invertase can be utilized repeatedly for many batch processes without significantly losing activity for the initial batches, its reusability was investigated. We assessed the immobilized enzyme's reusability under the best possible circumstances. The immobilized invertase was recovered by centrifugation after each enzyme test cycle, repeatedly cleaned with distilled water, and utilized to measure the activity of the enzyme.

IV. Rennet Immobilization on Alginate-Copper Nanoparticles

IV.1. Rennet Extraction:

The extraction was carried out according to the protocol used by (Wangoh, Farah, & Puhan, 1993).The camel abomasum was cut into slices (1 cm^2), a maceration is made in a 6% NaCl solution (1:10 w/v) containing 2% boric acid. The mixture was then filtered and centrifuged. The pH of the supernatant was then lowered to 4.7 and the extracts were kept at 25°C. The pH was then increased to 5.5, followed by a final centrifugation. The protein content was then measured using Bradford's technique (Pedrol & Tamayo, 2001). The enzyme extract was stored at (-18°C) until use.

IV.2. Preparation of immobilized rennet enzyme system

Immobilized enzyme was prepared by adding 2 mL of enzyme extract to 2 mL of concentrated alginate CuNPs. The volume was made up to 10 mL using tartaric buffer solution (tartaric acid / hydrogen-tartarate), mix thoroughly and kept under stirring at constant speed 500 rpm. After four hours, the samples were centrifuged and rinsed 3 times with distilled water after that the prepared immobilized enzyme was kept in a refrigerator at 4°C for further studies (H R et al., 2020).

IV.3. Efficiency of rennet immobilization

The efficiency of immobilization process was evaluated by determining the coagulant activity of the immobilized rennet. Coagulant activity (CAU) or rennet unit RU is defined by the quantity of enzyme contained in 1ml of enzymatic solution which can coagulate 10ml of BERRIDGE substrate (Berridge, 1995) in 100s at 30°C (Andrén, 2002). The technique consists of adding to the milk, 1ml of the enzymatic extract followed by homogenization (3 turns), then noting when visible casein flakes are formed on walls of the test tube (Mahaut, Jeantet, & Brulé, 2003)

IV.4. Berridge substrate

Skimmed milk powder (12 g) was used for Berridge substrate preparation (100 mL) which is dissolved in 100 mL of $CaCl_2$ solution (0.01 M). The pH of the prepared milk solution was adjusted to 6.4 with HCl or NaOH (1N) solutions.

IV.5. Optimization of rennet enzyme immobilization using Response Surface Methodology

The influence of key independent variables: pH (X_1), temperature (X_2), and the concentration of Alg-CuNPs (X_3), on the response outcomes of coagulant activity (Y_1) and protein concentration (Y_2) in immobilized rennet was systematically evaluated using Response Surface Methodology (RSM). Table 04 outlines the RSM design, incorporating both coded and actual (uncoded) factor levels. A central composite design (CCD) with five levels and a quadratic model framework was employed to structure the experimental runs. In total, twenty experimental treatments were executed in a randomized sequence, comprising six axial points, eight factorial points at fractional levels, and six replicates at the center point. The conversion of actual values of the independent variables into coded levels was carried out using the equation provided Eq.(2).

$$Z= Z_0 - Z_C /\Delta Z \qquad \textbf{Eq. (2)}$$

Where Z demonstrate the coded value of an independent variable, while Z_0 represents its corresponding actual level. The symbol ΔZ refers to the incremental change or step size between levels, and Z_C signifies the actual value at the central level of the experimental range.

Table 04: Independent variables and their corresponding levels for rennet immobilization.

Independent variable	Symbol	Coded levels				
		-alpha	-1	0	+1	+alpha
pH	X1	2.16364	2.3	2.5	2.7	2.83636
Temperature (°C)	X2	17.18	24	34	44	50.81
Alg-CuNP Concentration (%)	X3	1.29552	3	5.5	8	9.70448

To visualize the interactions among independent variables and their effects on the responses, 3D response surface plots and contour plots were generated. These plots helped in identifying optimal regions for both coagulant activity and protein concentration.

Furthermore, numerical optimization was carried out using the desirability function approach within the same software, targeting maximum coagulant activity and protein retention. The optimal conditions were selected based on the highest composite desirability score.

IV.6. Thermal Stability

In order to determine the thermal stability of free and immobilized rennet, the enzymes were incubated at different temperatures (30-60 °C) for 24 h. After that, enzymes were cooled immediately and then assayed at standard conditions to determine the coagulant activity.

IV.7. PH Stability

For the pH stability of immobilized rennet, the enzyme was incubated in different pH values using the 50 mM buffer solutions in acidic (sodium citrate, pH 4 and 5), neutral (sodium phosphate, pH 6 and 7), and basic (Tris/HCl, pH 8.0) pH ranges, at 4 °C for 24h. Then the remaining activity was estimated using the standard activity assay procedure.

IV.8. Storage stability of enzymes

The storage stability of free and immobilized rennet was investigated by measuring the coagulant activity after storage at 4 °C every 7 days for a period time of 6 weeks.

V. Biological Activity of Silver Nanoparticles

V.1. Antioxidant Activity Assays

V.1.1 FRAP Assay

The antioxidant capacity of the samples was evaluated using the ferric reducing antioxidant power (FRAP) assay, as outlined by (Rahman, Islam, Biswas, & Khurshid Alam, 2015). This method is based on the reduction of ferric ions (Fe^{3+}) to ferrous ions (Fe^{2+}), which subsequently form a blue-colored Prussian complex upon reaction with ferric chloride ($FeCl_3$). The intensity of the color, indicative of antioxidant activity, was quantified spectrophotometrically at 700 nm.

To perform the assay, 500 µL of the sample was combined with 1.25 mL of phosphate buffer (0.2 M, pH 6.6) and 1.25 mL of 1% potassium ferricyanide ($K_3Fe(CN)_6$). This mixture was incubated in a water bath at 50°C for 20 minutes. The reaction was halted by adding 1.25 mL of 10% trichloroacetic acid (TCA), followed by centrifugation at 3000 rpm for 5 minutes. After centrifugation, 1.25 mL of the clear supernatant was transferred into a clean tube, mixed with an equal volume (1.25 mL) of distilled water and 250 µL of 0.1% $FeCl_3$ solution. Absorbance was then recorded at 700 nm using a UV-VIS spectrophotometer, with a blank serving as the control.

$$\text{FRAP (\%)} = 100 - \frac{\text{OD controle}}{\text{OD sample}} \times 100$$

V.1.2 DPPH Assay

A DPPH radical scavenging assay was employed to determine, by a spectroscopic method, relative nanoparticle antioxidant ability. Different concentrations of St-AgNPs, Alg-AgNPs, and ascorbic acid were prepared in distilled water. A DPPH solution (0,1 mM) was prepared in ethanol. Thereafter, from each working solution 20 µl was mixed with 160 µl of the reagent solution and 20 µL of H2O in separate test tubes and vortexed thoroughly. The reaction mixture was incubated in dark place at 37 °C for 15 min. Sample absorbance was read at 517 nm, as described in (R. Singh, Singh, Saini, & Rao, 2008)

$$\text{Inhibition percentage (\%)} = \frac{\text{OD control} - \text{OD sample}}{\text{OD control}} \times 100$$

V.2. Anti-inflammatory Activity Assays

V.2.1 Protein denaturation assay

To assess anti-inflammatory activity, the reaction mixtures were prepared using varying concentrations of nanoparticle samples along with 1% bovine serum albumin (BSA). The mixtures were incubated at room temperature for 30 minutes. Following incubation, the pH was carefully adjusted to 2.0 by the gradual addition of concentrated hydrochloric acid (HCl). The acidified samples were then heated at 72 °C for 30 minutes. After allowing the mixtures to cool to room temperature, the degree of protein denaturation inhibition was determined by measuring absorbance at 660 nm using a UV-Visible spectrophotometer. Diclofenac served as the reference standard in this assay, as reported by (Djouadi & Derouiche, 2021). The inhibition efficiency was expressed in terms of IC_{50} values, calculated from the inhibition percentage (IP) using the following formula:

$$\text{Inhibition percentage (\%)} = \frac{\text{OD control} - \text{OD sample}}{\text{OD control}} \times 100$$

V.2.2 Hemolysis assay

The hemolytic activity of the test samples was evaluated following the protocol established by (Djouadi & Derouiche, 2021). Fresh human red blood cells (RBCs) were collected in tubes containing EDTA to prevent clotting. The samples were centrifuged to separate plasma, and the packed RBCs were subsequently washed three times with 150 µL of phosphate-buffered saline

(PBS) to obtain a concentrated erythrocyte suspension. From this suspension, 50 µL was combined with 100 µL of the test samples. PBS (1X) served as the active control. The mixtures were incubated at 37 °C in a water bath for one hour. To bring the final volume to 1 mL, 850 µL of PBS was added. Following incubation, the samples were centrifuged at 3000 rpm for 3 minutes, and the absorbance of the released hemoglobin in the supernatant was measured at 560 nm using a UV-Vis spectrophotometer.

The degree of hemolysis inhibition was expressed as a percentage, calculated using the following formula:

$$\text{Hemolysis inhibition (\%)} = 100 - \frac{\text{OD sample}}{\text{OD control}} \times 100$$

VI. Statistical Analysis

All experiments were conducted in triplicate, and results were expressed as mean ± standard deviation (SD). The optimization of rennet immobilization process, was performed using Response Surface Methodology (RSM) through the Design-Expert software (Version 12.0.3.0, Stat-Ease Inc., USA), which enabled the analysis of variable interactions and the generation of predictive models. Analysis of variance (ANOVA) was employed to evaluate the significance of the models and individual terms at a 95% confidence level ($p < 0.05$). Graphical representation and additional statistical treatment of data were performed using Microsoft Excel and OriginPro 2018 (OriginLab Corporation, USA).

Chapter II
Results

I. Characterization of Copper and Silver Nanoparticles

I.1. scanning electron microscopy (SEM) and size distribution

The scanning electron microscopy image (Figure 05 a) of the synthesized Alg-CuNPs reveals an aggregated, irregular surface morphology with particles exhibiting varied shapes and rough textures. The accompanying histogram (Figure 05 b) provides a quantitative size distribution of the nanoparticles. It shows that the majority of particles fall within the 100–300 nm range, the mean particle size was determined to be 152 nm.

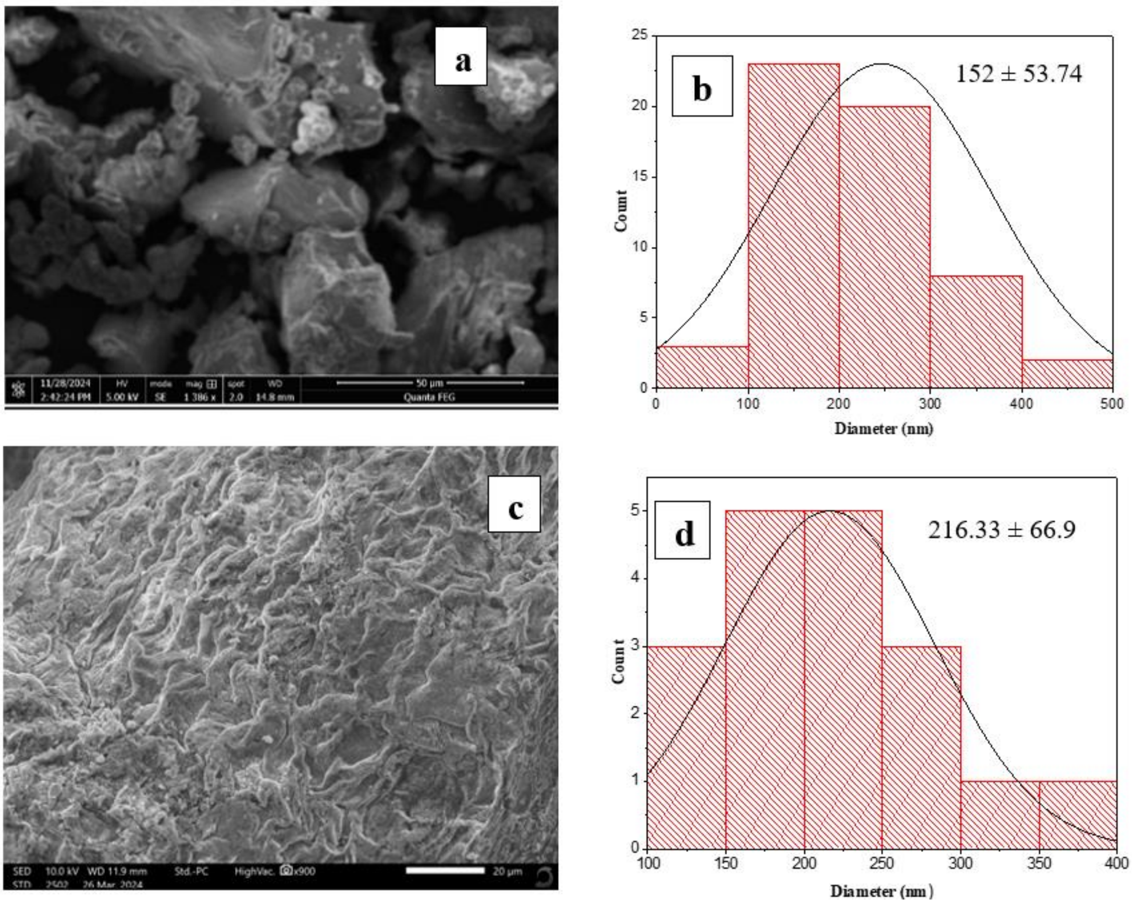

Figure 05: (a) SEM image and (b) particle size distribution histogram of alginate-copper nanoparticles; (c) SEM image and (d) particle size distribution histogram of starch-copper nanoparticles.

The SEM micrograph of St-CuNPs (Figure 05 c) reveals an irregular, wrinkled surface structure, indicating successful incorporation of the copper nanoparticles within the starch matrix. The image shows a relatively uniform distribution of particles with no significant signs of agglomeration. SEM analysis revealed that the majority of St-CuNPs had the size ranging from 150 nm to 250 nm with a mean size of 216.33 nm (Figure 05 d).

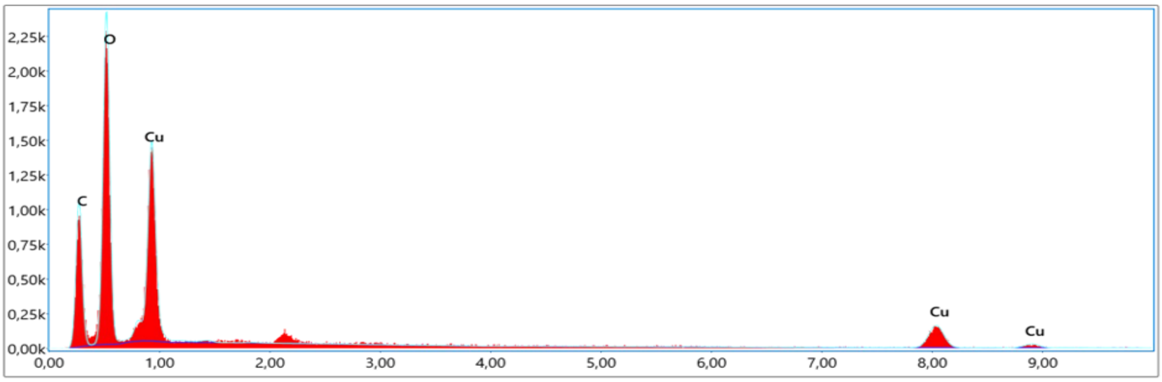

Figure 06: EDX spectrum of starch-copper nanoparticles.

The EDX spectrum (Figure 06) further confirmed the elemental composition of the sample. Strong signals corresponding to copper (Cu) were detected, confirming the successful synthesis of copper nanoparticles. Additionally, signals for carbon (C) and oxygen (O) were also observed, which are characteristic of the starch biopolymer used as a stabilizing and reducing agent. The presence of these elements supports the hypothesis that starch effectively capped the nanoparticles and contributed to their stability.

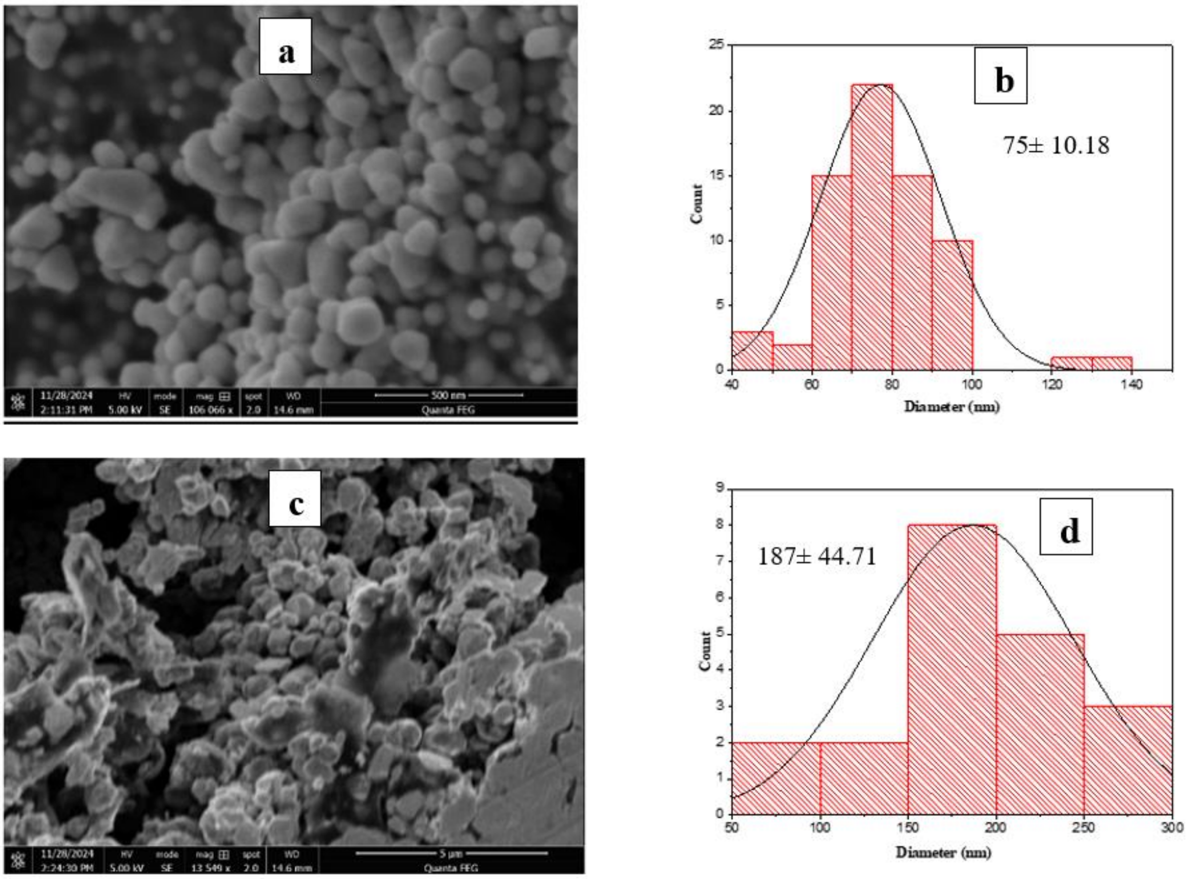

Figure 07: SEM images and particle size distribution histograms of alginate silver nanoparticles (a, b) and starch silver nanoparticles (c, d)

The surface morphology and size distribution of the synthesized Alg-AgNPs are shown in Figure (07 a, b). SEM images revealed that the nanoparticles predominantly exhibit a spherical to slightly irregular shape. The corresponding size distribution histogram showed that most nanoparticles ranged between 60 nm and 100 nm in diameter, with a mean size of 75 nm.

The SEM micrograph of St-AlgNPs (Figure 07 c) reveals a relatively aggregated structure with particles exhibiting a predominantly spherical to quasi-spherical shape with the most particle diameters ranging from approximately 150 nm to 250 nm (Figure 07 d). St-AlgNPs size was measured to be 187 nm.

I.2. Fourier Transform Infrared (FTIR) Spectroscopy

The FTIR spectrum of starch (Figure 08 C) exhibited a broad absorption band around 3250 cm^{-1}, which corresponds to the O–H stretching vibrations due to inter- and intramolecular hydrogen bonding of hydroxyl groups, this pic was shifted to 3253 cm^{-1} in St-AgNPs (Figure 08 B) and 3204 cm^{-1} in St-CuNPs (Figure 08 A) with a reduced intensity in both of them. A peak near 2920 cm^{-1} is assigned to C–H stretching vibrations of $–CH_2$ groups of starch was disappeared in St-AgNPs spectrum and reduced in intensity in St-CuNPs spectrum. The band observed at 1630 cm^{-1} in starch spectrum is related to O–H bending of absorbed water molecules, was shifted to 1749 cm^{-1} and 1611 cm^{-1} in St-AgNPs and St-CuNPs respectively. A pic appeared at 1320 cm^{-1} in starch spectrum concern C–H bending vibrations and O–H bending coupled to C–O vibration was shifted to 1340 cm^{-1} in St-CuNPs and disappeared in St-AgNPs. Strong band at 994 cm^{-1} in starch represent C–O–C and C–O stretching vibrations of the polysaccharide skeleton with reduced intensity and shifting to 990 $cm^{-1}$and 998 cm^{-1} for St-AgNPs and St-CuNPs respectively. some peaks around 550 cm^{-1} in starch are attributed to skeletal vibrations of the pyranose ring, which are typical features of starch. Additionally, new pics with high intensity are observed in the lower wavenumber region (400-600 cm^{-1}) at the nanoparticles spectrums, which may correspond to Cu–O and Ag–O vibrations, confirming nanoparticle formation.

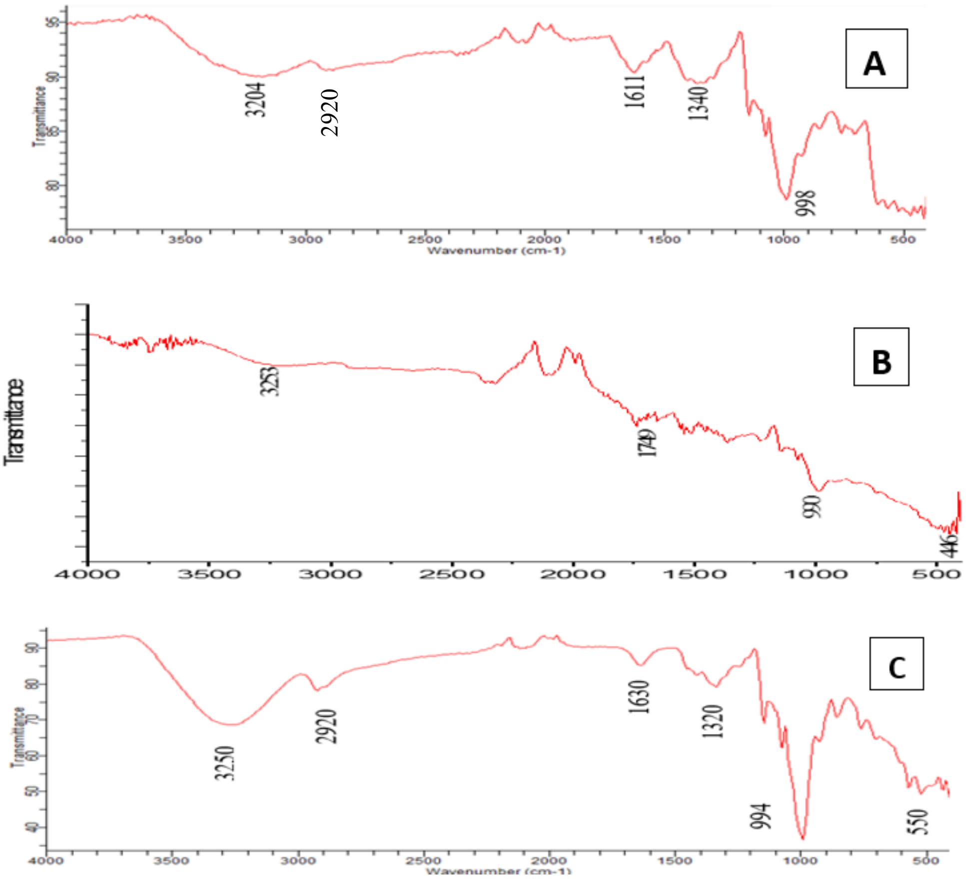

Figure 08: FT-IR Spectra of St-CuNPs (A), St-AgNPs (B) and starch (C).

The FTIR spectrum of pure alginate (Figure 09C) shows a broad absorption band at 3350 cm^{-1} attributed to O–H stretching vibrations, and a peak at 2900 cm^{-1} corresponding to C–H stretching. The strong band observed at 1700 cm^{-1} is assigned to the stretching of carbonyl groups (C=O). A band at 1208 cm^{-1} corresponds to C–O–C stretching vibrations in the glycosidic linkage. Strong pic at 1032 cm^{-1} corresponds to C–O stretching vibration, while the band at 410 cm^{-1} indicates skeletal vibrations related to the polysaccharide backbone.

In the Alg-CuNPs spectrum (Figure 09A), characteristic bands of alginate are still present but with noticeable shifts. The O–H stretching band appears at 3344 cm^{-1}, the band of C–H stretching shifted to 2919 cm^{-1} with reduced intensity, while the stretching of carboxylate groups is observed at 1721 cm^{-1}. The C–O–C stretching band shifted to 1227 m^{-1}, the peak near 1022 cm^{-1} corresponds to C–O stretching, while the intense band around 444 cm^{-1} may be attributed to metal–oxygen interactions between copper and alginate.

In Alg-AgNPs (Figure 09B), the O–H stretching vibration appears at 3322 cm^{-1}, while the band of C–H stretching appeared with reduced intensity. The asymmetric stretching of the carboxylate group is detected at 1693 cm^{-1}. The 1208 cm^{-1} band is still there but with reduced intensity. A distinct peak is also observed at 1010 cm^{-1}, associated with C–O stretching vibrations. A high-intensity band is detected at 411 cm^{-1}, which is related to Ag–O bonding, indicating the formation of silver nanoparticles.

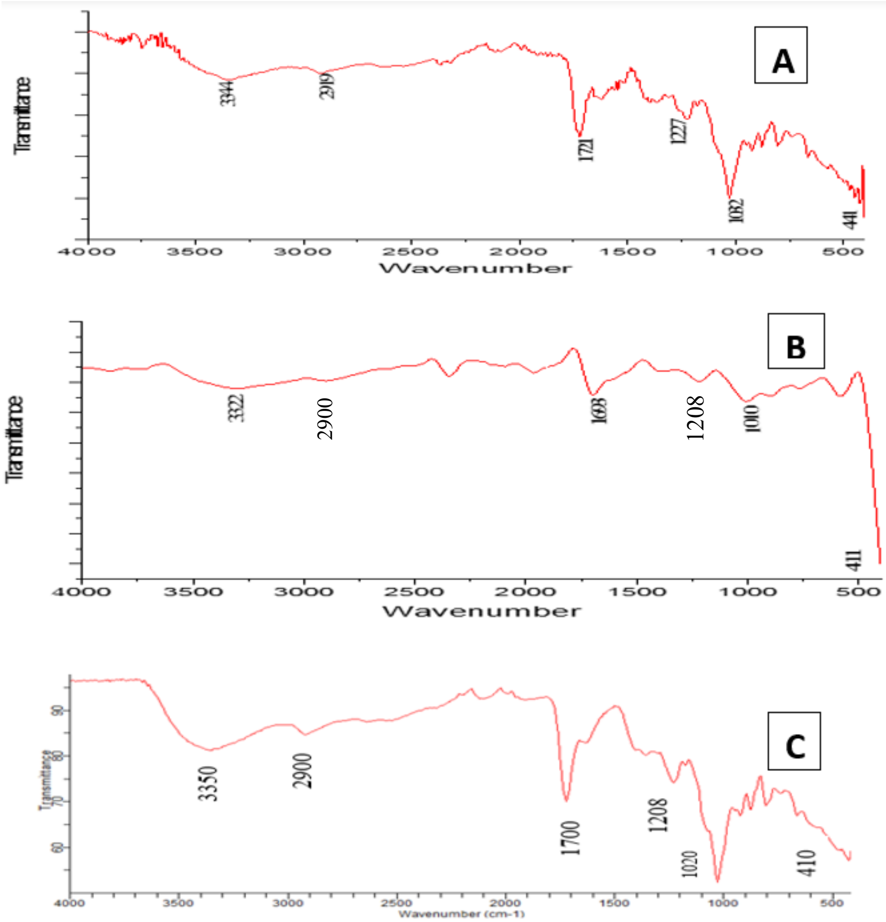

Figure 09: FT-IR Spectra of Alg-CuNPs (A), Alg-AgNPs (B) and alginate (C).

I.3. X-Ray Diffractometry (XRD)

The XRD pattern of St-CuNPs (Figure 10) indicated a strong diffraction peak at 30.9° indexed to the (200) plane, assigned to tetragonal Cu_4O_3 (JCPDS No. 00-033-0480), indicating the presence of a mixed-valence oxide phase that often forms under intermediate oxidation states of copper. Additional reflections are observed for CuO, including the (200) plane at 38.7° and the (−112) plane at 46.7°, which are consistent with the characteristic peaks of CuO (JCPDS No 00-005-0661) which crystallizes in the monoclinic system. Furthermore, distinct peaks corresponding to Cu_8O are identified at 59° (006) and $2\theta \approx 73.3°$ (107), in agreement with the orthorhombic phase of Cu_8O (JCPDS No. 01-078-1588). The crystallite size was calculated using Scherrer equation which can be written as: $D = 0{,}9\lambda/\beta\cos\theta$, where λ is the X-ray wavelength, β is the line broadening at half the maximum intensity (FWHM) and θ is the Bragg angle (Shende, Ingle, Gade, & Rai, 2015). The result demonstrates an average size of 19,34 nm for St-CuNPs.

Concerning Alg-CuNPs, the most intense diffraction peak was observed at 43.1°, indexed to the (111) plane, corresponds to face-centered cubic (fcc) metallic copper (Cu) (JCPDS No 00-003-1005). Additional Cu reflections are detected at 50.2° (200) and 74° (220), confirming the formation of crystalline copper nanoparticles. Besides metallic Cu, diffraction peaks at 38.2° and 44.4° corresponding to (202) and (220) respectively, are assigned to orthorhombic Cu_8O (JCPDS No. 01-078-1588). A further diffraction peak at $2\theta \approx 77.3°$, assigned to the (222) plane, corresponds to cubic CuO (JCPDS No. 01-078-0428). The crystallite size was found to be 14.75 nm.

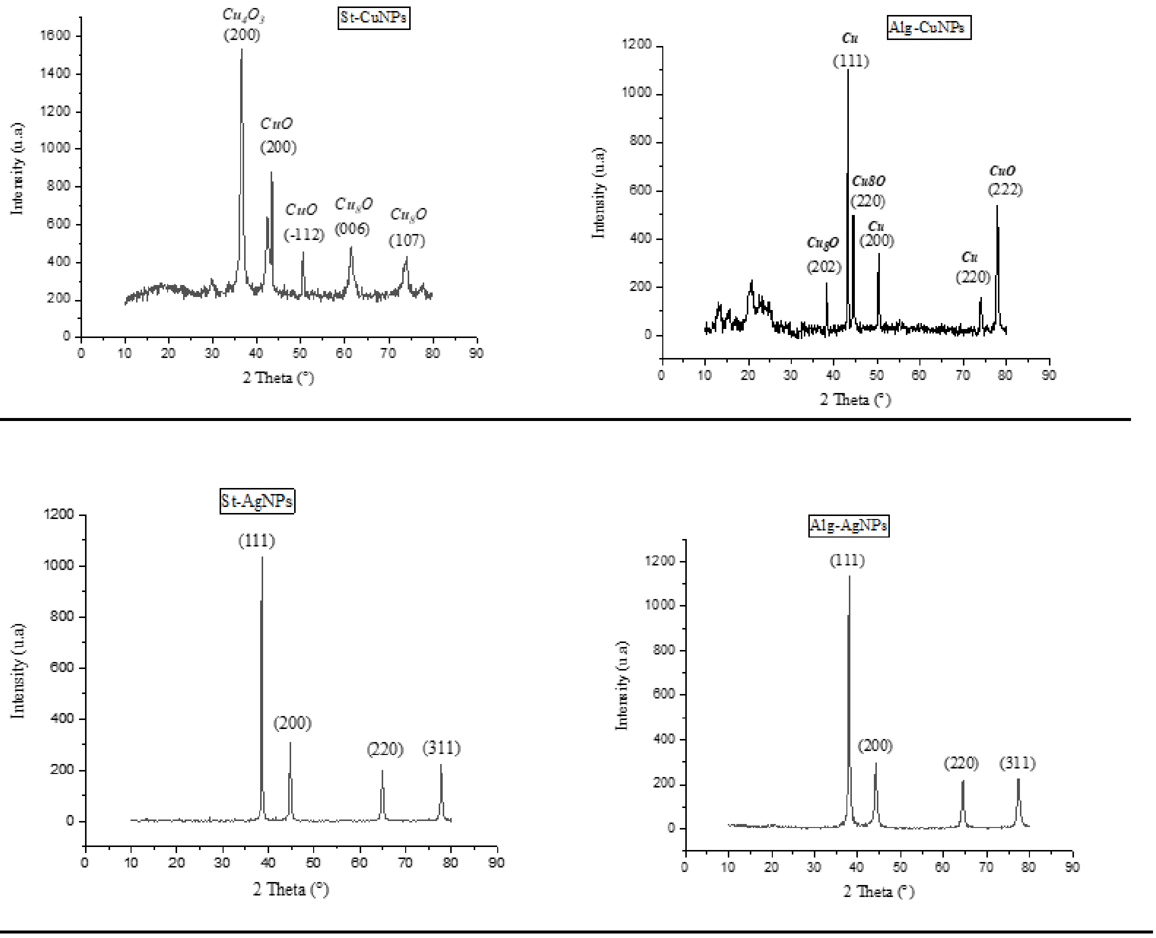

Figure 10: XRD patterns of St-CuNPs, Alg-CuNPs, St-AgNPs and Alg-AgNPs.

In the case of St-AgNPs, the highest diffraction pic was observed at 38.5° indexed to the (111) plane, corresponds to face-centered cubic metallic silver (Ag) (JCPDS No 00-003-0931), additional peaks at 44.7° (200), 64.9° (220), and 77.8° (311) also confirm the face-centered cubic structure of silver according to JCPDS card No 00-003-0921. The crystallite size was calculated to be 9.17 nm.

For Alg-AgNPs, four distinct diffraction peaks were observed at 38°, 44.1°, 64.4°, and 77.3°, corresponding to the (111), (200), (220), and (311) planes, respectively. These peaks are in good agreement with the standard values reported for face-centered cubic silver (JCPDS No 00-004-0783). The crystallite size was estimated at 8.42 nm.

II. Invertase Immobilization on Starch-Copper Nanoparticles

II.1. Optimization of invertase immobilization

II.1.1 Effect of incubation time

Under ideal circumstances, invertase raw extract was incubated with St-CuNPs at various intervals, over time, the invertase enzyme's immobilization on St-CuNPs changed. Enzyme binding began during the second hour of incubation, and this was verified by 0.5% immobilization yield and invertase activity. The maximum enzyme activity was measured at 4.28 µmol/min/mL during the fourth hour of incubation. The highest immobilization yield (1.43%) was obtained after 8 hours of incubation, but Table 05 shows that the enzyme activity began to decline after that.

Table 05: Effect of incubation time on invertase immobilization

Parameters	2h	4h	8h	18h
Enzymatic activity(µmol/min/mL)	2.63± 0,243	4.28± 0,015	2.77± 0.023	1.26± 0.18
Amount of Protein (mg/mL)	0.07±0.05	0.18±0.11	0.20±0.03	0.18±0.08
Relative activity %	18.31±0,243	29.8± 0,015	19.28±0.023	8.77± 0.18
Immobilization yield %	0.5±0.05	1.3±0.11	1.43±0.03	1.3± 0.08

Reaction conditions: buffer solution pH 07, temperature T =20 °C, St-CuNPs concentration = 5%.

II.1.2 Effect of pH and temperature

The optimal incubation time from previous experiments was used in pH optimization. The results presented in Table 06 demonstrate that pH significantly influences the enzymatic activity, protein immobilization, relative activity, and immobilization yield of invertase. The enzymatic activity increased with pH, reaching a maximum at pH 9 (8.02 µmol/min/mL) before decreasing at pH 10 (6.50 µmol/min/mL), whereas lower pH values (pH 6 and 7) resulted in considerably lower activity. Similarly, the immobilization yield followed a comparable trend, peaking at pH 9 (3.14 %), before slightly declining at pH 10. The relative activity was also highest at pH 9 (55.90%), whereas pH 6 and 7 resulted in significantly reduced enzymatic efficiency, this indicates that invertase exhibits optimal catalytic efficiency under mildly alkaline conditions.

Table 06: Effect of pH on invertase immobilization.

Parameters	pH=6	pH=7	pH=8	pH=9	pH=10
Enzymatic activity (µmol/min/mL)	1.89± 0.0064	3.13± 0.233	4.01± 0.312	8.02±0.530	6 .50±2.50
Amount of Protein mg /mL	0.12±0.0002	0.15±0.022	0.38±0.354	0.43±0.205	0.35±0.933
Relative activity %	13.16±0.0064	21.79±0.233	27.92±0.312	55.90 ±0.530	45.26 ±2.50
Immobilization yield %	0.86±0.00003	1.09±0.0212	2.78±0.354	3.14±0.205	2.55±0.933

Reaction conditions: reaction period = 04 hours, temperature T =20 °C, St-CuNPs concentration = 5%.

While using the determined optimal pH, Table 07 shows that the enzymatic activity was highest at 20 °C (8.02 µmol/min/mL) and slightly decreased at 30 °C (7.79 µmol/min/mL). However, a further increase in temperature led to a significant decline in activity, dropping to 6.11 µmol/min/mL at 40 °C and 5.02 µmol/min/mL at 50 °C. The relative activity followed the same trend, with the highest value at 20 °C (55.90%), slightly decreasing at 30 °C (54.27%), and significantly dropping at 40 °C (42.58%) and 50 °C (34.97%), indicating that higher temperatures negatively affect enzyme stability. The immobilization yield was highest at 30 °C (6.67%), then decreasing at 40 °C (4.94%) and 50 °C (0.85%).

Table 07: Effect of temperature on invertase immobilization.

Parameters	T=20 C°	T=30 C°	T=40 C°	T=50 C°
Enzymatic activity(µmol/min/ml)	8.02± 0.530	7.79± 0.001	6.11± 0.0530	5.02± 0.365
Amount of Protein (mg/ml)	0.43± 0.0004	0.93± 0.002	0.68± 0.0566	+0.11± 0.615
Relative activity %	55.90 ± 0.530	54.27 ± 0.001	42.58±0.0530	34.97 ± 0.365

Immobilization yield %	3.14± 0.002	6.67± 0.005	4.94± 0.0566	0.85± 0.615

Reaction conditions: buffer solution pH 09, reaction period = 04 hours, St-CuNPs concentration = 5%.

II.1.3 Effect of concentration of St-CuNPs

The optimization of the concentration of St-CuNPs for immobilizing the invertase enzyme is presented in Table 08. Invertase was incubated at percent concentrations ranging from 0.5 to 7 (w/v) in the optimal time, pH and temperature. St-CuNPs bound to the enzyme were collected at the conclusion of the incubation period, and the enzyme's activity was examined.

The enzymatic activity of immobilized invertase increased slightly as the St-CuNPs concentration increased from 0.5% to 3%, reaching a maximum of 9.01 µmol/min/mL at 3% St-CuNPs. However, further increases in St-CuNPs concentration to 5% and 7% resulted in a decline in enzymatic activity, with the lowest recorded activity at 7% St-CuNPs (6.56 µmol/min/mL) possibly due to enzyme denaturation or excessive crosslinking that hindered enzyme activity. The immobilization yield exhibited a significant increase, reaching its highest value at 5% St-CuNPs (3.14%), suggesting efficient enzyme attachment at this concentration. However, beyond that point, the yield decreased at 7% St-CuNPs (1.50%). Overall, the results indicate that 3% St-CuNPs provides the optimal conditions for achieving high enzymatic activity and relative activity, whereas 5% St-CuNPs yields the highest immobilization efficiency. However, excessive St-CuNPs concentrations beyond these values appear to reduce enzyme stability and performance.

Table 08: Effect of concentration of SCN on invertase immobilization.

Parameters	0.5%	1%	3%	5%	7%
Enzymatic activity (Umol/min/mL)	8.05±0.0997	8.19± 0.146	9.01±0.1171	8.02± 0.530	6.56±0.384
Amount of Protein mg /mL	0.11 ± 0.198	0.16±0.0006	0.19±0.0008	0.43±0.191	0.21±0.141
Relative activity %	56.05±0.0997	57.03 ±0.146	62.74±0.1171	55.84 ± 0.530	45.68 ±0.384
Immobilization yield %	0.79±0.198	1.15±0.002	1.36±0.001	3.14±0.191	1.50±0.141

Reaction conditions: buffer solution pH 09, reaction period 04 hours, T=20 °C.

II.2. Effect of pH and temperature on free and immobilized enzyme activity

In the temperature range of 30 to 50 °C, the temperature dependency of the sucrose hydrolysis reaction catalyzed by free and immobilized invertase was investigated. The findings are displayed in (Figure 11 A, B). The temperature was discovered to have an impact on the enzyme's activity. It was discovered that 35 °C was the ideal temperature for free invertase, and that it increased to 40 °C after immobilization. Both enzymes showed a considerable decrease in activity by 50 °C as the temperature was raised higher. The free enzyme's activity was much higher than the immobilized enzyme's during the 30–50 °C range, and they were roughly equal at 40 °C.

Invertase activity is impacted by pH, as seen in (Figure 11 C, D). It was discovered that the invertase activity changed with pH levels. It was discovered that the ideal pH ranges for the activity of free and immobilized enzymes were 5 and 4.5, respectively. At lower pH values, the immobilized enzyme exhibited increased activity compared to the free enzyme, and conversely, at higher pH values.

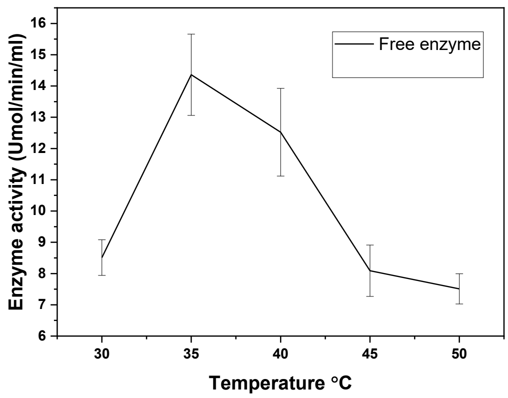

(A)

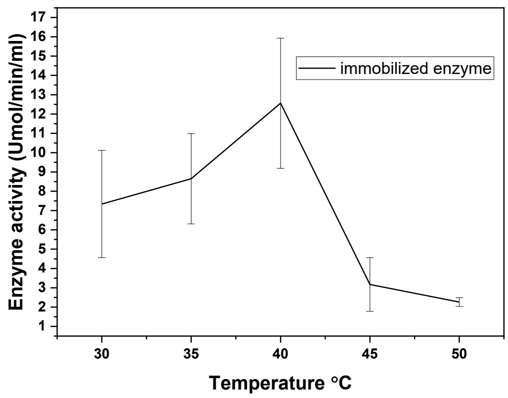

(B)

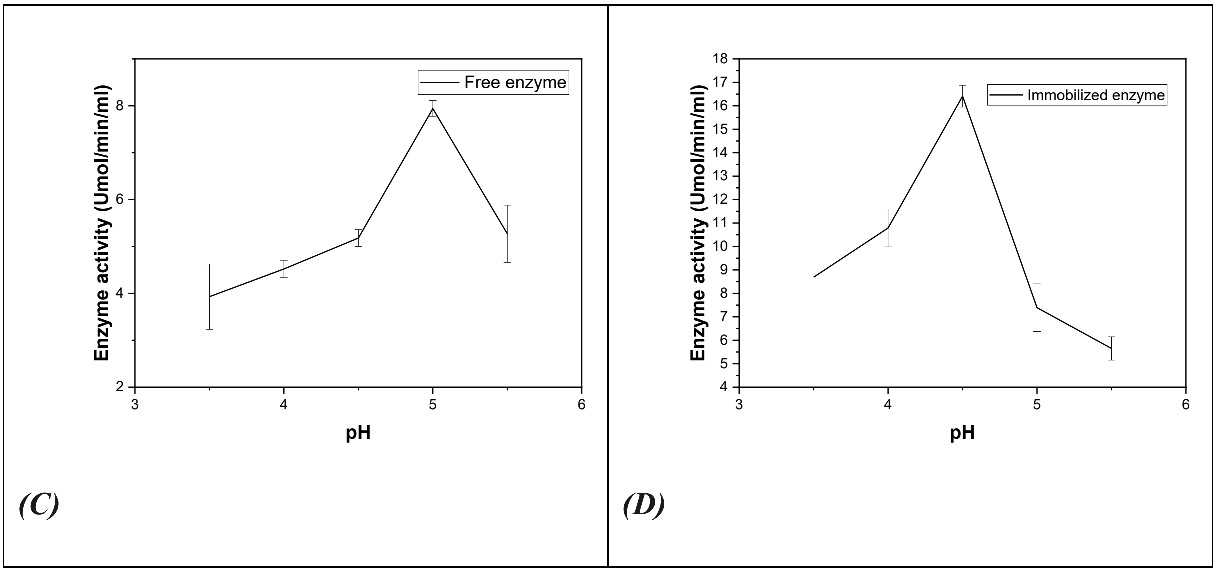

Figure 11: Effect of temperature and pH on free enzyme (A and C respectively) and immobilized enzyme (B and D respectively).

II.3. Reusability of immobilized enzyme

Ten cycles of immobilized invertase activity were measured. The results shown in figure 12 show that 67% of the enzyme activity was still present after the fifth cycle. However, after the tenth cycle of reuse, the enzyme was able to maintain 49% of its activity.

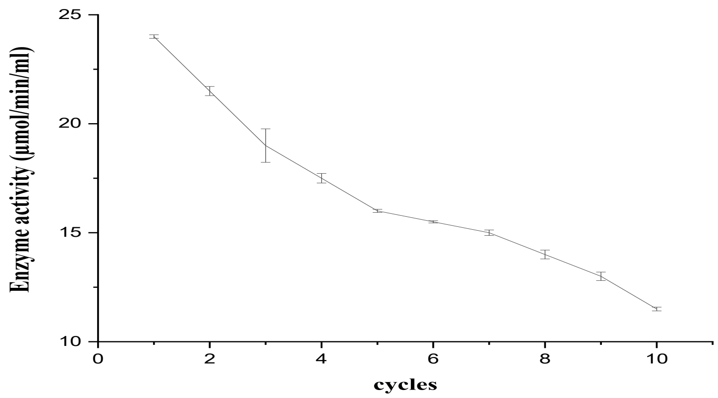

Figure 12: Reusability of immobilized enzyme.

III. Rennet Immobilization on Alginate-Copper Nanoparticles

III.1. Characterization of camel rennet extract

The analysis of camel rennet extract presented in Table 09 revealed a protein concentration of. The coagulant activity was measured at RU/mL. Furthermore, the specific activity of the extract was RU/mg.

Table 09: Properties of Camel rennet extract.

	Protein (mg/mL)	Coagulant activity ($RU.mL^{-1}$)	Specific activity ($RU.mg^{-1}$)
Camel rennet extract			

III.2. Fitting the model

Response surface methodology (RSM) was used to model and optimize the levels of independent variables. The effects of the independent variables on coagulant activity (Y_1) and protein concentration (Y_2) are shown in Table 10. The regression coefficients for these responses are also provided in Table 11.

Polynomial equations were derived from the experimental data to predict the values of the response variables (Eq. 3 and 4). Differences between experimental and predicted values were less than 0.98 $RU.mL^{-1}$ for coagulant activity and 0.57 mg/mL for protein concentration, except for one value where the difference exceeded 0.98 $RU.mL^{-1}$.

Table 10: predicted and experimental values of Coagulant activity and Protein concentration in immobilized rennet.

Coagulant activity = **Eq. (3)**

Protein concentration = **Eq. (4)**

Statistical analysis using ANOVA showed that the experimental data were well represented by a quadratic polynomial model. The coefficients of determination (R^2) for coagulant activity (Y_1) and protein concentration (Y_2) were and, respectively (Table 11). The significance levels of the model coefficients were also determined through ANOVA.

Table 11: Regression Coefficients values of different responses for immobilized rennet preparation.

III.3. Effect of independent variables on response variables

III.3.1 Coagulant Activity

The coagulant activity of immobilized rennet was significantly influenced by the pH and temperature of the immobilization medium at the linear level ($p < 0.01$). However, the quadratic and interaction effects of pH and temperature were not significant. Additionally, Alg-CuNPs concentration had no significant effect on coagulant activity, indicating it did not influence rennet immobilization.

Figure 13 A illustrates the combined effects of pH and temperature on coagulant activity. A decreasing trend in coagulant activity was observed with increasing pH and temperature. The highest activity was recorded at approximately pH and °C.

III.3.2 Protein Concentration

The protein concentration of rennet immobilized on Alg-CuNPs was significantly affected by temperature and Alg-CuNPs concentration at the quadratic level ($p < 0.01$). In contrast, pH was not statistically significant at any level ($p > 0.05$), and the linear and interaction effects of temperature and Alg-CuNP concentration were non-significant.

As shown in Figure 13 B, the response surface revealed a quadratic relationship, where protein concentration increased to a peak and then decreased. Maximum protein concentration was observed at intermediate Alg-CuNPs concentrations and moderate temperatures. At both lower and higher concentrations or extreme temperatures, protein concentration decreased. Concentric ellipses in the contour plot indicate a nonlinear interaction between the two variables.

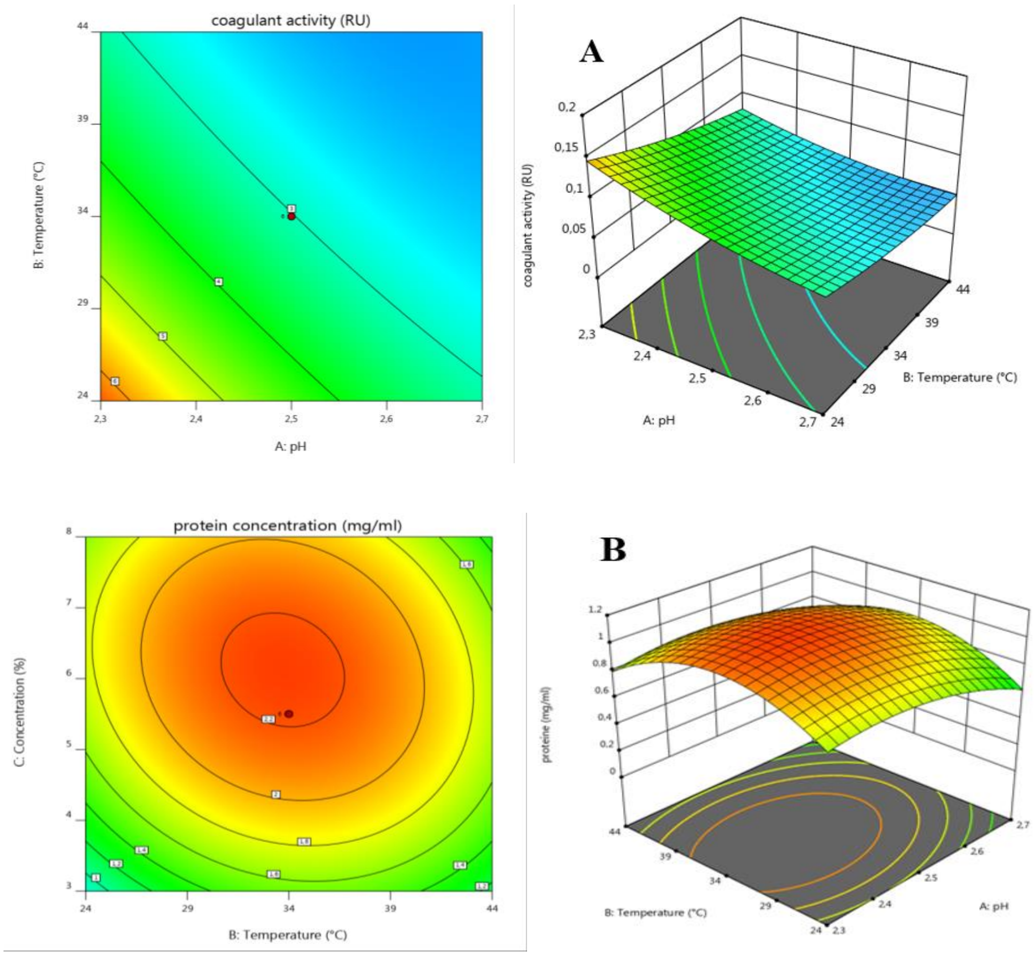

Figure 13: contour plots and 3D surface graph of coagulant activity (A) and protein concentration (B) of immobilized rennet.

III.4. Numerical Optimization

Numerical optimization was carried out using the desirability function approach via Design Expert Software to determine the ideal conditions for maximizing the coagulant activity of immobilized rennet.

A total of 58 candidate solutions were generated, each representing a different combination of the three independent variables (pH, temperature, and Alg-CuNP concentration). Among these, the solution with the highest desirability value (0.933) was selected as the optimal condition. The optimal values for the independent variables were:

- **pH:**
- **Temperature:**
- **Alg-CuNPs**:

Under these conditions, the maximum coagulant activity recorded was $RU.mL^{-1}$ (Table 10).

III.5. Verification of the RSM Model

The validity of the RSM model was confirmed by comparing the predicted coagulant activity at optimal conditions with the experimentally observed values. The optimal conditions identified were already part of the tested runs.

- Predicted value from the model: $RU.mL^{-1}$
- Observed experimental value: $RU.mL^{-1}$

As shown in Table 12, the results indicate a close agreement between the predicted and experimental values, supporting the reliability of the model for predicting coagulant activity within the studied parameter range.

Table 12: Optimum conditions, experimental and predicted values of responses at optimized conditions.

Optimum condition	Coded levels	Actual levels
pH	-1	
Temperature (°C)	-1	
Alg-CuNP Concentration (%)	+1	
Response	Predicted values	Experimental Values
Coagulant activity	($RU.mL^{-1}$)	($RU.mL^{-1}$)
Protein concentration	(mg/mL)	(mg/mL)

III.6. Thermal stability of free and immobilized rennet

As shown in Figure 14, the coagulant activity of both free and immobilized enzymes decreased with increasing temperature in the range of 30°C to 60°C.

For the free enzyme, activity was highest at 30°C and gradually declined with temperature. At 50°C, the activity remained relatively high, but at 60°C, a marked decrease was observed.

For the immobilized enzyme, the initial activity at 30°C was approximately $RU.mL^{-1}$. The activity gradually decreased with rising temperature, reaching about $RU.mL^{-1}$ at 50°C, around $RU.mL^{-1}$ at 55°C, and no activity observed at 60°C.

Figure 14: Thermal stability of free and immobilized enzyme.

III.7. PH stability of immobilized rennet

Figure 15 presents the pH stability of the immobilized enzyme, highlighting its coagulant activity across a pH range of 4 to 8. The highest activity was observed at pH 4. As the pH increases, the enzyme activity gradually declines, reaching its lowest value at pH 8.

Figure 15: PH stability of immobilized enzyme.

III.8. Storage of free and immobilized rennet

The stability of both free and immobilized enzymes over a storage period of six weeks was illustrated in Figure 16. The results indicate a gradual decline in coagulant activity for both enzyme forms, however, the rate of activity loss differs significantly between them.

For the free enzyme, the initial coagulant activity was approximately RU.mL^{-1}. Over the six-week storage period, the enzyme exhibited a steady decline, reaching around RU.mL^{-1} by the final week. In contrast, the immobilized enzyme demonstrated a more stable profile, starting with an activity close to RU.mL^{-1} and declining more gradually to about RU.mL^{-1} by week six.

Figure 16: Free and immobilized enzyme storage.

IV. Biological Activity of Silver Nanoparticles

IV.1. Antioxidant assay

IV.1.1 FRAP assay

The results of Ferric Reducing Antioxidant Power (FRAP) assay were expressed as IC50 values. As shown in Figure 17, the IC50 value for starch-AgNPs was found to be µg/mL, while alginate-AgNPs exhibited a slightly higher IC50 of µg/mL. These values reflect a moderate antioxidant activity for both formulations. Notably, starch-AgNPs demonstrated better performance. In comparison, the standard antioxidant, vitamin C, showed a significantly lower IC50 value (10 µg/mL), as expected due to its well-known potent antioxidant properties.

Figure 17: Frap IC50 values of Starch AgNPs, Alginate AgNPs and Vit C.

IV.1.2 DPPḢ assay

The IC50 values of DPPH radical scavenging assay are presented in Figure 18, the results clearly demonstrate that both types of synthesized AgNPs possess considerable antioxidant activity. Notably, the starch-AgNPs exhibited a significantly lower IC50 value compared to the alginate-AgNPs, indicating a stronger radical scavenging ability. Although vitamin C showed the highest antioxidant potential, the starch-AgNPs came remarkably close, confirming their effective antioxidant performance.

Figure 18: DPPH IC50 values of Starch AgNPs, Alginate AgNPs and Vit C.

IV.2. Anti-inflammatory assay

IV.2.1 Protein denaturation assay

The inhibitory effects of the synthesized nanoparticles on protein denaturation were evaluated by determining their IC_{50} values, using diclofenac sodium as a standard reference. As shown in Figure 19, the Starch AgNPs exhibited the highest IC_{50} value, indicating the lowest efficacy in preventing protein denaturation among the tested samples. In contrast, the alginate-capped silver nanoparticles (Alginate AgNPs) demonstrated a significantly lower IC_{50}. When compared to the standard drug, diclofenac sodium, which displayed the lowest IC_{50}, both types of nanoparticles showed promising but less potent activity.

Figure 19: IC50 values of protein denaturation assay of Starch AgNPs, Alginate AgNPs and diclofenac.

IV.2.2 Hemolysis assay

The antihemolytic effect of the synthesized silver nanoparticles was assessed by measuring their IC50 values in a hemolysis assay (Figure 20). The synthesized nanoparticles displayed a concentration-dependent inhibition of red blood cell hemolysis. Alginate-AgNPs demonstrated the highest IC50 value, followed by Starch-AgNPs, whereas the reference drug, diclofenac sodium, showed a significantly lower IC50.

Figure 20: IC50 values of hemolysis assay of Starch AgNPs, Alginate AgNPs and diclofenac.

Chapter III
Discussion

Starch and alginate were selected because they are natural, biocompatible, non-toxic, and biodegradable polymers, which makes them suitable for applications related to food, biotechnology, and enzyme immobilization (Martău, Mihai, & Vodnar, 2019) (Vardhan et al., 2025). Copper was chosen for its high surface reactivity, strong coordination with biomolecules, and suitability for enzyme immobilization. As an essential trace element, it offers good biocompatibility and safety for food and biological applications. Invertase was chosen in this study because of its significant industrial importance and well-defined catalytic activity (Wang et al., 2020). Invertase produce invert sugars which are widely used in food processing, fermentation, and confectionery industries. It is a well-characterized enzyme, making it suitable as a model for studying enzyme behavior, stability, and immobilization efficiency. (Manoochehri, Hosseini, et al., 2020) Rennet is used because it is one of the most important enzymatic applications in food biotechnology, especially given the limited supply of animal rennet worldwide, which is no longer sufficient to meet the increasing demand for cheese (Zhang et al., 2025).

Characterization of Copper and Silver Nanoparticles

The SEM analyses confirm the successful synthesis and stabilization of copper and silver nanoparticles using biopolymer matrices. The SEM and size distribution results of our Alg-CuNPs align with findings from previous studies. Pricop et al. (Pricop et al., 2025) synthesized copper nanoparticles using trisodium citrate, reporting well-dispersed, spherical particles averaging 37 nm. Similarly, Chiniforoshan et al. (Chiniforoshan, Ensafi, Heydari-Bafrooei, Khalesi, & Tabrizi, 2015) obtained nearly spherical particles around 80 nm using a polymeric ligand, with minimal aggregation. These comparable morphologies highlight the role of different stabilizing agents in guiding nanoparticle formation. The morphology observed in the SEM micrograph of St-CuNPs suggests that starch effectively capped and stabilized the copper nanoparticles, preventing significant agglomeration. The EDX analysis supports this interpretation, as the presence of copper alongside carbon and oxygen confirms the dual role of starch as both a reducing and stabilizing agent.

The Alg-AgNPs were mostly spherical with minimal aggregation and a narrow size distribution centered around 75 nm. This uniformity suggests controlled synthesis and effective stabilization by alginate. These findings are consistent with those of Andreescu et al. (Andreescu, Eastman, Balantrapu, & Goia, 2007), who observed well-dispersed, spherical silver nanoparticles using alginate, and (Skiba, Vorobyova, Pivovarov, & Makarshenko, 2020), who reported similarly shaped particles within the 25–35 nm range. Although the particle sizes in our study are somewhat larger, the shape and distribution patterns support alginate's role in stabilizing and controlling nanoparticle growth. In contrast, the St-AgNPs exhibited more aggregation and a broader size range (70–280 nm), with a dominant size of 187 nm. Compared to the more uniform results reported by Iqbal et al. (Iqbal, Zafar, Mahmood, Niazi, & Aslam, 2020) and Krishnakumar et al. (Krishnakumar, Ramanathan, & Rj, 2017), both of whom found spherical particles under 100 nm using starch, our findings indicate a higher degree of polydispersity. These differences may stem from variations in starch source, concentration, or synthesis conditions. These findings highlight the potential of using natural polymers in green synthesis approaches to produce stable and functional metal nanoparticles (Marta et al., 2023).

The analysis of FTIR spectra of starch–CuNPs and starch–AgNPs demonstrates the successful stabilization of copper nanoparticles by starch molecules. The broad O–H stretching band (3250 cm^{-1}) shows a noticeable shift and intensity reduction in the nanoparticles spectrums, suggesting that hydroxyl groups of starch participate in capping and stabilizing of CuNPs and AgNPs through hydrogen bonding or weak coordination with copper ions. Similarly, the changes observed in the 1630 cm^{-1} band (O–H bending of water) indicate modifications in the hydration environment during nanoparticle formation. More importantly, the strong characteristic peak of starch at 994 cm^{-1}, assigned to C–O and C–O–C stretching, shift slightly and broaden in the nanoparticles spectrums (Raghavendra, Raichur, & Jayaramudu, 2016). This implies the involvement of glycosidic linkages and hydroxyl groups of starch in the reduction and stabilization processes. The appearance of new absorption features in the lower frequency region (<600 cm^{-1}) supports the formation of Cu–O and Ag–O bonds, providing further evidence for starch copper and silver nanoparticle synthesis. The band shifts and intensity changes in starch functional groups, together with the appearance of a new intense bands below 600 cm^{-1} assigned to Cu–O vibrations confirms that copper nanoparticles form coordination bonds with hydroxyl groups of starch, indicating chemical immobilization. However, since most of the characteristic starch bands remain present, the interaction can be described as partial or weak chemical immobilization (Ponsanti, Tangnorawich, Ngernyuang, & Pechyen, 2020).

In St-AgNPs, the loss of the 1320 cm^{-1} band suggests the involvement of hydroxyl and C–O groups in coordination with silver, while the disappearance of the 2920 cm^{-1} band reflects conformational reorganization of the starch backbone due to its interaction with the metal surface. These spectral modifications confirm the chemical interactions between starch functional groups and silver, further supporting a chemical immobilization mechanism.

The FTIR spectra of both Alg-CuNPs and Alg-AgNPs demonstrated clear shifts in the characteristic bands of alginate, confirming the involvement of functional groups in metal binding. In both nanocomposites, the broad O–H stretching band (3350 cm^{-1}) was shifted to lower wavenumbers, suggesting hydrogen bonding and participation of hydroxyl groups. Similarly, the carboxyl C=O stretching band of alginate (1700 cm^{-1}) shifted to 1720 cm^{-1} in Alg-CuNPs and to 1653 cm^{-1} in Alg-AgNPs, indicating coordination of the carboxyl groups with metal ions (Nandiyanto, Oktiani, & Ragadhita, 2019). Furthermore, new low-frequency bands were observed at 444 cm^{-1} and 411 cm^{-1}, corresponding to Cu–O and Ag–O vibrations, respectively, which confirm the formation of metal–oxygen linkages. Importantly, the glycosidic C–O–C band at 1208 cm^{-1} remained unchanged, indicating that the alginate backbone was preserved. These results suggest that in both systems, immobilization occurs predominantly through coordination of hydroxyl and carboxylate groups with the metal ions. Overall, FTIR analysis confirms that starch and alginate not only act as a reducing agent for copper and silver ions but also serve as a stabilizing and capping agents, preventing agglomeration of CuNPs and AgNPs through interactions of hydroxyl and glycosidic groups with metals (Papageorgiou et al., 2010).

The XRD-derived average crystallite sizes of our starch-stabilized AgNPs (St-AgNPs, 9.17 nm) and alginate-stabilized AgNPs (Alg-AgNPs, 8.42 nm) fall in the lower-nanometer range and are substantially different from some literature reports depending on the synthesis route and the measurement technique. For example, a study (Sibiya, Xaba, & Moloto, 2016) reported very small particles of starch-capped AgNPs by TEM, with particle diameters in the 0.5–4 nm range under their optimal conditions, together with XRD showing cubic reflections consistent with Ag. This shows that starch can yield extremely small AgNPs when reaction parameters are tuned. By contrast, a chitosan-capped AgNPs study reported a much larger XRD crystallite size ≈ 26 nm, with HR-TEM particle sizes mostly in the 10–50 nm range, demonstrating that biopolymer type and synthesis conditions can produce significantly larger coherent domains/particles (Vijayakumar et al., 2019). The average crystallite sizes of the synthesized copper nanoparticles were found to be 19.34 nm for St-CuNPs and 14.75 nm for Alg-CuNPs. These results clearly demonstrate the influence of the capping agent on nanoparticle growth and stabilization, with alginate showing a greater ability to limit crystallite expansion compared to starch. the study of Díaz-Visurraga et al. (2012) reported alginate-stabilized CuNPs with average particle sizes of 3–10 nm as determined by TEM. These values are smaller than our XRD-derived crystallite sizes, highlighting both methodological differences and synthesis-dependent variations.

Invertase immobilization

In relation to the impact of experimental parameters on immobilization efficiency, the findings indicate that an 8-hour incubation period provides a high immobilization yield, with a maximum activity reached after 4 hours. Regarding the effect of temperature, the highest activity was observed at 20 °C, but the maximum immobilization yield was observed at 30°C with 6,67%. This temperature range was also reported by Amaya et al.(Amaya-Delgado, Hidalgo-Lara, & Montes-Horcasitas, 2006) who discovered that the maximum immobilization yield of invertase occurs at a temperature of 30°C. Our findings suggest that high temperatures reduce the enzyme's ability to bind effectively to the support material. These findings indicate that temperatures between 20°C and 30 °C are optimal for invertase immobilization, while temperatures above 30°C led to a gradual loss of activity and immobilization efficiency, likely due to enzyme denaturation and structural instability.

Regarding the pH effect, the results showed that the best immobilization yield and highest activity were found at pH 9, with an immobilization yield of 3.14%. In contrast, Amaya et al. (Amaya-Delgado et al., 2006) reported that invertase exhibited maximum activity when immobilized at pH 5.0 on nylon-6 microbeads. Additionally, Marquez et al. (Marquez, Cabral, Freitas, Cardoso, & Ribeiro, 2008) discovered that a pH of 5.0 was the maximum for invertase immobilization via adsorption in ionic exchange resin. This difference can result from the employment of various immobilization methods and support materials. On the other hand, 3% of starch CuNPs had the highest immobilized enzyme activity, despite 5% having the maximum immobilization yield.

Regarding the ideal pH values for the activity of free and immobilized enzymes, the findings indicate that they correspond to 4,5 and 5, respectively, for these circumstances. At lower pH values, the immobilized enzyme exhibited increased activity compared to the free enzyme, and conversely, at higher pH values. Since enzymes are proteins, pH variations will have a significant impact on the ionic character of amino and carboxylic acid groups on proteins, which will in turn have a significant impact on the catalytic site and conformation of an enzyme. This helps to explain how pH affects enzymatic activity (Rouzer & Marnett, 2020).

Apart from purely ionic effects, significant denaturation and subsequent inactivation of the enzyme protein can be caused by either high or low pH levels. Furthermore, because many substrates have an ionic nature, an enzyme's active site could need a certain ionic species in order to function at its best. These factors most likely determine the majority of an average enzyme activity-pH relationship (Aburigal, Elkhalifa, Sulieman, & Elamin, 2014). The results show that, when compared to the free enzyme, the usage of starch CuNPs in conjunction with invertase can enhance the activity of immobilized invertase at acidic pHs and demonstrate good stability of invertase at this pH range.

The temperature was discovered to have an impact on the enzyme's activity. It was discovered that 35°C was the ideal temperature for free invertase, and that it rose to 40°C after immobilization. A decrease in activity may result from an enzyme's inactivation at low temperatures and thermal denaturation at high temperatures (Naqash et al., 2019). In line with our findings, Hakkoymaz and Mazi (2020) reported that the optimal temperature for free invertase was 55 °C, whereas immobilized invertase showed a higher optimal temperature of 70 °C, confirming that immobilization enhanced thermal stability.

Ten cycles of immobilized invertase activity were measured, the findings showed that 67% of the enzyme activity remained after the fifth cycle and 49% after the tenth cycle of reuse. The reduction of support strength, which caused enzyme leakage from the starch-CuNPs, was the cause of the drop-in activity with subsequent cycles. In the work of Malhotra and Basir (2020) after 9 batches of reusing invertase immobilized on chitosan, there was a 70% retention in activity. Unlike free invertase, the immobilized form could be reused several times and it is more stable against environmental factors like temperature fluctuations, pH variations, and enzymatic degradation (Hakkoymaz & Mazi, 2020).

Rennet immobilization

The properties of rennet extract indicate a moderate protein content and demonstrate the extract's effectiveness in milk coagulation. The relatively high specific activity suggests strong enzymatic efficiency per milligram of protein. Our results are consistent with the findings of (Bouras, Ouarda, Krid, Djeghim, & Zidoune, 2022), who reported that camel rennet exhibited a coagulant activity of 111.12 ± 1.23 RU/mL and a specific activity of 7.21 ± 0.03 RU/mg.

Response surface methodology (RSM) is a statistical, theoretical and mathematical technique for model building in order to optimize the level of independent variables (Homayoonfal, Khodaiyan, & Mousavi, 2015). The low differences between experimental and predicted values indicate that the RSM models are reliable and accurate for predicting coagulant activity and protein concentration. These results confirm the effectiveness of the chosen model in optimizing the enzymatic properties. The close agreement between experimental and predicted values supports the adequacy of the regression models derived from RSM

R^2 values close to unity indicate a good fit of the model to the actual data, while lower values suggest the model may not adequately explain the variation (Jensen, 2017). In our study, the R^2 values suggest that the model provides a reasonably good prediction of coagulant activity and protein concentration. This implies that the influence of pH (X_1), temperature (X_2), and Alg-CuNP concentration (X_3) on the response variables can be effectively described using a quadratic polynomial model.

The enzyme's ability to maintain activity at low pH is consistent with the findings of Earl and Paul (Struble & Sharp, 1940), who reported that commercial rennet remains active at pH 2 when heated to 49 °C, with a decline in stability as temperature increases. Similarly, reference (Mickelsen & Ernstrom, 1967) noted moderate stability of rennet below pH 3. The observed decrease in coagulant activity at higher pH and temperature suggests that the immobilization process is sensitive to environmental conditions. This is likely due to changes in surface charge interactions and material stability. High temperatures may reduce enzyme activity through denaturation, thus lowering immobilization efficiency (Che Man, Ab Rahim, Mohd Arshad, & Sulaiman, 2022). In comparison, prior studies on laccase immobilization reported optimum pH ranges of 4.5–6.5 on chitosan–alginate hydrogel (H. Zhang et al., 2024) and pH 5 on magnetic nanoparticles (Fortes, Daniel-da-Silva, Xavier, & Tavares, 2017), indicating that rennet may have a broader or lower pH tolerance range under immobilization conditions.

The presence of an optimal concentration and temperature range for protein immobilization suggests that enzyme-support interactions are strongly influenced by these conditions. This observation aligns with previous findings on the immobilization of cyclodextrin glucanotransferase on hollow fiber membranes, where high enzyme concentrations (12–14%) led to a drop in immobilization yield (Jamil et al., 2018). Additionally, enzyme crowding on the support surface has been associated with reduced activity due to spatial restrictions, limited access to active sites, and even enzyme denaturation (Talbert & Goddard, 2012). These results highlight the importance of optimizing enzyme loading and environmental parameters to achieve high immobilization efficiency without compromising enzyme functionality.

The optimization via desirability function supports these interpretations, showing that enzymatic activity is maximized under low pH, low temperature, and relatively high support concentration. This confirms that enzyme immobilization is strongly influenced by physicochemical interactions, and that controlling the immobilization environment can greatly enhance functional outcomes.

The comparison between the predicted and actual values confirms that the quadratic RSM model is statistically sound and experimentally reliable. Although the predicted value (7.49 RU) was slightly higher than the observed experimental result (6.5 RU), the small deviation demonstrates that the model is capable of accurately forecasting enzyme activity under various experimental conditions. This level of agreement suggests that the model is well-calibrated and suitable for use in process optimization and scale-up strategies. Minor discrepancies are expected in biological systems and can be attributed to experimental variability, enzyme sensitivity, or micro-environmental factors during immobilization. These findings affirm that RSM can be effectively used as a predictive and optimization tool in biotechnological applications involving enzyme immobilization.

Biological activity of silver nanoparticles

Antioxidant activity

The FRAP assay results suggest that both starch- and alginate-stabilized silver nanoparticles possess inherent antioxidant activity, though markedly lower than the standard antioxidant vitamin C. Among the synthesized nanoparticles, starch-AgNPs showed superior antioxidant performance with a lower IC_{50} value than alginate-AgNPs, indicating a more effective capacity to reduce ferric ions. Furthermore, the observed antioxidant activity is consistent with previous reports by Zeng et al. (Zeng, Zhang, Zhang, Cui, & Sun, 2015), who identified significant ferric-reducing power in polysaccharide fractions—particularly those rich in starch and mannose—from *Cordyceps militaris*.

The DPPH assay results confirm that both starch- and alginate-stabilized silver nanoparticles possess effective free radical scavenging capabilities, although to varying degrees. The markedly lower IC_{50} value for starch-AgNPs compared to alginate-AgNPs reflects a significantly greater antioxidant performance. Although both nanoparticle types demonstrated antioxidant potential, starch clearly served as a more favorable capping agent, likely offering better electron-donating ability and surface accessibility. These findings support the idea that the choice of stabilizing agent critically influences the biological functionality of metal nanoparticles. These results are in agreement with Taha et al. (Taha et al., 2022), who also observed lower IC_{50} values for starch-AgNPs and confirmed the superior antioxidant performance of vitamin C. Furthermore, similar trends have been reported by Abdellatif et al. (Abdellatif, Alturki, & Tawfeek, 2021), who demonstrated that AgNPs stabilized with natural cellulosic polymers like ethylcellulose and methylcellulose showed significant radical scavenging activity. Likewise, the findings of Cernei et al. (Mohandoss et al., 2023), using ulvan—a polysaccharide from green algae—as a capping agent. This reinforces the idea that carbohydrate-based materials can contribute to the antioxidant potential of nanostructures and supports their application in biomedical or food-related fields.

Anti-inflammatory activity

The protein denaturation inhibition assay revealed a marked difference in anti-inflammatory potential between the two types of silver nanoparticles. Alginate-AgNPs outperformed starch-AgNPs, as indicated by their significantly lower IC_{50} value. This suggests that alginate provides a more favorable surface chemistry for interacting with and stabilizing proteins, thereby preventing denaturation more effectively. These findings are consistent with prior research. Nasim et al. (Nasim, Shamly, Jaju, Vishnupriya, & Jabin, 2022) and Tehrim et al. (Tehrim et al., 2024) demonstrated that silver nanoparticles, whether capped with organic acids or loaded with therapeutic agents, exhibit meaningful anti-inflammatory activity. Our results add to this body of evidence by confirming that capping with biopolymers like alginate can significantly enhance the efficacy of AgNPs in protein denaturation inhibition. Additionally, recent studies have highlighted the effectiveness of biopolymer-based nanoparticles in modulating inflammation. For example, Saravanan et al. (Saravanan et al., 2025) reported substantial anti-inflammatory effects using sodium alginate nanoparticles loaded with marine plant extracts, while Kulpreechanan and Sorasitthiyanukarn (Kulpreechanan & Sorasitthiyanukarn, 2023) achieved enhanced activity with astaxanthin-loaded chitosan oligosaccharide/alginate nanocarriers. Despite differing compositions, these studies—along with ours—underscore the growing relevance of biopolymer-coated nanoparticles in developing safe and efficient anti-inflammatory agents.

The experimental findings revealed that polysaccharide-stabilized silver nanoparticles effectively inhibited red blood cell hemolysis in a concentration-dependent manner. Notably, alginate-modified nanoparticles demonstrated superior hemocompatibility compared to their starch-stabilized counterparts, though both formulations showed significantly improved blood compatibility relative to unmodified nanoparticles. These observations correlate well with existing literature on polysaccharide-based biomaterials. Previous work by Noga et al. (Noga, Edinger, Wagner, Winter, & Besheer, 2014) on starch-containing copolymers similarly reported excellent hemocompatibility, reinforcing our findings regarding starch's stabilizing effects. The hemolytic profiles observed in our study align with Sattari et al. (Sattari et al., 2017) demonstration of starch-based composites exhibiting minimal blood cell damage. Furthermore, our results with alginate-stabilized nanoparticles complement Elbayomi et al.

(Elbayomi, Wang, Tamer, & You, 2021) reports on the outstanding blood compatibility of alginate formulations. This collective evidence strongly supports the strategic use of natural polysaccharides as stabilizing agents to develop safer, more biocompatible nanoparticle systems for therapeutic applications.

Conclusion & Perspectives

Conclusion

By embracing environmentally friendly synthesis approaches, this study underscores the value of green nanotechnology in the design of efficient, biocompatible platforms for enzyme immobilization and biomedical applications. Through the use of naturally derived materials such as starch and alginate, we have successfully developed copper and silver nanoparticles (CuNPs and AgNPs) with significant bio-functional capabilities. The key findings are summarized as follows:

✓ Eco-friendly synthesis methods allowed for the successful fabrication of four distinct bio-nanostructures: starch-copper (St-CuNPs), alginate-copper (Alg-CuNPs), starch-silver (St-AgNPs), and alginate-silver nanoparticles (Alg-AgNPs), all characterized using FTIR, SEM, and XRD. These nanoparticles exhibited distinct morphological traits and nanoscale sizes.

✓ Immobilization of invertase from *Saccharomyces cerevisiae* on St-CuNPs yielded a robust biocatalyst, with optimal parameters determined as 4 hours, pH 9, temperature 30 °C, and 3% nanoparticle concentration. Immobilization slightly shifted the optimal conditions of invertase, from pH 4.5 and 35 °C (free enzyme) to pH 5.0 and 40 °C (immobilized form). The immobilized enzyme maintained 49% of its activity after 10 reuses, signifying improved operational stability and potential for industrial reusability.

✓ Rennet extract was effectively immobilized on Alg-CuNPs. Using response surface methodology (RSM), optimal enzyme activity was observed at pH 2.3, 24 °C, and 8% Alg-CuNPs concentration. The resulting coagulant activity reached a peak of 6.5 RU/mL under these conditions.

✓ Thermal and pH stability studies demonstrated that while the free enzymes showed higher initial activity, the immobilized forms offered greater resilience to temperature fluctuations (below 50°C) and long-term storage, preserving enzymatic function over six weeks.

✓ The synthesized St-AgNPs and Alg-AgNPs also demonstrated potent antioxidant and anti-inflammatory properties. The FRAP and DPPH assays confirmed that St-AgNPs had superior radical scavenging and ferric-reducing capabilities compared to Alg-AgNPs, while Alg-AgNPs excelled in protein stabilization and anti-inflammatory response.

✓ These nanomaterials, acting as both capping agents and active biofunctional entities, showcase a dual role in both enzyme immobilization and therapeutic potential, thus offering a green alternative to synthetic chemical methods.

In summary, this investigation successfully demonstrates that bio-based nanomaterials synthesized via green chemistry can serve as stable, reusable enzyme carriers and hold promising antioxidant and anti-inflammatory properties. These findings support the future integration of such nanomaterials in various biotechnological and biomedical fields, from drug delivery systems to functional foods and therapeutic agents.

Despite the promising results, this study has some limitations. The experiments were conducted under controlled laboratory conditions, which may not fully reflect industrial or in vivo environments. Long-term stability and large-scale applicability of the synthesized nanomaterials were not evaluated. Additionally, the interactions of these nanoparticles with complex biological systems require further investigation to ensure safety and efficacy. Future studies should address these aspects to validate and expand the practical applications of these materials.

Perspectives

Building upon the promising results of our research, several future directions can be considered to further expand the scientific and practical implications of green-synthesized bio-nanomaterials:

- ✓ **In vivo evaluation**: While in vitro results confirmed the antioxidant and anti-inflammatory potential of St-AgNPs and Alg-AgNPs, future studies should include in vivo testing on animal models to assess biocompatibility, pharmacokinetics, and potential toxicological effects under physiological conditions.
- ✓ **Formulation and delivery**: Encapsulation of the synthesized nanoparticles into hydrogels, films, or controlled-release systems could create novel drug delivery platforms suitable for wound healing, skin applications, or oral therapeutics.
- ✓ **Environmental applications**: Given the safe and sustainable nature of the synthesized NPs, future research could investigate their potential in environmental biotechnology, such as wastewater treatment, microbial remediation, or biosensing of pollutants.
- ✓ **Stability enhancement**: Investigating surface modifications or cross-linking strategies could further improve the thermal and pH stability of immobilized enzymes, enhancing their long-term usability in industrial settings.

References

Abdel-Hameed, M., Hameed, A., & Ebrahim, O. (2007). Biotechnological potential uses of immobilized algae. *International Journal of Agriculture & Biology, 9*, 9-1.

Abdel Wahab, W. A., Karam, E. A., Hassan, M. E., Kansoh, A. L., Esawy, M. A., & Awad, G. E. A. (2018). Optimization of pectinase immobilization on grafted alginate-agar gel beads by 2(4) full factorial CCD and thermodynamic profiling for evaluating of operational covalent immobilization. *Int J Biol Macromol, 113*, 159-170.

Abdellatif, A. A. H., Alturki, H. N. H., & Tawfeek, H. M. (2021). Different cellulosic polymers for synthesizing silver nanoparticles with antioxidant and antibacterial activities. *Scientific Reports, 11*(1), 84. doi: 10.1038/s41598-020-79834-6

Aburigal, A., Elkhalifa, E., Sulieman, A. M., & Elamin, H. (2014). Extraction and Partial Kinetic Properties of Invertase from Schizosaccharomyces pombe. *International Journal of Food Science and Nutrition Engineering, 4*, 80-85.

Agostinelli, E., Belli, F., Tempera, G., Mura, A., Floris, G., Toniolo, L., . . . Stevanato, R. (2007). Polyketone polymer: A new support for direct enzyme immobilization. *Journal of biotechnology, 127*(4), 670-678.

Al-Adhami, A. J., Bryjak, J., Greb-Markiewicz, B., & Peczyńska-Czoch, W. (2002). Immobilization of wood-rotting fungi laccases on modified cellulose and acrylic carriers. *Process Biochemistry, 37*(12), 1387-1394.

Alam, I., Hubbard, S. J., Oliver, S. G., & Rattray, M. (2007). A kingdom-specific protein domain HMM library for improved annotation of fungal genomes. *BMC Genomics, 8*(1), 97.

Ali, A., Wu, H., Ponnampalam, E. N., Cottrell, J. J., Dunshea, F. R., & Suleria, H. A. (2021). Comprehensive profiling of most widely used spices for their phenolic compounds through LC-ESI-QTOF-MS2 and their antioxidant potential. *Antioxidants, 10*(5), 721.

Amaya-Delgado, L., Hidalgo-Lara, M. E., & Montes-Horcasitas, M. C. (2006). Hydrolysis of sucrose by invertase immobilized on nylon-6 microbeads. *Food Chemistry, 99*(2), 299-304.

Aminabad, N. S., Farshbaf, M., & Akbarzadeh, A. (2019). Recent advances of gold nanoparticles in biomedical applications: state of the art. *Cell biochemistry and biophysics, 77*, 123-137.

Andreescu, D., Eastman, C., Balantrapu, K., & Goia, D. V. (2007). A simple route for manufacturing highly dispersed silver nanoparticles. *Journal of Materials Research, 22*(9), 2488-2496.

Andrén, A. (2002). CHEESE | Rennets and Coagulants. In H. Roginski (Ed.), *Encyclopedia of Dairy Sciences* (pp. 281-286). Oxford: Elsevier.

Anis, S., Muhamad, I., Selvakumaran, S., Mohd Marsin, A., Liew, W., & Kamaludin, M. (2021). Ionically Gelled Polysaccharide-Based Floating Drug Delivery Systems (pp. 161-185).

AS, B., & BR, R. (2004). *Biocatalysis: fundamentals and applications* (Wiley-VCH, Weinheim ed.).

Azeem, M. N. A., Ahmed, O. M., Shaban, M., & Elsayed, K. N. (2022). RETRACTED ARTICLE: In vitro antioxidant, anticancer, anti-inflammatory, anti-diabetic and anti-Alzheimer potentials of innovative macroalgae bio-capped silver nanoparticles. *Environmental Science and Pollution Research, 29*(39), 59930-59947.

References

Batsalova, K., Kunchev, K., Popova, Y., Kozhukharova, A., & Kirova, N. (1987). Hydrolysis of lactose by β-galactosidase immobilized in polyvinylalcohol. *Applied Microbiology and Biotechnology, 26*(3), 227-230.

Beatriz, B., Paula, G., & Batista-Viera, F. (2013). Immobilization of enzymes: A literature survey. *Immobilization of Enzymes and Cells:*, 15-31.

Benucci, I., Caso, M. C., Bavaro, T., Masci, S., Keršienė, M., & Esti, M. (2020). Prolyl endopeptidase from Aspergillus niger immobilized on a food-grade carrier for the production of gluten-reduced beer. *Food Control, 110*, 106987.

Berridge, N. J. (1995). Purification and assay of rennin. In G. E. Perlmann & L. Acad (Eds.), *Methods in Enzymology* (Vol. 2, pp. 69-77.). New York: Press.

Bhalla, T. C., Thakur, N., & Thakur, N. (2017). Invertase of Saccharomyces cerevisiae SAA-612: Production, characterization and application in synthesis of fructo-oligosaccharides. *LWT, 77*, 178-185.

Bhatia, S. (2018). Introduction to enzymes and their applications *Introduction to Pharmaceutical Biotechnology, Volume 2* (pp. 1-1-1-29): IOP Publishing.

Biswas, R., Alam, M., Sarkar, A., Haque, M. I., Hasan, M. M., & Hoque, M. (2022). Application of nanotechnology in food: processing, preservation, packaging and safety assessment. *Heliyon, 8*.

Boller, T., Meier, C., & Menzler, S. (2002). Eupergit oxirane acrylic beads: how to make enzymes fit for biocatalysis. *Organic Process Research & Development, 6*(4), 509-519.

Bouras, B., Ouarda, A., Krid, F. a., Djeghim, F., & Zidoune, M. (2022). Optimization of flocculation and clotting time of camel milk with camel and goat rennets, and chicken pepsin in comparison with cow milk using response surface method (RSM). *Emirates Journal of Food and Agriculture*.

Cabrera, K. (2004). Applications of silica-based monolithic HPLC columns. *Journal of separation science, 27*(10-11), 843-852.

Cadinoiu, A. N., Rata, D. M., Daraba, O. M., Ichim, D. L., Popescu, I., Solcan, C., & Solcan, G. (2022). Silver nanoparticles biocomposite films with antimicrobial activity: In vitro and in vivo tests. *International Journal of Molecular Sciences, 23*(18), 10671.

Cao, L., van Langen, L., & Sheldon, R. A. (2003). Immobilised enzymes: carrier-bound or carrier-free? *Current opinion in Biotechnology, 14*(4), 387-394.

Cerreti, M., Markošová, K., Esti, M., Rosenberg, M., & Rebroš, M. (2017). Immobilisation of pectinases into PVA gel for fruit juice application. *International Journal of Food Science and Technology, 52*(2), 531-539.

Chang, M.-Y., & Juang, R.-S. (2007). Use of chitosan–clay composite as immobilization support for improved activity and stability of β-glucosidase. *Biochemical Engineering Journal, 35*(1), 93-98.

Che Man, R., Ab Rahim, R., Mohd Arshad, Z. I., & Sulaiman, S. Z. (2022). Effect of process parameters on immobilization of cyclodextrin glucanotranferase (CGTase) from Bacillus licheniformis on pineapple waste. *Materials Today: Proceedings, 57*, 1036-1039.

Chellaram, C., Murugaboopathi, G., John, A. A., Sivakumar, R., Ganesan, S., Krithika, S., & Priya, G. S. (2014). Significance of Nanotechnology in Food Industry. *APCBEE Procedia, 8*, 109-113.

Chen, J., Wang, Q., Hua, Z., & Du, G. (2007). Research and application of biotechnology in textile industries in China. *Enzyme and microbial technology, 40*(7), 1651-1655.

Chiniforoshan, H., Ensafi, A. A., Heydari-Bafrooei, E., Khalesi, S. B., & Tabrizi, L. (2015). Polymeric nanoparticle of copper(II)-4,4′-dicyanamidobiphenyl ligand: Synthetic, spectral and structural aspect; application to electrochemical sensing of dopamine and ascorbic acid. *Applied Surface Science, 347*, 315-320.

Chiou, S. H., & Wu, W. T. (2004). Immobilization of Candida rugosa lipase on chitosan with activation of the hydroxyl groups. *Biomaterials, 25*(2), 197-204.

Costa, S., Azevedo, H. S., & Reis, R. L. (2005). Enzyme immobilization in biodegradable polymers for biomedical applications.

Datta, S., Christena, L. R., & Rajaram, Y. R. (2013). Enzyme immobilization: an overview on techniques and support materials. *3*(1), 1-9.

David, A. E., Wang, N. S., Yang, V. C., & Yang, A. J. (2006). Chemically surface modified gel (CSMG): An excellent enzyme-immobilization matrix for industrial processes. *Journal of biotechnology, 125*(3), 395-407.

De Castro Leite Júnior, B. R., De Oliveira Martins, F., Trevizano, L. M., da Capela, A. P., de Melo Carlos Dias, T., Pacheco, A. F. C., & Martins, E. M. F. (2022). Chapter 7 - Applications of enzymes in food processing. In B. Prakash (Ed.), *Research and Technological Advances in Food Science* (pp. 175-194): Academic Press.

De Oliveira, R. C., Amoresi, R. A. C., Marana, N. L., Zaghete, M. A., Ponce, M., Chiquito, A. J., . . . Simões, A. Z. (2020). Influence of synthesis time on the morphology and properties of CeO2 nanoparticles: an experimental–theoretical study. *Crystal Growth & Design, 20*(8), 5031-5042.

Dessale, M., Mengistu, G., & Mengist, H. M. (2022). Nanotechnology: A Promising Approach for Cancer Diagnosis, Therapeutics and Theragnosis. *International Journal of Nanomedicine, 17*, 3735 - 3749.

Díaz-Visurraga, C., Bruna, J., Palma, P., Saavedra, N., Correa, M., & Planes, J. (2012). Antibacterial alginate films with silver or copper nanoparticles for active food packaging. Nanomaterials, 2(3), 275–288.

Díaz-Visurraga, J., Daza, C., Pozo, C., Becerra, A., von Plessing, C., & García, A. (2012). Study on antibacterial alginate-stabilized copper nanoparticles by FT-IR and 2D-IR correlation spectroscopy. [Research Support, Non-U S Gov't]. *Int J Nanomedicine, 7*, 3597-3612.

Djouadi, A., & Derouiche, S. (2021). Spinach mediated synthesis of zinc oxide nanoparticles: Characterization, In vitro biological activities study and in vivo acute toxicity evaluation. *Current Research in Green and Sustainable Chemistry, 4*, 100214.

Edalli, V. A., Mulla, S. I., Eqani, S. A., Mahadevan, G. D., Sharma, R., Shouche, Y., & Kamanavalli, C. M. (2016). Evaluation of p-cresol degradation with polyphenol oxidase (PPO) immobilized in various matrices. *6*(2), 016-0547.

Edis, Z., Haj Bloukh, S., Ashames, A., & Ibrahim, M. (2019). Copper-Based Nanoparticles, Their Chemistry and Antibacterial Properties: A Review (pp. 401-428).

El-Khawaga, A. M., Zidan, A., & Abd El-Mageed, A. I. (2023). Preparation methods of different nanomaterials for various potential applications: A review. *Journal of Molecular Structure, 1281*, 135148.

Elbayomi, S. M., Wang, H., Tamer, T. M., & You, Y. (2021). Enhancement of Antioxidant and Hydrophobic Properties of Alginate via Aromatic Derivatization: Preparation, Characterization, and Evaluation. *Polymers, 13*(15).

Elnashar, M., & Hassan, M. (2017). Development of functionalized carrageenan, chitosan and alginate as polymeric chelating ligands for water softening. *International journal of Environmental Science and Technology, 14*.

Enrico, C. (2019). Nanotechnology-Based Drug Delivery of Natural Compounds and Phytochemicals for the Treatment of Cancer and Other Diseases. *Studies in Natural Products Chemistry*.

Fernández-Lorente, G., Terreni, M., Mateo, C., Bastida, A., Fernández-Lafuente, R., Dalmases, P., . . . Guisán, J. M. (2001). Modulation of lipase properties in macro-aqueous systems by controlled enzyme immobilization: enantioselective hydrolysis of a chiral ester by immobilized Pseudomonas lipase. *Enzyme and microbial technology, 28*(4-5), 389-396.

Ferreira, M. V., Rossler, A. F., Toralles, R. P., Ruiz, W. A., & Rombaldi, C. V. (2018). Optimized extraction and partial purification of invertase isolated from S. cerevisiae in peach puree. Brazilian Journal of Fruit Growing, 40, e-489.

Flores-Maltos, A., Rodríguez-Durán, L. V., Renovato, J., Contreras, J. C., Rodríguez, R., & Aguilar, C. N. (2011). Catalytical properties of free and immobilized Aspergillus niger tannase. *Enzyme research, 2011*(1), 768183.

Fortes, C. C. S., Daniel-da-Silva, A. L., Xavier, A. M. R. B., & Tavares, A. P. M. (2017). Optimization of enzyme immobilization on functionalized magnetic nanoparticles for laccase biocatalytic reactions. *Chemical Engineering and Processing: Process Intensification, 117*, 1-8.

Fox, K. E., Tran, N., Nguyen, T. A. H., Nguyen, T. T., & Tran, P. A. (2019). Surface modification of medical devices at nanoscale—recent development and translational perspectives. *Biomaterials in Translational Medicine*.

Fujiwara, R., Yokoi, T., & Nakajima, M. (2016). Structure and Protein-Protein Interactions of Human UDP-Glucuronosyltransferases. [Review]. *Front Pharmacol, 7*(388).

Garman, S. C. (2007). Structure-function relationships in alpha-galactosidase A. [Research Support, Non-U S Gov't]. *Acta Paediatr, 96*(455), 6-16.

Giannakopoulou, A., Gkantzou, E., Polydera, A., & Stamatis, H. (2020). Multienzymatic nanoassemblies: recent progress and applications. *Trends in biotechnology, 38*(2), 202-216.

Girelli, A. M., & Mattei, E. (2005). Application of immobilized enzyme reactor in on-line high performance liquid chromatography: a review. *Journal of Chromatography B, 819*(1), 3-16.

Gomes-Ruffi, C. R., da Cunha, R. H., Almeida, E. L., Chang, Y. K., & Steel, C. J. (2012). Effect of the emulsifier sodium stearoyl lactylate and of the enzyme maltogenic amylase on the quality of pan bread during storage. *LWT, 49*(1), 96-101.

Govardhan, C. P. (1999). Crosslinking of enzymes for improved stability and performance. [Review]. *Curr Opin Biotechnol, 10*(4), 331-335.

Guan, T., Liu, B., Wang, R., Huang, Y., Luo, J., & Li, Y. (2021). The enhanced fatty acids flavor release for low-fat cheeses by carrier immobilized lipases on O/W Pickering emulsions. *Food Hydrocolloids, 116*, 106651.

Guisan, J. M. (2013). New Opportunities for Immobilization of Enzymes. In J. M. Guisan (Ed.), *Immobilization of Enzymes and Cells: Third Edition* (pp. 1-13). Totowa, NJ: Humana Press.

H R, S. a. H., Hosamani, P., D N, G., & Sneharani, A. H. (2020). Immobilization of trypsin enzyme on silver nanoparticles. *Biomedicine, 40*.

Hakkoymaz, O., & Mazi, H. (2020). An immobilized invertase enzyme for the selective determination of sucrose in fruit juices. Analytical Biochemistry, 611, 27.

Haleem, A., Javaid, M., Singh, R. P., Rab, S., & Suman, R. (2023). Applications of nanotechnology in medical field: a brief review. *Global Health Journal, 7*(2), 70-77.

Hamad, A. F., Han, J.-H., Kim, B.-C., & Rather, I. A. (2017). The intertwine of nanotechnology with the food industry. *Saudi Journal of Biological Sciences, 25*, 27 - 30.

Handayani, W., Ningrum, A., & Imawan, C. (2020). *The role of pH in synthesis silver nanoparticles using pometia pinnata (matoa) leaves extract as bioreductor.* Paper presented at the Journal of Physics: Conference Series.

Hartmann, M. (2005). Ordered mesoporous materials for bioadsorption and biocatalysis. *Chemistry of materials, 17*(18), 4577-4593.

Hashem, A. M., Gamal, A. A., Hassan, M. E., Hassanein, N. M., & Esawy, M. A. (2016). Covalent immobilization of Enterococcus faecalis Esawy dextransucrase and dextran synthesis. [Research Support, Non-U S Gov't]. *Int J Biol Macromol, 82*, 905-912.

Hassan, M., Haroun, M., Hassan, E., El Enshasy, H., Soliman, E. A., & Eldin, M. S. (2012). Covalent Immobilization of penicillin G Acylase onto chemically activated Surface of PVC Membranes for 6-APA production from penicillin Hydrolysis Process. M.E. Hassan, B.M. Haroun, E.A. Hassan, H.A. El Enshasy, E.A. Soliman, M.S. Mohy Eldin. Journal of Applied Polymer Science, Vol. 124, E27–E36 (2012). *Applied Polymer Science, 124*, E27–E36.

Hassan, M. A., Haroun, B. M., Amara, A. A., & Serour, E. A. (2013). Production and Characterization of Keratinolytic Protease from New Wool-Degrading Bacillus Species Isolated from Egyptian Ecosystem. *BioMed Research International, 2013*(1), 175012.

Helman, G., Pacheco-Colón, I., & Gropman, A. L. (2014). The urea cycle disorders. *Seminars in neurology*, *34*(3), 341–349.

Hernandez, K., & Fernandez-Lafuente, R. (2011). Control of protein immobilization: coupling immobilization and site-directed mutagenesis to improve biocatalyst or biosensor performance. *Enzyme Microb Technol, 48*(2), 107-122.

Homaei, A. A., Sariri, R., Vianello, F., & Stevanato, R. (2013). Enzyme immobilization: an update. [Review]. *J Chem Biol, 6*(4), 185-205.

Homayoonfal, M., Khodaiyan, F., & Mousavi, M. (2015). Modelling and optimising of physicochemical features of walnut-oil beverage emulsions by implementation of response surface methodology: Effect of preparation conditions on emulsion stability. *Food Chemistry, 174*, 649-659.

Horowitz, B. (1918). What are Enzymes? *The Scientific Monthly, 6*(3), 253-259.

Hsieh, H.-J., Liu, P.-C., & Liao, W.-J. (2000). Immobilization of invertase via carbohydrate moiety on chitosan to enhance its thermal stability. *Biotechnology letters, 22*, 1459-1464.

Huang, H., Wang, D., Zhu, J., Seeger, S., & Chu, Z. (2022). Sand-Based Economical Micro/Nanocomposite Materials for Diverse Applications. *ACS applied materials & interfaces*.

Iqbal, M., Zafar, H., Mahmood, A., Niazi, M. B. K., & Aslam, M. W. (2020). Starch-Capped Silver Nanoparticles Impregnated into Propylamine-Substituted PVA Films with Improved Antibacterial and Mechanical Properties for Wound-Bandage Applications. *Polymers, 12*(9), 2112.

Jahan, I., Erci, F., & Isildak, I. (2021). Facile microwave-mediated green synthesis of non-toxic copper nanoparticles using Citrus sinensis aqueous fruit extract and their antibacterial potentials. *Journal of Drug Delivery Science and Technology, 61*, 102172.

Jain, A. S., Pawar, P. S., Sarkar, A., Junnuthula, V., & Dyawanapelly, S. (2021). Bionanofactories for Green Synthesis of Silver Nanoparticles: Toward Antimicrobial Applications. *Int J Mol Sci, 22*(21).

Jaiswal, L., Limayem, A., & Shankar, S. (2022). Chapter 4 - Polysaccharide-based nanomaterials. In K. Pal, A. Sarkar, P. Sarkar, N. Bandara & V. Jegatheesan (Eds.), *Food, Medical, and Environmental Applications of Nanomaterials* (pp. 95-111): Elsevier.

Jamil, N., Che Man, R., Suhaimi, S., Md Shaarani, S., Iffah Mohd Arshad, Z., Kholijah Abdul Mudalip, S., & Zubaidah Sulaiman, S. (2018). Effect of enzyme concentration and temperature on the immobilization of cyclodextrin glucanotransferase (CGTase) on hollow fiber membrane. *Materials Today: Proceedings, 5*(10, Part 2), 22036-22042.

Jegannathan, K. R., Abang, S., Poncelet, D., Chan, E. S., & Ravindra, P. (2008). Production of biodiesel using immobilized lipase--a critical review. *Crit Rev Biotechnol, 28*(4), 253-264.

Jensen, W. (2017). Book Review of Response Surface Methodology: Process and Product Optimization Using Designed Experiments 4th edition. *Journal of Quality Technology, 49*, 186-188.

Kanniah, P., Chelliah, P., Thangapandi, J. R., Thangapandi, E. J. J. S. B., Kasi, M., & Sivasubramaniam, S. (2022). Benign fabrication of metallic/metal oxide nanoparticles from algae. In K. A. Abd-Elsalam, R. Periakaruppan, & S. Rajeshkumar (Eds.), *Agri-waste and microbes for production of sustainable nanomaterials* (pp. 465–493). Elsevier

Karuvantevida, N., Razia, M., Bhuvaneshwar, R., Sathishkumar, G., Prabukumar, S., & Sivaramakrishnan, S. (2022). Bioactive flavonoid used as a stabilizing agent of mono and bimetallic nanomaterials for multifunctional activities. *Journal of Pure and Applied Microbiology, 16*(3), 1652-1662.

Katchalski-Katzir, E., & Kraemer, D. M. (2000). Eupergit® C, a carrier for immobilization of enzymes of industrial potential. *Journal of molecular catalysis B: enzymatic, 10*(1-3), 157-176.

Kaushal, J., Singh, G., & Arya, S. K. (2022). Chapter 36 - Emerging trends and future prospective in enzyme technology. In M. Kuddus & C. N. Aguilar (Eds.), *Value-Addition in Food Products and Processing Through Enzyme Technology* (pp. 491-503): Academic Press.

Khan, A., Rashid, A., Younas, R., & Chong, R. (2016). A chemical reduction approach to the synthesis of copper nanoparticles. *International Nano Letters, 6*(1), 21-26.

Khandekar, D. C., Palai, T., Agarwal, A., & Bhattacharya, P. K. (2014). Kinetics of sucrose conversion to fructo-oligosaccharides using enzyme (invertase) under free condition. *Bioprocess and Biosystems Engineering, 37*(12), 2529-2537.

Kierstan, M. P., & Coughlan, M. P. (1991). Immobilization of proteins by noncovalent procedures: principles and applications. *Bioprocess Technol, 14*, 13-71.

Klein, M. P., Scheeren, C. W., Lorenzoni, A. S. G., Dupont, J., Frazzon, J., & Hertz, P. F. (2011). Ionic liquid-cellulose film for enzyme immobilization. *Process Biochemistry, 46*(6), 1375-1379.

Klis, M., Karbarz, M., Stojek, Z., Rogalski, J., & Bilewicz, R. (2009). Thermoresponsive poly (N-isopropylacrylamide) gel for immobilization of laccase on indium tin oxide electrodes. *The Journal of Physical Chemistry B, 113*(17), 6062-6067.

Klouda, L., & Mikos, A. G. (2008). Thermoresponsive hydrogels in biomedical applications. *European journal of pharmaceutics and biopharmaceutics, 68*(1), 34-45.

Kotwal, S. M., & Shankar, V. (2009). Immobilized invertase. *Biotechnology Advances, 27*(4), 311-322.

Kress, J., Zanaletti, R., Amour, A., Ladlow, M., Frey, J. G., & Bradley, M. (2002). Enzyme accessibility and solid supports: which molecular weight enzymes can be used on solid supports? An investigation using confocal Raman microscopy. *Chemistry, 8*(16), 3769-3772.

Krishnakumar, S., Ramanathan, G., & Rj, H. (2017). Polysaccharide induced production of silver nanoparticles (Ag-NPs) and their antibacterial efficacy against selected bacterial pathogens. *International Journal of Pharma and Bio Sciences, 8*, 1–7.

Kulpreechanan, N., & Sorasitthiyanukarn, F. N. (2023). Astaxanthin-loaded chitosan oligosaccharide/alginate nanoparticles: Exploring the anti-inflammatory and anticancer potential as a therapeutic nutraceutical: An *in vitro* study. *Research Journal of Pharmacy and Technology, 16*(11), 5378–5383.

Kumar, A., Asthana, M., Jain, K. G., & Singh, V. (2017). 5. Microbial production of enzymes: An Overview. In G. Vijai Kumar, Z. Susanne, X. F. F. Edivaldo, D.-D.-d.-B. Maria Carmen & P. Diane (Eds.), *Microbial Applications* (pp. 107-138). Berlin, Boston: De Gruyter.

Kumar, V., Shriram, V., Shukla, R., & Gosavi, S. (2022). *Nano-Strategies for Addressing Antimicrobial Resistance*. Springer.

Kumari, A., Kaur, B., Srivastava, R., & Sangwan, R. S. (2015). Isolation and immobilization of alkaline protease on mesoporous silica and mesoporous ZSM-5 zeolite materials for improved catalytic properties. *Biochemistry and Biophysics Reports, 2*, 108-114.

Kurzbaum, E., Raizner, Y., Kuc, M. E., Kulikov, A., Hakimi, B., Kruh, L. I., & Menashe, O. (2020). Phenol biodegradation by bacterial cultures encapsulated in 3D microfiltration-membrane capsules. *Environmental Technology, 41(22), 2875–2883.*.

Le Corre, D., Bras, J., & Dufresne, A. (2010). Starch nanoparticles: a review. *Biomacromolecules*, *11*(5), 1139–1153.

Liang, J. F., Li, Y. T., & Yang, V. C. (2000). Biomedical application of immobilized enzymes. *Journal of pharmaceutical sciences, 89*(8), 979-990.

Linde, D., Rodríguez-Colinas, B., Estévez, M., Poveda, A., Plou, F. J., & Fernández Lobato, M. (2012). Analysis of neofructooligosaccharides production mediated by the extracellular β-fructofuranosidase from Xanthophyllomyces dendrorhous. *Bioresource Technology, 109*, 123-130.

Liu, D.-M., & Dong, C. (2020). Recent advances in nano-carrier immobilized enzymes and their applications. *Process Biochemistry, 92*, 464-475.

Liu, Y., Wang, X., Shi, X., Sun, M., Wang, L., Hu, Z., Liu, F., Liu, Q., Wang, P., Li, J., & Zhao, C. (2022). A colorimetric sensor for *Staphylococcus aureus* detection based on controlled click chemical-induced aggregation of gold nanoparticles and immunomagnetic separation. *Mikrochimica Acta, 189*(3), 104.

Lombard, V., Golaconda Ramulu, H., Drula, E., Coutinho, P. M., & Henrissat, B. (2014). The carbohydrate-active enzymes database (CAZy) in 2013. *Nucleic acids research, 42*(D1), D490-D495.

Maghraby, Y. R., El-Shabasy, R. M., Ibrahim, A. H., & Azzazy, H. M. E.-S. (2023). Enzyme Immobilization Technologies and Industrial Applications. *ACS Omega, 8*(6), 5184-5196.

Mahaut, M., Jeantet, R., & Brulé, G. (2003). *Initiation à la Technologie Fromagère*. Paris, France: Lavoisier Tech Doc.

Makarov, V. V., Love, A. J., Sinitsyna, O. V., Makarova, S. S., Yaminsky, I. V., Taliansky, M. E., & Kalinina, N. O. (2014). Green nanotechnologies: Synthesis of metal nanoparticles using plants. *Acta Naturae, 6*(1), 35–44.

Makler, M. T., Piper, R. C., & Milhous, W. K. (1998). Lactate dehydrogenase and the diagnosis of malaria. *Parasitol Today, 14*(9), 376-377.

Malhotra, I., & Basir, S. F. (2020). Application of invertase immobilized on chitosan using glutaraldehyde or tris(hydroxymethyl)phosphine as cross-linking agent to produce bioethanol. *Applied Biochemistry and Biotechnology, 191*, 838–851.

Manoochehri, H., Hosseini, N. F., & [other authors]. (2020). A review on invertase: Its potentials and applications. *Biocatalysis and Agricultural Biotechnology, 25,* 101599.

Mansoori, G. A., & Soelaiman, T. A. F. (2005). Nanotechnology — An Introduction for the Standards Community. *Journal of ASTM International, 2*, 1-21.

Marquez, L. D. S., Cabral, B. V., Freitas, F. F., Cardoso, V. L., & Ribeiro, E. J. (2008). Optimization of invertase immobilization by adsorption in ionic exchange resin for sucrose hydrolysis. *Journal of Molecular Catalysis B: Enzymatic, 51*(3), 86-92.

Marrazza, G. (2014). Piezoelectric biosensors for organophosphate and carbamate pesticides: a review. *Biosensors, 4*(3), 301-317.

Marta, H., Rizki, D. I., Mardawati, E., Djali, M., Mohammad, M., & Cahyana, Y. (2023). Starch Nanoparticles: Preparation, Properties and Applications. *Polymers, 15*(5), 1167.

Martău, G. A., Mihai, M., & Vodnar, D. C. (2019). The use of chitosan, alginate, and pectin in the biomedical and food sector: Biocompatibility, bioadhesiveness, and biodegradability. *Polymers, 11*(11), 1837

Maslova, O. V., Senko, O. V., & Efremenko, E. N. (2018). Aspartic and glutamic acids polymers: preparation and applications in medicinal chemistry and pharmaceutics. *Russian Chemical Bulletin, 67*(4), 614-623.

Massolini, G., & Calleri, E. (2005). Immobilized trypsin systems coupled on-line to separation methods: Recent developments and analytical applications. *Journal of separation science, 28*(1), 7-21.

Matto, M., & Husain, Q. (2009). Calcium alginate–starch hybrid support for both surface immobilization and entrapment of bitter gourd (Momordica charantia) peroxidase. *Journal of molecular catalysis B: enzymatic, 57*(1), 164-170.

Memarpoor-Yazdi, M., Karbalaei-Heidari, H. R., & Khajeh, K. (2017). Production of the renewable extremophile lipase: Valuable biocatalyst with potential usage in food industry. *Food and Bioproducts Processing, 102*, 153-166.

Mickelsen, R., & Ernstrom, C. A. (1967). Factors Affecting Stability of Rennin1, 2. *Journal of Dairy Science, 50*(5), 645-650.

Mohamad, N. R., Marzuki, N. H. C., Buang, N. A., Huyop, F., & Wahab, R. A. (2015). An overview of technologies for immobilization of enzymes and surface analysis techniques for immobilized enzymes. *Biotechnology & Biotechnological Equipment, 29*(2), 205-220.

Mohamed, E. A. (2020). Green synthesis of copper & copper oxide nanoparticles using the extract of seedless dates. *Heliyon, 6*(1), e03123.

Mohammadi, M., Rezaei Mokarram, R., Ghorbani, M., & Hamishehkar, H. (2019). Inulinase immobilized gold-magnetic nanoparticles as a magnetically recyclable biocatalyst for facial and efficient inulin biotransformation to high fructose syrup. *Int J Biol Macromol, 123*, 846-855.

Mohandoss, S., Murugaboopathy, V., Haricharan, P. B., Hebbal, M. I., Saadaldin, S., Soliman, M., & Eldwakhly, E. (2023). Ulvan as a Reducing Agent for the Green Synthesis of Silver Nanoparticles: A Novel Mouthwash. *Inorganics, 11*(1), 5.

Mohy Eldin, M., Hassan, E., & El-Aassar, M. (2005). β -Galactosidase Covalent Immobilization on the Surface of Alginate Beads and its Application in Lactose Hydrolysis. *Deutsche Lebensmittel-Rundschau: Zeitschrift für Lebensmittelkunde und Lebensmittelrecht, 101*, 255-259.

Mtibe, A., Mokhothu, T. H., John, M. J., Mokhena, T. C., & Mochane, M. J. (2018). Chapter 8 - Fabrication and Characterization of Various Engineered Nanomaterials. In C. Mustansar Hussain (Ed.), *Handbook of Nanomaterials for Industrial Applications* (pp. 151-171): Elsevier.

Nagpal, K., Singh, S. K., & Mishra, D. N. (2010). Chitosan nanoparticles: a promising system in novel drug delivery. *Chem Pharm Bull, 58*(11), 1423-1430.

Namdeo, M., & Bajpai, S. (2009). Immobilization of α-amylase onto cellulose-coated magnetite (CCM) nanoparticles and preliminary starch degradation study. *Journal of molecular catalysis B: enzymatic, 59*(1), 134-139.

Nandiyanto, A. B. D., Oktiani, R., & Ragadhita, R. (2019). How to Read and Interpret FTIR Spectroscope of Organic Material. *Indonesian Journal of Science & Technology, 4*(1), 97-118.

Naqash, F., Masoodi, F. A., & Rather, S. A. (2019). Food enzymes and nanotechnology. In M. Kuddus (Ed.), Enzymes in food biotechnology (pp. 769–784). Academic Press.

Nasim, I., Shamly, M., Jaju, K., Vishnupriya, V., & Jabin, Z. (2022). Antioxidant and anti-inflammatory activity of a nanoparticle based intracanal drugs. *Bioinformation, 18*(5), 450-454.

Nguyen, H. H., & Kim, M. (2017). An overview of techniques in enzyme immobilization. *Applied Science and Convergence Technology, 26*(6), 157-163.

Noga, M., Edinger, D., Wagner, E., Winter, G., & Besheer, A. (2014). Characterization and compatibility of hydroxyethyl starch-polyethylenimine copolymers for DNA delivery. *J Biomater Sci Polym Ed, 25*(9), 855-871.

O'Driscoll, K. F. (1976). Techniques of enzyme entrapment in gels. *Methods Enzymol, 44*, 169-183.

Oroojalian, F., Charbgoo, F., Hashemi, M., Amani, A., Yazdian-Robati, R., Mokhtarzadeh, A., Ramezani, M., & Hamblin, M. R. (2020). Recent advances in nanotechnology-based drug delivery systems for the kidney. *Journal of Controlled Release, 321*, 442–462.

Palecek, M. (2020). The evolution of ‘culture’: Juggling a concept. *Anthropological Theory, 20*(1), 53-76.

Papageorgiou, S. K., Kouvelos, E. P., Favvas, E. P., Sapalidis, A. A., Romanos, G. E., & Katsaros, F. K. (2010). Metal–carboxylate interactions in metal–alginate complexes studied with FTIR spectroscopy. *Carbohydrate Research, 345*(4), 469-473.

Patil, J., Kamalapur, M., Marapur, S., & Kadam, D. (2010). Ionotropic gelation and polyelectrolyte complexation: the novel techniques to design hydrogel particulate sustained, modulated drug delivery system: a review. *Digest Journal of Nanomaterials and Biostructures, 5*(1), 241-248.

Pedrol, N., & Tamayo, P. (2001). Protein content quantification by Bradford method. In M. J. Reigosa Roger (Ed.), *Handbook of plant ecophysiology techniques* (pp. 283–295). Springer.

Ponsanti, K., Tangnorawich, B., Ngernyuang, N., & Pechyen, C. (2020). A flower-shape green synthesis and characterization of silver nanoparticles (AgNPs) with different starch as reducing agent. *Journal of Materials Research and Technology, 9*(5), 11003-11012.

Porath, J., & Axén, R. (1976). Immobilization of enzymes to agar, agarose, and Sephadex supports. *Methods Enzymol, 44*, 19-45.

Pricop, A., Negrea, A., Pascu, B., Nemeş, N. S., Ciopec, M., Negrea, P., Ianăşi, C., Svera, P., Muntean, D., Ivan, A., & Cristea, I. M. (2025). Copper nanoparticles synthesized by chemical reduction with medical applications. *International Journal of Molecular Sciences, 26*(4), 1628.

Raafat, A. I., Araby, E., & Lotfy, S. (2012). Enhancement of fibrinolytic enzyme production from Bacillus subtilis via immobilization process onto radiation synthesized starch/dimethylaminoethyl methacrylate hydrogel. *Carbohydrate polymers, 87*(2), 1369-1374.

Raghavendra, A. K., Raichur, A. M., & Jayaramudu, J. (2016). Starch-based synthesis of silver nanoparticles and their characterization. *Carbohydrate Polymers*, **152**, 296–303.

Rahman, M. M., Islam, M. B., Biswas, M., & Khurshid Alam, A. H. (2015). In vitro antioxidant and free radical scavenging activity of different parts of Tabebuia pallida growing in Bangladesh. *BMC Res Notes, 8*(621), 015-1618.

Rajdeo, K., Harini, T., Lavanya, K., & Fadnavis, N. W. (2016). Immobilization of pectinase on reusable polymer support for clarification of apple juice. *Food and Bioproducts Processing, 99*, 12-19.

Rashidi, L. (2021). Different nano-delivery systems for delivery of nutraceuticals. *Food bioscience, 43*, 101258.

Raspopova, E. A., & Krasnoshtanova, A. A. (2016). Characterizing the properties and evaluating the efficiency of biocatalysts based on immobilized fungal amylase. *Catalysis in Industry, 8*(1), 75-80.

Ren, G., Xu, X., Cheng, J., Yuan, X., Wu, L., & Wan, Y. (2006). Electrospun poly(vinyl alcohol)/glucose oxidase biocomposite membranes for biosensor applications. *Reactive and Functional Polymers, 66*, 1559-1564.

Ricardi, N. C., de Menezes, E. W., Valmir Benvenutti, E., da Natividade Schöffer, J., Hackenhaar, C. R., Hertz, P. F., & Costa, T. M. H. (2018). Highly stable novel silica/chitosan support for β-galactosidase immobilization for application in dairy technology. *Food Chemistry, 246*, 343-350.

Robinson P. K. (2015). Enzymes: principles and biotechnological applications. *Essays in biochemistry*, *59*, 1–41.

Roszek, B., Jong, W. H., & Re, G. (2005). *Nanotechnology in medical applications: State-of-the-art in materials and devices*. Springer.

Rouzer, C. A., & Marnett, L. J. (2020). Structural and Chemical Biology of the Interaction of Cyclooxygenase with Substrates and Non-Steroidal Anti-Inflammatory Drugs. *Chem Rev, 120*(15), 7592-7641.

Saallah, S., Naim, M. N., Lenggoro, I. W., Mokhtar, M. N., Abu Bakar, N. F., & Gen, M. (2016). Immobilisation of cyclodextrin glucanotransferase into polyvinyl alcohol (PVA) nanofibres via electrospinning. *Biotechnology Reports, 10*, 44-48.

Safaya, M., & Rotliwala, Y. (2022). Neem oil based nano-emulsion formulation by low energy phase inversion composition method: Characterization and antimicrobial activity. *Materials Today: Proceedings, 57*, 1793-1797.

Sahu, T., Ratre, Y. K., et al. (2021). Nanotechnology based drug delivery system: Current strategies and emerging therapeutic potential for medical science. *Journal of Drug Delivery Science and Technology, 63*, 102487.

Salatin, S., & Yari Khosroushahi, A. (2017). Overviews on the cellular uptake mechanism of polysaccharide colloidal nanoparticles. *J Cell Mol Med, 21*(9), 1668-1686.

Saravanan, M., Mahalakshmi, B., K L G, A., Subriya, S., Sridevi, M., & E, D. (2025). Formulation and Characterization of Sodium Alginate-based Nanoparticle Doped with Seagrass (Syringodium isoetifolium) Extract: In vitro Anti-inflammatory, Antioxidant and Anti-diabetic Activities. *Natural and Life Sciences Communications, 24*, E2025035.

Sattari, M., Fathi, M., Daei, M., Erfan-Niya, H., Barar, J., & Entezami, A. A. (2017). Thermoresponsive graphene oxide - starch micro/nanohydrogel composite as biocompatible drug delivery system. *Bioimpacts, 7*(3), 167-175.

Scott, A., Vadalasetty, K. P., Chwalibog, A., & Sawosz, E. (2018). Copper nanoparticles as an alternative feed additive in poultry diet: a review. *Nanotechnology Reviews, 7*(1), 69-93.

Sheldon, R. (2007). Cross-linked enzyme aggregates (CLEA® s): Stable and recyclable biocatalysts. *Biochemical Society Transactions, 35*(6), 1583-1587.

Sheldon, R. A. (2007). Cross-linked enzyme aggregates (CLEAs): stable and recyclable biocatalysts. *Biochem Soc Trans, 35*(6), 1583-1587.

Shen, Q., Yang, R., Hua, X., Ye, F., Zhang, W., & Zhao, W. (2011). Gelatin-templated biomimetic calcification for β-galactosidase immobilization. *Process Biochemistry, 46*(8), 1565-1571.

Shende, S., Ingle, A. P., Gade, A., & Rai, M. (2015). Green synthesis of copper nanoparticles by Citrus medica Linn. (Idilimbu) juice and its antimicrobial activity. World Journal of Microbiology and Biotechnology, 31, 865-873.

Shivaramakrishnan, B., Gurumurthy, B., & Balasubramanian, A. (2017). Potential biomedical applications of metallic nanobiomaterials: a review. *International Journal of Pharmaceutical Sciences and Research, 8*(3), 985.

Sibiya, P., Xaba, T., & Moloto, M. (2016). Green synthetic approach for starch capped silver nanoparticles and their antibacterial activity. *Pure and Applied Chemistry, 88*(1-2), 61-69.

Singh, R., Kumar, M., Mittal, A., & Mehta, P. K. (2016). Microbial enzymes: industrial progress in 21st century. *6*(2), 016-0485.

Singh, R., Singh, A., & Sachan, S. (2019). Chapter 48 - Enzymes Used in the Food Industry: Friends or Foes? In M. Kuddus (Ed.), *Enzymes in Food Biotechnology* (pp. 827-843): Academic Press.

Singh, R., Singh, N., Saini, B. S., & Rao, H. S. (2008). In vitro antioxidant activity of pet ether extract of black pepper. *Indian J Pharmacol, 40*(4), 147-151.

Singh, T., Shukla, S., Kumar, P., Wahla, V., Bajpai, V. K., & Rather, I. A. (2017). Application of nanotechnology in food science: Perception and overview. *Frontiers in Microbiology, 8*, 1501.

Skiba, M. I., Vorobyova, V. I., Pivovarov, A., & Makarshenko, N. P. (2020). Green Synthesis of Silver Nanoparticles in the Presence of Polysaccharide: Optimization and Characterization. *Journal of Nanomaterials, 2020*(1), 3051308.

Struble, E. B., & Sharp, P. F. (1940). Effect of Heat and pH on the Inactivation of Rennin in Whey. *Journal of Dairy Science, 23*(7), 587-591.

Sugahara, V. H., & Varéa, G. S. (2014). Immobilization of *Beauveria bassiana* lipase on silica gel by physical adsorption. *Brazilian Archives of Biology and Technology, 57*(6), 842–850.

Suye, S.-i., Kumon, Y., & Ishigaki, A. (2010). Immobilization of glucose oxidase on poly-(L-lysine)-modified polycarbonate membrane. *Biotechnology and Applied Biochemistry, 27*, 245-248.

Taha, I. M., Zaghlool, A., Nasr, A., Nagib, A., El Azab, I. H., Mersal, G. A. M., Ibrahim, M. M., & Fahmy, A. (2022). Impact of Starch Coating Embedded with Silver Nanoparticles on Strawberry Storage Time. *Polymers, 14*(7), 1439.

Talbert, J. N., & Goddard, J. M. (2012). Enzymes on material surfaces. *Colloids Surf B Biointerfaces, 93*, 8-19.

Tamer, T., Omer, A., & Hassan, M. (2016). Methods of Enzyme Immobilization. *International Journal of Current Pharmaceutical Review and Research, 7*, 385-392.

Taylor, I. N., Brown, R. C., Bycroft, M., King, G., Littlechild, J. A., Lloyd, M. C., Praquin, C., Toogood, H. S., & Taylor, S. J. (2004). Application of thermophilic enzymes in commercial biotransformation processes. *Biochemical Society transactions*, *32*(2), 290–292.

Tehrim, F., Hina, A., Noor, J., Sana, S., Nazia, A., Besharat, A. A., & Waqas, A. (2024). Molecular marker identification, antioxidant, antinociceptive, and anti-inflammatory responsiveness of malonic acid capped silver nanoparticle. *Frontiers in Pharmacology, 14, 1319613.*

Thanh, N. T., Maclean, N., & Mahiddine, S. (2014). Mechanisms of nucleation and growth of nanoparticles in solution. *Chemical reviews, 114*(15), 7610-7630.

Trbojević Ivić, J., Veličković, D., Dimitrijević, A., Bezbradica, D., Dragačević, V., Gavrović Jankulović, M., & Milosavić, N. (2016). Design of biocompatible immobilized Candida rugosa lipase with potential application in food industry. *Journal of the Science of Food and Agriculture, 96*(12), 4281-4287.

Van de Velde, F., Lourenço, N. D., Pinheiro, H. M., & Bakker, M. (2002). Carrageenan: A food-grade and biocompatible support for immobilisation techniques. *Advanced Synthesis & Catalysis, 344*(8), 815-835.

Vardhan, H., Singhal, N., Vashistha, P., Jain, R., Bist, Y., Gaur, A., & Wagri, N. K. (2025). Starch–biomacromolecule complexes: A comprehensive review of interactions, functional materials, and applications in food, pharma, and packaging. *Carbohydrate Polymer Technologies and Applications, 11,* 101001.

Vianello, F., Zennaro, L., Di Paolo, M. L., Rigo, A., Malacarne, C., & Scarpa, M. (2000). Preparation, morphological characterization, and activity of thin films of horseradish peroxidase. *Biotechnology and bioengineering, 68*(5), 488-495.

Vijayakumar, S., Malaikozhundan, B., Parthasarathy, A., Saravanakumar, K., Wang, M.-H., & Vaseeharan, B. (2019). Nano biomedical potential of biopolymer chitosan-capped silver nanoparticles with special reference to antibacterial, antibiofilm, anticoagulant and wound dressing material. *Journal of Cluster Science, 31*, 355-366.

Wahba, M. I., & Hassan, M. E. (2015). Novel grafted agar disks for the covalent immobilization of β-D-galactosidase. *Biopolymers, 103*(12), 675-684.

Wang, P., Yuan, Y., Xu, K., Zhong, H., Yang, Y., Jin, S., Yang, K., & Qi, X. (2020). Biological applications of copper-containing materials. *Bioactive Materials, 6*(4), 916–927.

Wangoh, J., Farah, Z., & Puhan, Z. (1993). Extraction of camel rennet and its comparison with calf rennet extract. *Milchwissenschaft-milk Science International, 48*, 322-325.

Wong, L. S., Thirlway, J., & Micklefield, J. (2008). Direct site-selective covalent protein immobilization catalyzed by a phosphopantetheinyl transferase. *Journal of the American Chemical Society, 130*(37), 12456-12464.

Xu, Q., Tan, Z., Liao, X., & Wang, C. (2021). Recent advances in nanoscale metal-organic frameworks biosensors for detection of biomarkers. *Chinese Chemical Letters*. *33*(1): 22-32

Yu, H., Park, J.-Y., Kwon, C. W., Hong, S.-C., Park, K. M., & Chang, P.-S. (2018). An Overview of Nanotechnology in Food Science: Preparative Methods, Practical Applications, and Safety. *Journal of Chemistry, 2018,* 5427978.

Zdarta, J., Kołodziejczak-Radzimska, A., Bachosz, K., Rybarczyk, A., Bilal, M., Iqbal, H. M. N., Buszewski, B., & Jesionowski, T. (2023). Nanostructured supports for multienzyme co-immobilization for biotechnological applications: Achievements, challenges and prospects. *Advances in Colloid and Interface Science, 315*, 102889.

Zeng, Y., Zhang, Y., Zhang, L., Cui, S., & Sun, Y. (2015). Structural characterization and antioxidant and immunomodulation activities of polysaccharides from the spent rice substrate of Cordyceps militaris. *Food Science and Biotechnology, 24*(5), 1591-1596.

Zhang, H., Zhang, X., Wang, L., Wang, B., Zeng, X., & Ren, B. (2024). Functionalized Chitosan and Alginate Composite Hydrogel-Immobilized Laccase with Sustainable Biocatalysts for the Effective Removal of Organic Pollutant Bisphenol A. *Catalysts, 14*(5), 304.

Zhang, J., Lovell, J. F., Shi, J., & Zhang, Y. (2025). Nanomaterials for co-immobilization of multiple enzymes. *BMEMat, 3*(1), e12080.

Zhang, X., Tao, L., Wei, G., Yang, M., Wang, Z., Shi, C., Shi, Y., & Huang, A. (2025). Plant-derived rennet: Research progress, novel strategies for their isolation, identification, mechanism, bioactive peptide generation, and application in cheese manufacturing. *Critical Reviews in Food Science and Nutrition, 65*(3), 444–456

Annex

Annex 01 shows the effect of incubation time on invertase immobilization, results were obtained using DNS method by mixing 1mL of sample and 1mL of DNS reagent (1:1 ratio) and the absorbance was measured using spectrophotometer.

Annex 01: Effect of incubation time on invertase immobilization

Parameters	2h	4h	8h	18h
Enzymatic activity(µmol/min/ml)	7.91± 0,418	12.86± 0,098	8.33± 0.0148	3.79± 0.00001
Amount of Protein (mg/ml)	0.71±0.453	1.415±0.476	1.845±1.294	1.67±1.002
Relative activity %	55.08 ±0.418	89.55 ± 0.098	58.00 ± 0.0148	26.39± 0.00001
Immobilization yield %	5.09±0.453	10.16±0.476	13.24±1.294	11.99± 1.002

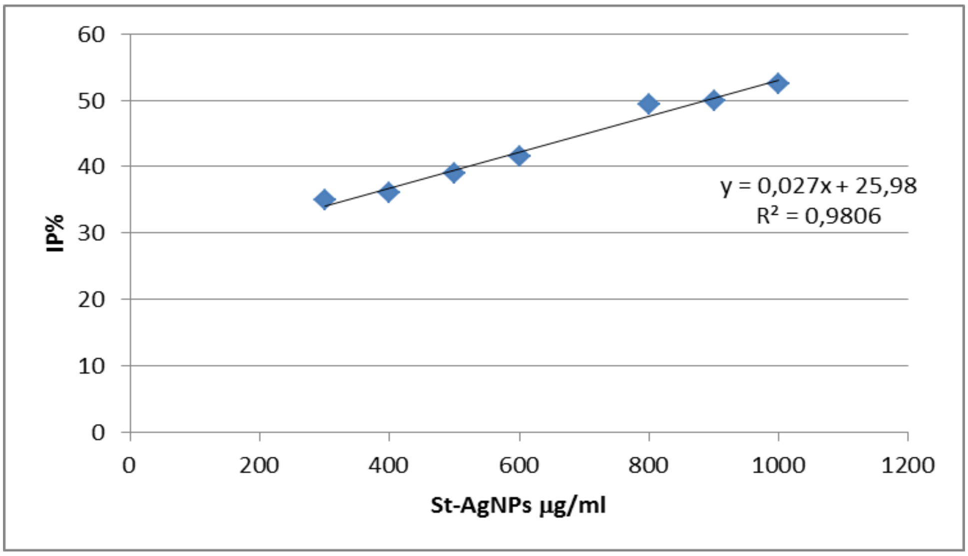

Annex 02: Inhibition percentage values of St-AgNPs (Hemolysis assay).

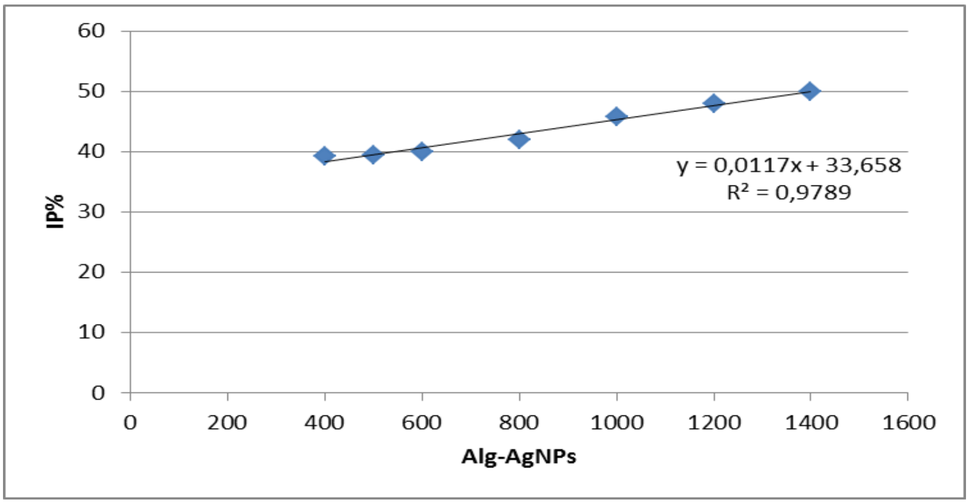

Annex 03: Inhibition percentage values of Alg-AgNPs (Hemolysis assay).

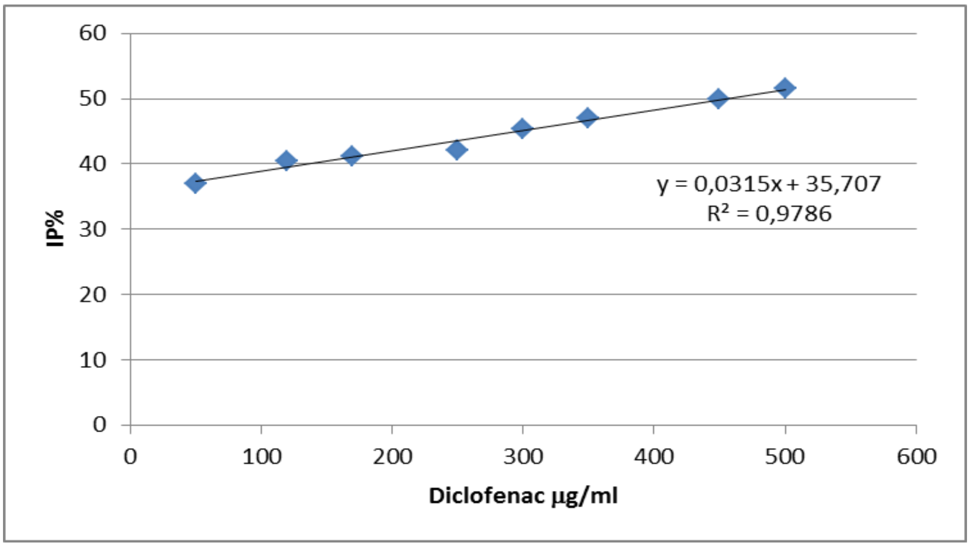

Annex 04: Inhibition percentage values of Diclofenac (Hemolysis assay).

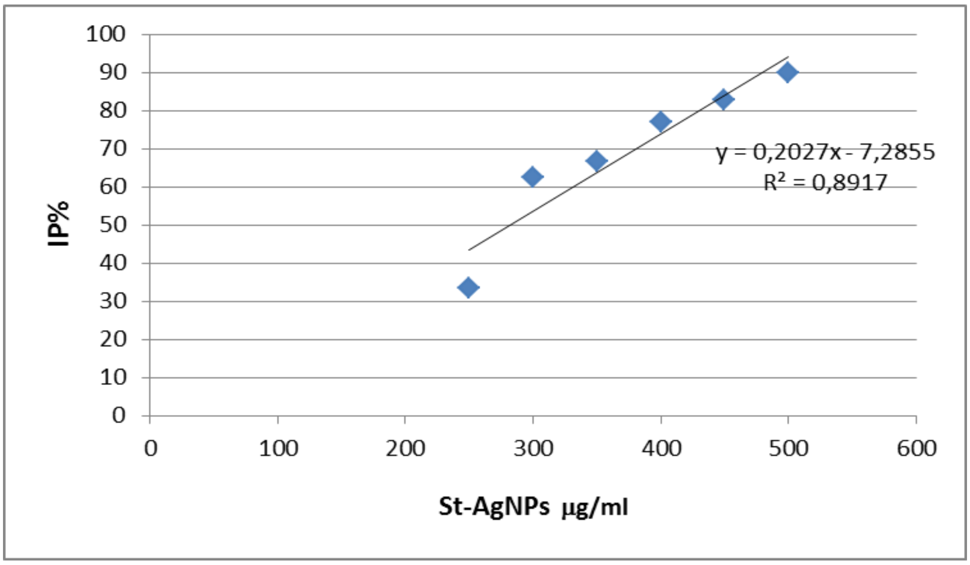

Annex 05: Inhibition percentage values of St-AgNPs (Protein denaturation assay)

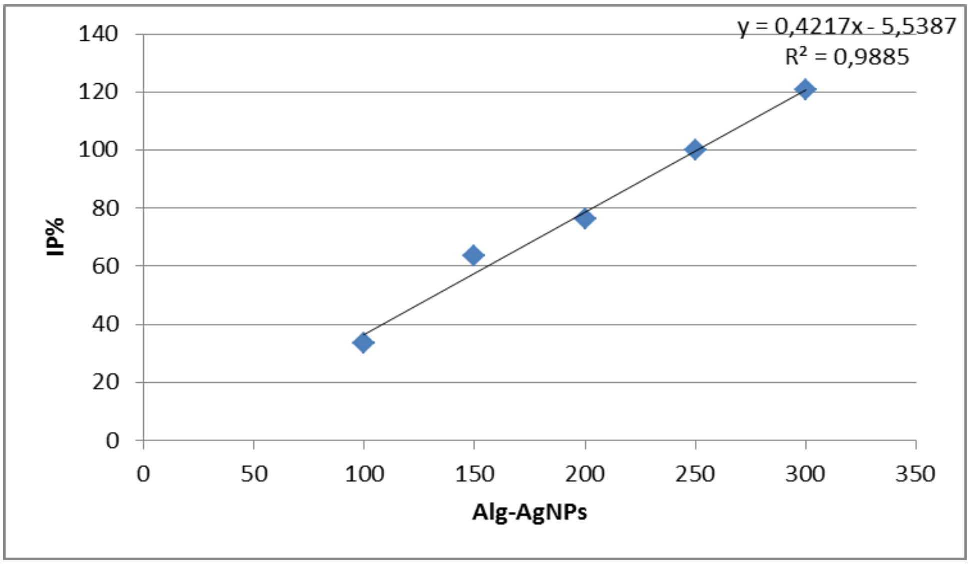

Annex 06: Inhibition percentage values of Alg-AgNPs (Protein denaturation assay)

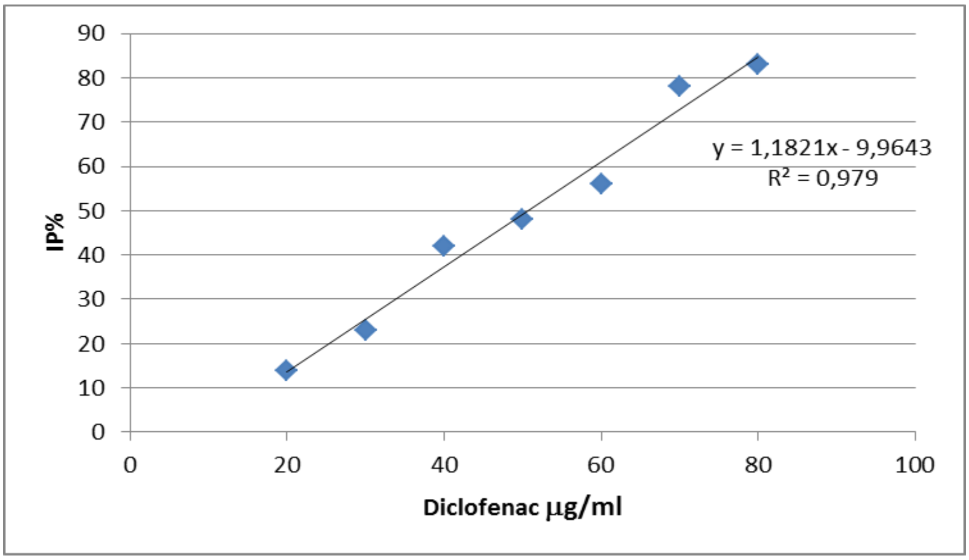

Annex 07: Inhibition percentage values of Alg-AgNPs (Protein denaturation assay)

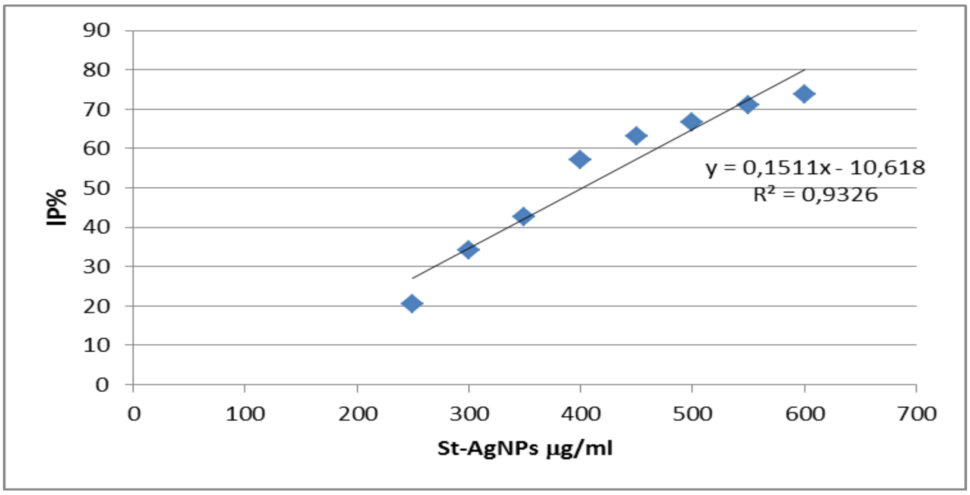

Annex 08: Inhibition percentage values of St-AgNPs (FRAP assay)

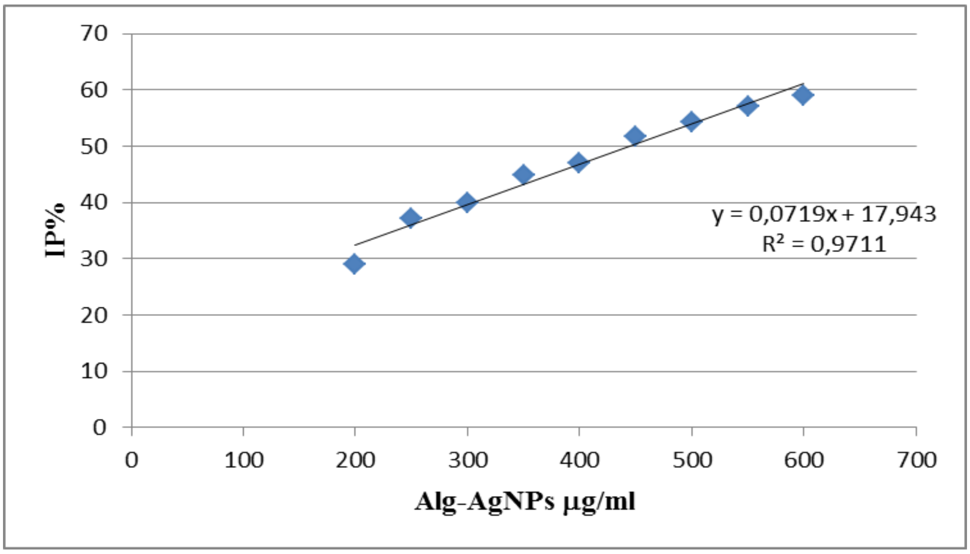

Annex 09: Inhibition percentage values of St-AgNPs (FRAP assay)

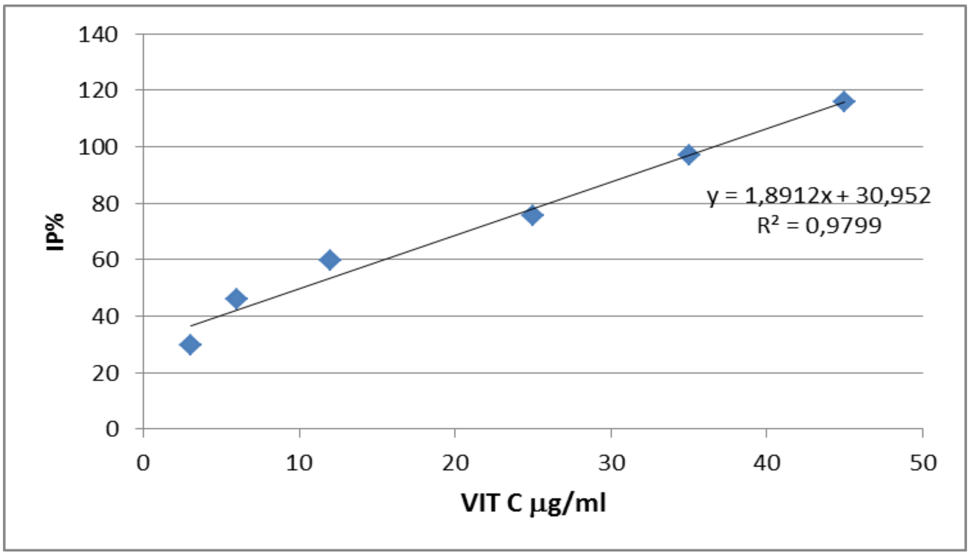

Annex 10: Inhibition percentage values of Vitamin C (FRAP assay)

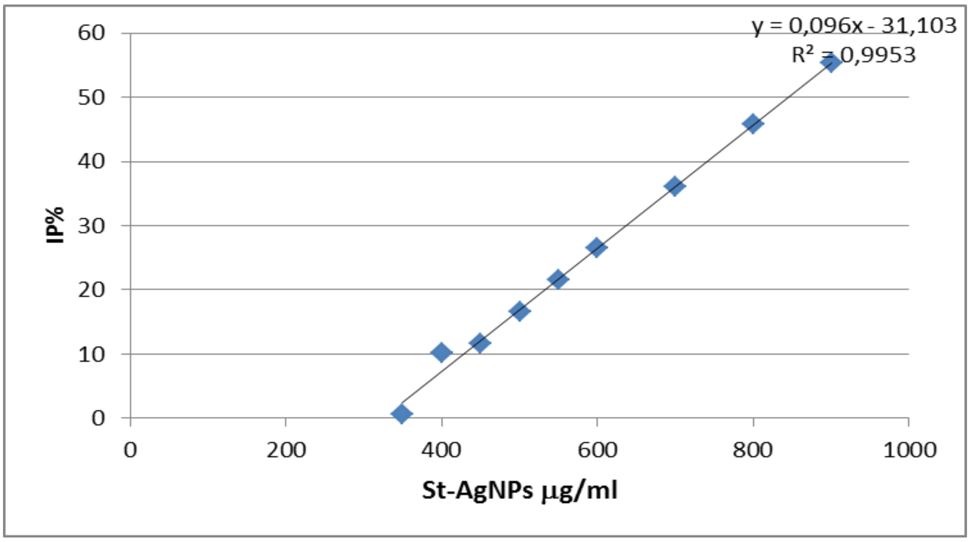

Annex 11: Inhibition percentage values of St-AgNPs (DPPH assay)

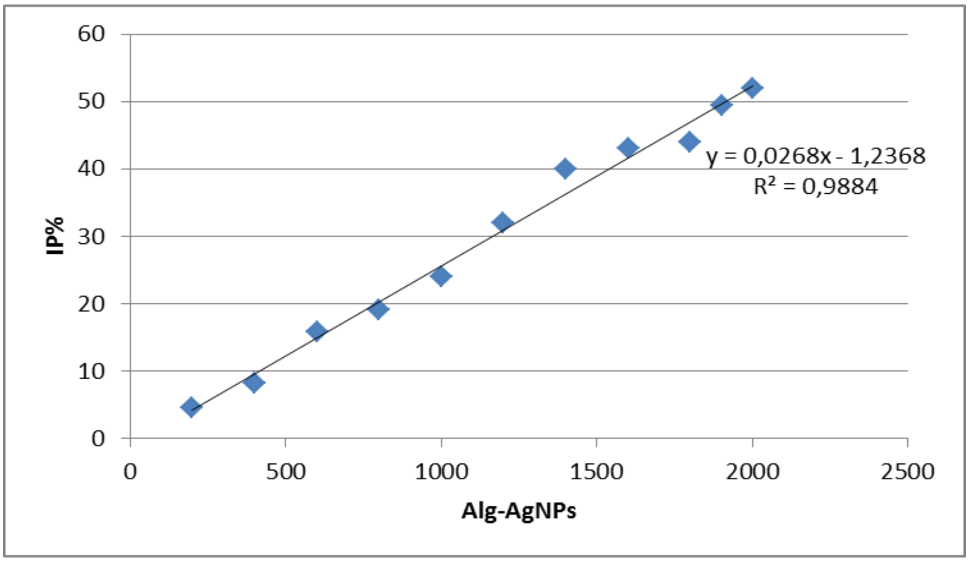

Annex 12: Inhibition percentage values of Alg-AgNPs (DPPH assay)

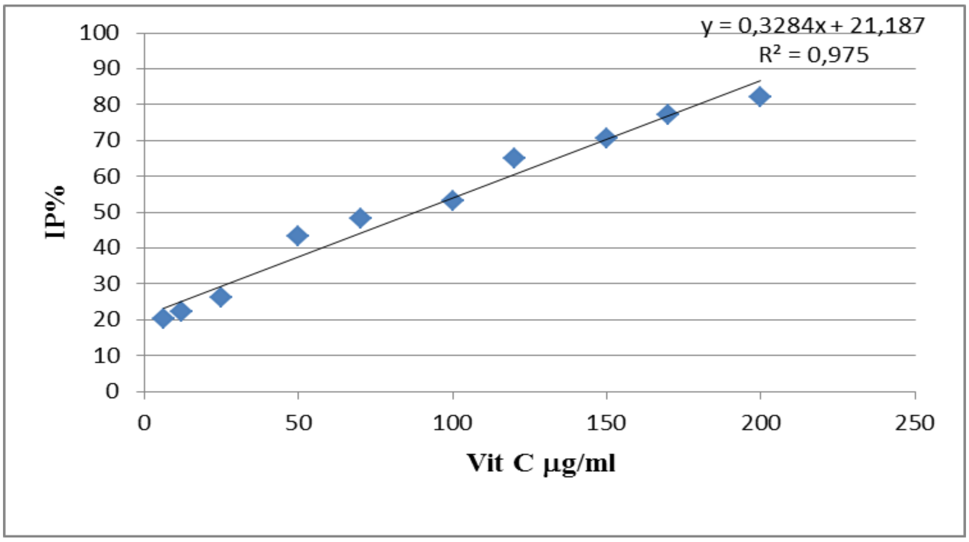

Annex 13: Inhibition percentage values of Vitamin C (DPPH assay)